MSc Program
Renewable Energy Systems

ACADEMY FOR CONTINUING EDUCATION

Sustainable energy supply system for consumers of city of Subotica based on geothermal energy of Pannonian geological basin

A Master's Thesis submitted for the degree of
“Master of Science”

supervised by
Dr. Mario Ortner

Nikolai Zalevskii

12129465

Vienna, 09.11.2023

Affidavit

I, **NIKOLAI ZALEVSKII**, hereby declare

1. that I am the sole author of the present Master's Thesis, "SUSTAINABLE ENERGY SUPPLY SYSTEM FOR CONSUMERS OF CITY OF SUBOTICA BASED ON GEOTHERMAL ENERGY OF PANNONIAN GEOLOGICAL BASIN", 95 pages, bound, and that I have not used any source or tool other than those referenced or any other illicit aid or tool, and
2. that I have not prior to this date submitted the topic of this Master's Thesis or parts of it in any form for assessment as an examination paper, either in Austria or abroad.

Vienna, 09.11.2023

_____
Signature

ACKNOWLEDGEMENTS

I would like to express my sincere gratitude to my supervisor Dr. Mario Ortner for his invaluable guidance and support. His expertise and encouragement helped me to complete my research and write this thesis.

I am grateful to NIS a.d. (Naftna Industrija Srbije) for providing me essential data for geological part of this research what had significant impact on the research. I would like to extend a special thanks to the Director of Department of exploration and field development Mikhail Kuznetsov, for his support, valuable advices and patient explanation of all geological aspects, which I faced with.

I would also like to thank my colleagues at Scientific and Technological Center of NIS a.d., where I used to work for great 6 years, and individually Director Leonid Stulov, for their help, support and collaboration during my research. In particular, I would like to thank Goran Bogicevic, Dr. Ivan Dulic, Ruslan Akhmetzyanov and Janko Sovilj for their help with assessment of geothermal potential of Pannonian Basin, geological modeling of Subotica region and maps preparing. Also, I would like to thank Maksim Pilipenko for his assistance with geothermal reservoir modeling, valuable suggestions about geothermal field development plan and interesting discussions. In addition, special thanks to Aleksandar Jevremovic for his help to pass all procedures and get permission for use NIS a.d. geological data in my research.

I would also like to thank Head of Strategy Department of NIS a.d. Ivan Pigalev for providing valuable feedback and suggestions for economical part of the project. His insights on a final stage helped me to finalize my research and write this thesis.

I am deeply thankful to me wife and my kids for their love and support during this process. Without their encouragement and motivation, I would not have been able to complete this journey.

ABSTRACT

According to the state energy balance, the total energy supply of Serbia in 2020 was 664,224 TJ and dominated by fossil fuels (coal, oil and gas) with a share of 84.2 %. Exactly electricity and heat producers with domination of carbon fossil fuels generate 68% of CO2 emission in Serbia. “Energy Sector Development Strategy of the Republic of Serbia for the period by 2025 with projections by 2030” foresees available technical potential of renewable energy production in Serbia around 154,158 TJ per annum. The largest potential, approximately 100,232 TJ per year, belongs to biomass than geothermal energy potential is 7,327TJ per year and could be underestimated as it is not included electricity production.

The Serbia's total installed geothermal capacity is 82.8 MW_{th} nowdays. Geothermal energy is used for agricultural, balneology, spa, district and individual heating. The share of district/space heating in total geothermal energy usage is 25%, what it is very small in comparison to its potential.

The density of the geothermal heat flow in the significant part of the territory of Serbia is higher than its average value for the continental part of Europe, which is about 60 mW/m^2. The highest values, over 100 mW/m^2, are in the Pannonian Basin, the central part of southern Serbia and in central Serbia. However, any geothermal energy system design has high risks related to geological uncertainties and it successful development depends from proven and reliable geological data.

Pannonian basin is located mostly in northern part of Serbia, Vojvodina province. This region is the center of oil and gas production of Serbia. That means that a lot of geological data were collected in a last 70 years of oil exploration activities in this area. In addition, is NIS (Naftna Industrija Srbije) Oil Company operates many oil fields in northern Serbia and available data and knowledge is reasonable to use.

As the city of Subotica is an economical and cultural center of northern Vojvodina with high energetic heat demand, the goal of this Mater Thesis was research of potential use-case of geothermal direct heat usage in city of Subotica. Overall study of this topic required systematic analyses of followings: exist technologies and expiries in geothermal worldwide, in Europe and Serbia, geothermal potential in Panonian basin with a focus on the area near the city of Subotica and technical challenges of design of geothermal heat plant.

As a result, doublet geothermal system power of 10 MW^{th} and temperature regime 85/55^oC was modeled and designed. Project evaluation took into account the anticipated reservoir performance in the context of heat generation strategies and well performance. As we have significant geological uncertainties, probabilistic approach was chosen for modeling and calculations as a common tool for such cases.

Economical evaluation of the project showed that due to high investment costs related to subsurface part and high electricity price geothermal heat production is positive only in a case of CO_2 trading that is not a common tool yet is Serbia as it is not a member of EU. Aiming to build sustainable business-case with a low carbon footprint additional scenario was set up - PV power plant and geothermal heat plant together, as one energy asset. This scenario proved its economic efficiency and feasibility as has a positive NPV and PI=1.02.

The development of geothermal power and heat generation could be an important part of renewable energy agenda in Serbia. However, to harness its geothermal potential, Serbia will need to invest in research and development, provide financial incentives for geothermal projects, and establish a clear legal and regulatory framework for the sector.

TABLE OF CONTENT

1. INTRODUCTION

Republic of Serbia is a country in south-east Europe with a population more than 6.6 million inhabitants. Serbia is landlock country and shares land borders with Hungary, Romania, Montenegro, Croatia, North Macedonia, and Bosnia and Hercegovina. According to The World Bank annual GDP of Serbia was $ 63,082,047,650 in 2021 or $ 9,230 per capita. The main economical sectors of Serbia energy, the automotive industry, machinery, mining, and agriculture.

According to the state energy balance the total energy supply of Serbia in 2020 was 664,224 TJ and dominated by fossil fuels (coal, oil and gas) with a share of 84.2 % or 559,436 TJ (figure 1.1). The share of oil products is 22% and it mainly use in a transport sector as coal (49.7%) and gas (12.5%) play significant role in electricity and heat production in Serbia. Exactly electricity and heat producers with domination of carbon fossil fuels generate 68% of CO_2 emission in Serbia (Energy balance of Republic of Serbia 2022; https://www.iea.org/countries/serbia).

Total energy consumption (TEC) in Serbia by sectors is presented in figure 1.2. It was 392,839 TJ in total in 2020. As we can see the main consumers are residential, industry and transport sectors with shares 37%, 21% and 23% respectively. Total energy consumption by sources is leaded by oil with a share of 33% which mainly used in the transport sector. The next biggest source is electricity with a share of 26% or 100,370 TJ. Heat has share of 8% in TEC or 31,391 TJ (https://www.iea.org/countries/serbia).

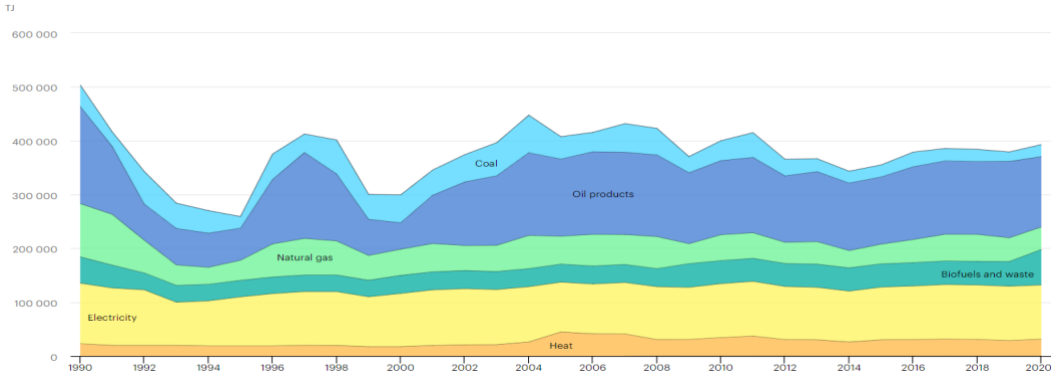

Figure 1.1.: Total energy consumption (TEC) in Serbia by sources (source: https://www.iea.org/countries/serbia)

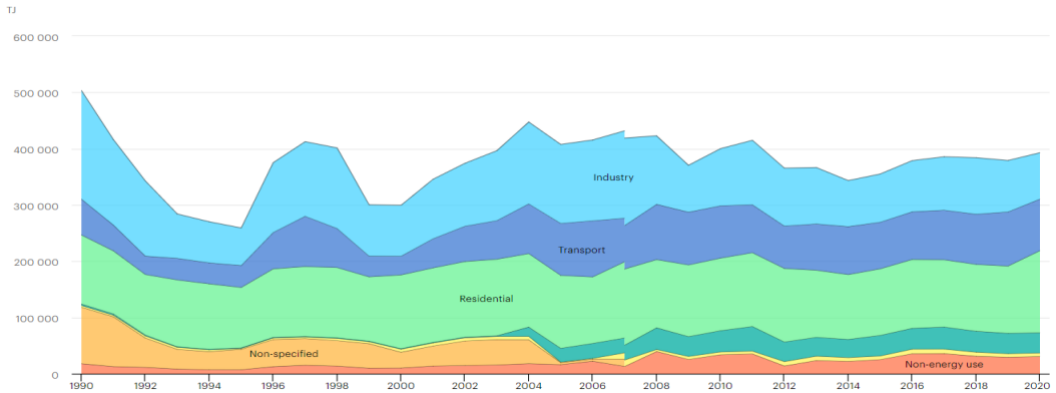

Figure 1.2.: Total energy consumption (TEC) in Serbia by sectors (source: https://www.iea.org/countries/serbia)

It is reasonable to review electricity and heat generation in details as they have different structure.

If we look on figure 1.3, we will notice that majority of electricity 26.5 TWh_e or 70% produced on coal power plants and 9.8 TWh_e or 25.7% on hydro power plants. The total electricity production was 37.96GWh_e in 2020.

The main producer of electricity in Serbia, with a share of 97%, is “Elektroprivreda Srbije” (EPS). The company has an installed capacity of 7,391 MW_e. Its installed capacity in 6 lignite-fired thermal power plant is 4,079 MW_e, 3 gas-fired and liquid fuel-fired combined heat and power plants is 297 MW_e, and 12 hydro power plants is 3,015 MW_e. Besides that, EPS is the main producer of lignite in Serbia with annual production around 39 million tons per year (https://www.eps.rs).

A smaller share of Serbia's electricity production in 2020 came from independent power producers and renewable energy producers, which together accounted for around 3% of the total electricity production. These include various small-scale hydro, solar, wind, and biomass power plants.

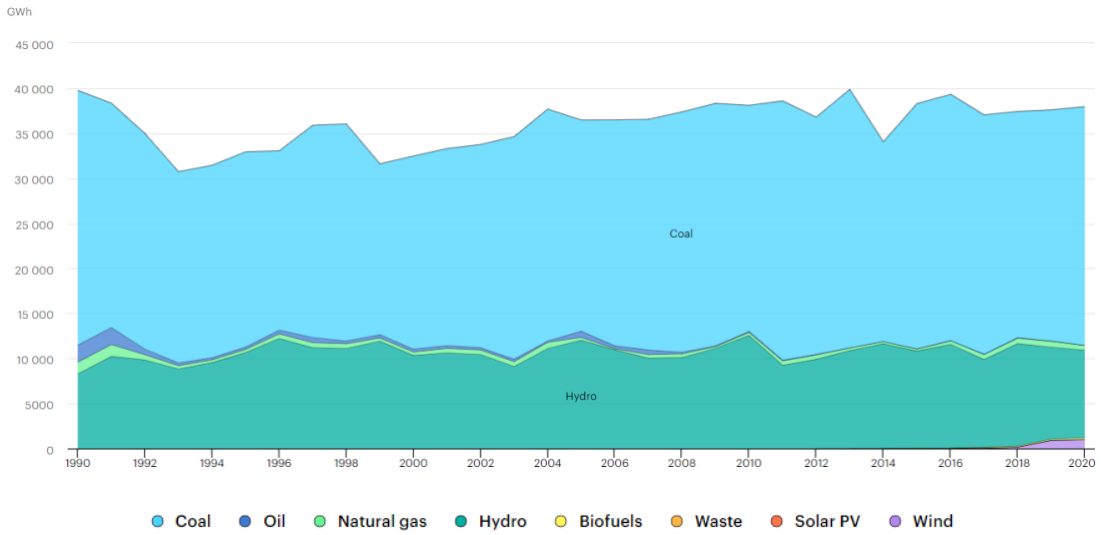

Figure 1.3.: Electricity generation by source in Serbia (https://www.iea.org/countries/serbia)

Annual heat production in Serbia was 40,172 TJ in 2021. You can see on figure 1.3, that 30,331 TJ or 75.8% of heat produce from gas, 4,122 TJ or 10.3% from coal and 4,922 TJ or 12.3% from oil. The rest of heat, around 1.6%, produced from biomass (Energy balance of Republic of Serbia 2022).

These numbers related to the next sources of heat production and distribution (figure 1.4.):

- District heating systems (DHS) in 64 municipalities which include heat generation facilities of installed capacity about 5987 MW_t with annual production 22,009 TJ or 55% of Annual heat production in Serbia.
- Thermal power plants “Kolubara,” “Kostolac” and “Nikola Tesla” which produce heat for Lazarevac, Obrenovac, Kostolac and Požarevac towns. The total heat installed capacity of them is 437.6 MW_t and annual heat production is 2,401 TJ or 6%.
- CHP power plants which have the total heat installed capacity of 558 MW_t and produces 7,203 TJ of heat annually or 18%.

- Industrial energy plants with total heat power of 712 MW_t, which are mostly used for industrial needs and work space heating. They generate about 21% of annual heat production in Serbia or 8,403 TJ per year.

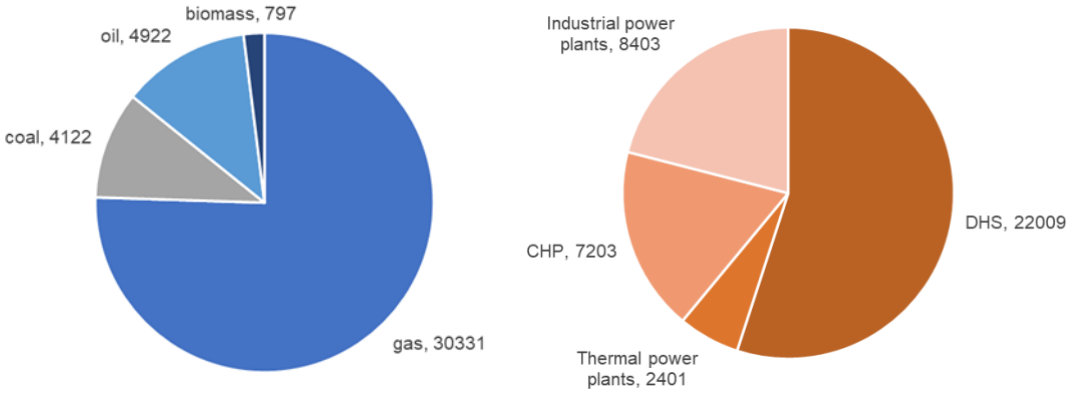

Figure 1.4.: Heat generation by source in Serbia in 2022, TJ
(data source: https://www.iea.org/countries/serbia)

Industrial consumers has part with share of 26%, and households and other sectors with share of 74% in the breakdown structure of heat consumption (Energy balance of Republic of Serbia 2022).

As it was mentioned above these numbers related to centralized heat production. However, significant number of households in Serbia even in big cities are not connected to district heating systems and direct use natural gas, biomass or coal for heating. So, these needs in energy sources for heating are included in related parts in the figure 1.1 and estimated around 100-125 PJ annually.

The share of households connected to the central district heating system is estimated around 24.5% (KWF 2016). Municipalities in Serbia with District Heating Systems are showen in the figure 1.5.

As country's energy sector predominantly dependent on fossil fuels power plants with domination of coal-fired, Serbia ranked among the highest per capita emitters of CO_2 in the region. CO_2 emissions were approximated 7.1 metric tons per capita in 2020. Additionally, the transportation, industry, and agriculture sectors contribute to the nation's CO_2 emissions. The burgeoning Serbian economy has intensified the demand for energy and mobility, thereby exacerbating CO_2 emissions in recent years. Air pollution is a pressing concern in Serbia, especially in urban areas such as Belgrade and other big cities. Moreover, the widespread use of solid fuels for household heating in urban and rural areas contributes to particulate matter emissions, particularly during winter months.

On a way of building sustainable, independent, and carbon-neutral energy system Serbia develops new projects in renewable energy. This is supported by government as a part of “Energy Sector Development Strategy of the Republic of Serbia for the period by 2025 with projections by 2030” with accordance to “National Renewable Energy Action Plan (NREAP) of the Republic of Serbia”. NREAP was developed in 2013 and set up the target to increase the share of RES in a gross final energy consumption (GFEC) to 27.0 % and the amount of GFEC from RES to 107,333 TJ by 2020.

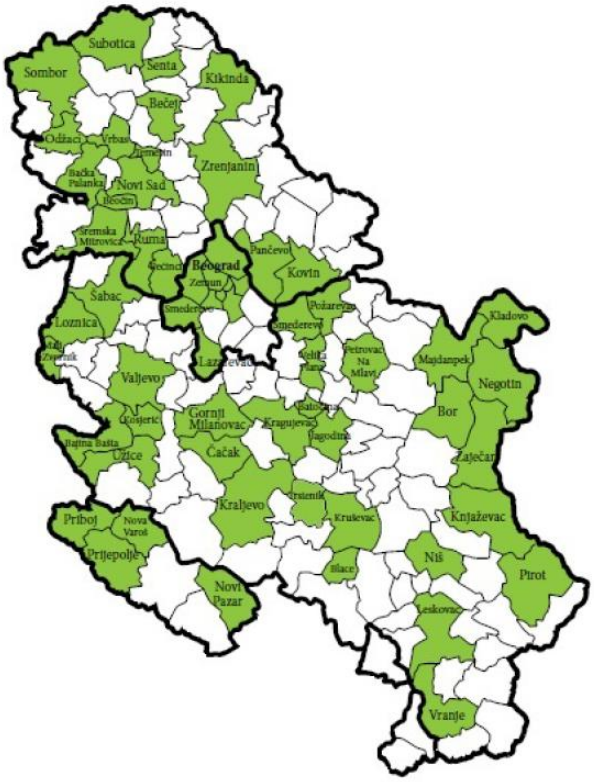

Figure 1.5: Municipalities in Serbia with District Heating Systems (KWF 2016).

According to "National Renewable Energy Action Plan (NREAP) Implementation Report for 2020" the share of RES was 26.3% and GFEC from RES was 106,922 TJ (table 1.1.).

Sectors	The share of RES, %	GFEC, TJ
RES – heating and cooling	35.68	66,708
RES – electricity	30.7	39,796
RES – transport	1.17	414
RES - total in GFEC	26.3	106,922

Table 1.1: The share of renewable energy sources and gross final energy consumption from RES by sectors in Serbia in 2020 (National Renewable Energy Action Plan (NREAP) Implementation Report for 2020)

The Republic of Serbia maintained a constant increase in the construction of new capacities for electricity production from RES. 226 RES power plant with total installed capacity 514.6 MW were built by 31 December 2020. The share of renewables in annual electricity generation reached 30.7% or 10,936 GWh dominating by hydro. New wind and solar projects with total installed capacity over 400 MW realized in Serbia in last years. As a result, the share of these types of renewables raised to 2.6% or 989 GWh in total annual electricity generation in Serbia.

As we can see in the table 1.1. the share of RES in total heating consumption is 35,68%. However, this share is mostly related to decentralized heating or industrial usage of heat as share of RES in district heating is only 1.6% or 435 TJ (Energy balance of Republic of Serbia 2022). The breakdown of RES in heating is presented in figure 1.6. As we can see most of the RES is related to usage of solid biomass in households than share of biogas and geothermal are significantly low – 1.1% and 0.3 % respectively.

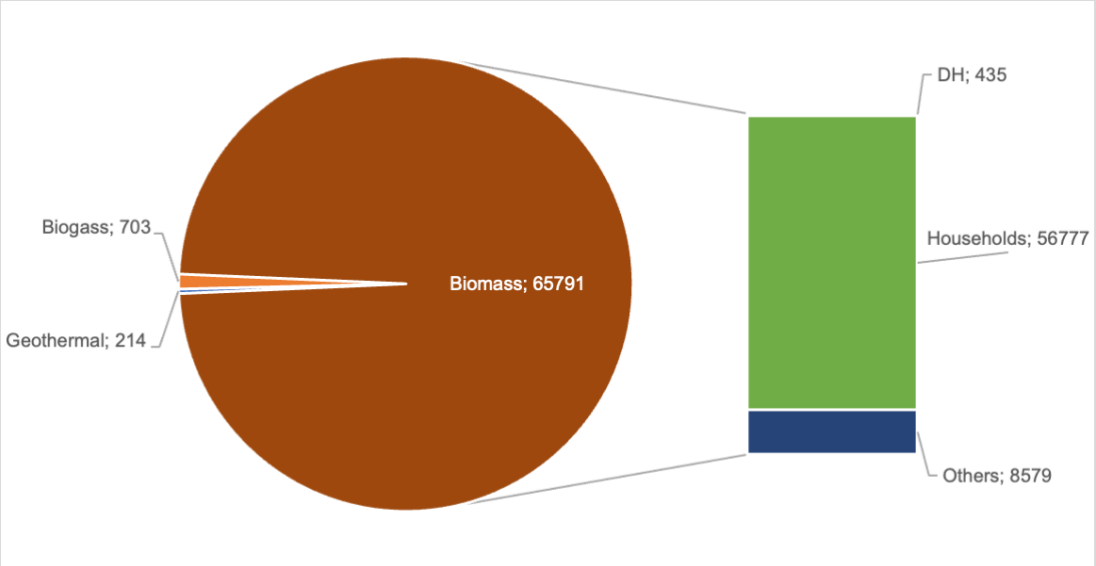

Figure 1.6.: Breakdown of RES in heating and cooling 2020, TJ (National Renewable Energy Action Plan (NREAP) Implementation Report for 2020)

Serbia has a lot of unrealized potential of renewable energy sources, as solar, wind, hydropower, biomass, and geothermal energy. Realizing this potential might make a significant difference in the national energy sector and help it become less dependent on fossil fuels and achieve its climate goals. Except hydro energy, all others sources of renewable energy are still in its early stages (Energy Sector Development Strategy of the Republic of Serbia for the period by 2025 with projections by 2030, 2016: 14). However, the development of renewable energy in Serbia faces numerous challenges, such as regulatory hurdles, financial barriers, and limited public awareness.

According to “Energy Sector Development Strategy of the Republic of Serbia for the period by 2025 with projections by 2030” the unused available technical potential of renewable energy sources in Serbia is around 154,158 TJ per annum. The breakdown of this potential is shown in table 1.2.

RES type	Unused available technical potential (TJ/per year)
Hydro	32,238
Biomass	100,232
Solar	10,048
Wind	4,312
Geothermal	7,327
Total	154,158

Table 1.2: Unused available technical potential of RES in Serbia (Energy Sector Development Strategy of the Republic of Serbia for the period by 2025 with projections by 2030)

As we can see the biomass has the largest potential approximately 100,232 TJ per year than geothermal energy potential is 7,327TJ per year. However, geothermal potential is underestimated, as it is not included electricity production.

Serbia has promising geothermal energy potential, with more than 60 known geothermal sites and reservoirs across the country. According to “National Renewable Energy Action Plan (NREAP) of the Republic of Serbia” 7GWh$_e$ of electricity and 420TJ or 116.4 GWh$_t$ of heat had to be produced from geothermal source in 2020. However, the utilization of geothermal energy for electricity generation remains largely unexplored in Serbia. As of 2021, there were no geothermal power plants in operation and heat production was 214 TJ or 59,4 GWh$_t$ (National Renewable Energy Action Plan (NREAP) Implementation Report for 2020).

The development of geothermal power and heat generation in Serbia faces several challenges, including limited geological data, upfront investment costs, limited local expertise, and complex regulatory frameworks. Serbia will need to make research and development investments, offer financial incentives for geothermal projects, and set up a clear legal and regulatory framework for the industry in order to fully realize its geothermal potential.

Any geothermal energy system design has high risks related to geological uncertainties and it successful development depends from proven and reliable geological data. Normally geology exploration stage should prior to project development.

The territory of Vojvodina (northern part of Serbia), which belongs to the Panonian geological basin, has high potential for geothermal energy research and use. This relates to drill-accessible thermal waters from natural springs and waters in rocky masses. In Vojvodina for hydrogeological systems are recognized and classified. There basic characteristic is preliminary defined on the basin level: ethological composition, stratigraphic references, type an quality of rock collectors, temperature and hydrodynamic features, physical and chemical features of geothermal water and accompanying released gases (Golusin et al. 2014: 870). However, they have to specifically researched and defined for required location. In addition, is NIS oil company operates a lot of oil fields in northern Serbia and available data and knowledge is reasonable to use.

As city of Subotica is an economical and cultural center of northern Vojvodina with high energetic heat demand, the goal of this Mater Thesis was research of potential use-case of geothermal direct heat usage in city of Subotica. Overall study of this topic required systematic analyses of followings: exist technologies and expiries in geothermal worldwide, in Europe and Serbia, geothermal potential in Panonian basin with a focus on the area near the city of Subotica, design of geothermal heat plant and finance analyses.

2. GEOTHERMAL ENERGY REVIEW IN REPUBLIC OF SERBIA

The density of the geothermal energy flow is the main parameter, which can give us the first understanding of the geothermal potential of an area. It shows the amount of geothermal heat that comes from the Earth's deep layers to its surface through an area of 1 m^2 per second. According to available data, the average value of the density of the geothermal heat flow is around 60 mW/m^2 for majority of continental Europe. At the same time, the value of the density of the geothermal heat flow exceed 100 mW/m^2 on the territory of Serbia which belongs to Pannonian Geological Basin (Stipić et al. 2012).

The geothermal energy resources of the Republic of Serbia are well-known and have been used in some locations for many years. Geothermal energy is used in Serbia mainly for heating and others similar purposes. However, its usage for energy production is still relatively underdeveloped despite the fact that Serbia has a large amount of this resource and high potential.

The majority of geothermal springs are located in Vojvodina (northern part of Serbia) and central Serbia (figure 2.17), where Pannonian Basin is located. They are used exclusively for sports, recreational, balneology and partly for space heating purposes. (Golusin et al. 2014: 870).

Figure 2.1: Map of geothermal sources in central and north part of Serbia (Stipić et al. 2012).

However, there are a lot of natural springs of geothermal water with a temperature higher than 15°C outside the Pannonian basin as well. The highest temperature of geothermal water were discovered in Vranjska Banja (96°C), Jošanička Banja (78°C) and Sijerinska Banja (72°C).

The country's total installed geothermal capacity is 82.8 MW_{th} of thermal energy and annual production is 648.6 GWh_{th} (without heat pumps). Geothermal energy is used for agricultural, balneology, spa, district and individual heating. The majority of geothermal heat, almost 50%, use for balneology, spas and recreation purposes (table 2.2). 59 spas and recreation centers all around Serbia use geothermal waters. The share of district/space heating in total geothermal energy usage is 25%, but it is very small in comparison to its potential. There is no geothermal power plants in Serbia.

Propose of usage	Installed Power, MW_{th}	Used Energy	
		GWh_{th}/year	%
Space heating	19.7	159.7	24.6
Bathing and pools	36.0	319.4	49.3
Agricultural drying	0.7	6.1	0.9
Greenhouses	15.4	71.1	11.0
Fish farming	6.4	58.6	9.0
Industrial process heat	4.6	33.6	5.2
TOTAL	**82.8**	**648.6**	**100**

Table 2.1: Geothermal heat in Sebia, GWh_{th}/year (Milivojevic & Martinovic 2005).

Outside of Pannonian Basin region, geothermal resources is also used in different locations. As a great example, direct use of geothermal water for space heating has started forty years ago in Vranjska Banja. Nowadays, geothermal water is being used there to heat flower greenhouses, poultry farms, textile workshops, hotel premises, and the spa rehabilitation center. In other locations, as Kursumlijska Banja, Sijarinska Banja Ribarska Banja, geothermal water is used for a heating purpose in rehabilitation and recreational facilities, hotels and swimming pools. Some geothermal heat exist facilities and consumers in Serbia are shown in figure 2.18.

Figure 2.2: Geothermal heat production map in Serbia (data source Milivojevic & Martinovic 2005).

3. GEOTHERMAL ENERGY TECHNOLOGIES REVIEW

Geothermal energy can be found at various depths and temperatures. Hydrothermal systems which consisting of hot water circulating through deep-seated permeable rock are the most developed.

The temperature of the geothermal resource is a key factor in a definition how it can be used in a best way. According with a temperature they can be divided into **three groups: high (greater than 150°C), medium (90-150°C)** and **low (less than 90°C).** The production of electricity is preferable from medium to high temperature geothermal resources. In order to generate electricity at commercial scale, the temperature of the resource must be between 150 and 180°C (depending on technology). However, existing technologies are able to create a profitable electricity production use-case even from temperatures as low 70°C. Geothermal medium-temperature resources are used in a variety of applications such as for buildings heating and cooling, industrial processing, and agricultural. It is possible to use combined heat and electricity for both heating and cooling. Geothermal heat pumps (GHPs) can be used for a variety of applications to increase the heat content in low-temperature sources. Aiming to maximise the use of geothermal resources and increase the efficiency cascaded utilisation is used.It means that the outlet of working fluid from the first application can be used further. For example, the hotwater collected after electricity production can be used for district heating (IRENA and IGA 2023: 14).

3.1 Lindal diagram

Lindal diagram is a great tool for technologies and their application classification depending on the temperature of geothermal reservoir. In figure 3.1 modified the Lindal Diagram from the U.S. GeoVision report by the U.S. Department of Energy is presented.

Most geothermal applications use of water in a range of temperatures. The applications at the upper end of the temperature range use steam while those in the lower part of the scale usually use hot liquid geothermal water. Conventional geothermal power plants use high temperature geothermal resources as dry or flash steam. Binary power system lies on a middle of range with a temperature up to 85°C. Direct use of geothermal waters covers the entire range, and can even be extended below 20°C with heat pumps usage. In general, the Lindle diagram shows industrial geothermal applications in the middle-to-high range, while the lower end is reserved for energy-efficient applications, such as agriculture and space heating.

This classification of current and potential application in an order of decreasing resource temperature gives rise to two important system design conditions. Firstly, there is a limit to the kind of use that is possible in any given project, and it is determined by the maximum resource temperature. Secondly, it is possible to extend the potential use of geothermal fluids through cascade and/or combined use, as well as through optimized process design and the use of high-efficiency components (Patsa et al. 2015).

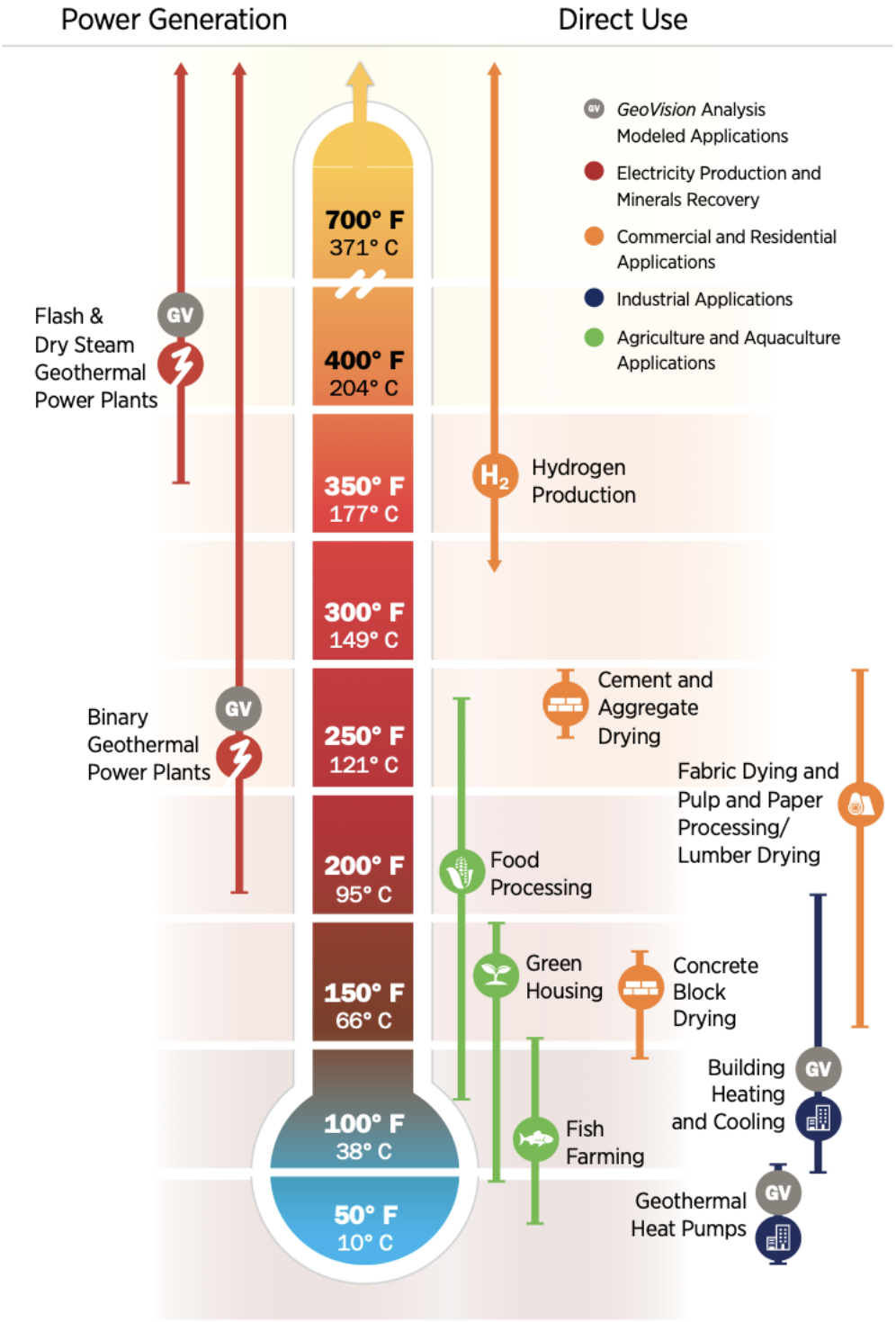

Figure 3.1: The continuum of geothermal energy technology applications and uses (U.S. Department of Energy 2015: 22)

3.2 Technologies for electricity generation from geothermal source

Three primary power plant technologies are used to convert the energy from geothermal resources to electricity: **dry steam, flash steam** and **the binary cycle** (figure 3.2). The majority of geothermal power plants are flash or dry steam plants, which use geothermal energy at temperatures above 150°C. Although lower-temperature resources are being increasingly developed for electricity production or combined heat and electricity using binary cycle technologies.

The dry steam technology is used when the geothermal reservoir produces dry steam which can be obtained and collected on a surface. Geothermal steam, that is saturated or superheated at high pressure, feeds directly to a steam turbine which rotates a generator to produce electricity. Steam exhaust from the turbine is discharged into a condenser at low pressure or partial vacuum. This ensures the higher drop pressure and increase the efficiency the thermodynamic cycle. Backpressure plants, which discharge exhaust steam directly to the atmosphere, are much cheaper and simpler and used in small modular units for early stages in geothermal power projects.

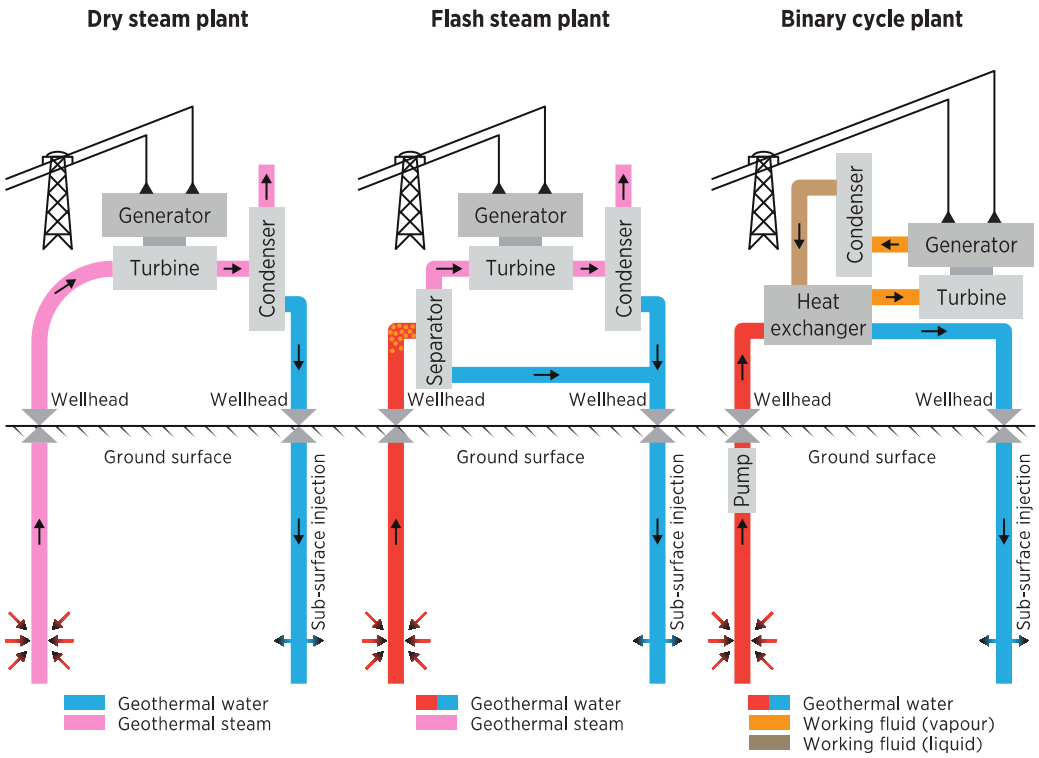

Figure 3.2: Geothermal power plant technologies (IRENA and IGA 2023: 16)

Globally, **flash steam** is the most common technology used in existing geothermal plants. This technology uses two-phase geothermal fluids at high temperatures and pressures to produce electricity. The two-phase geothermal fluid separates for a steam and a liquid before a turbine. This process known as "flashing". After that steam is expanded in a turbine which rotates a generator for electricity production (single-flash). Similar to the dry steam process, the steam exhaust from the turbine is

discharged into a condenser at low pressure or released directly into the atmosphere in backpressure plant solutions. The separated liquid component of the geothermal fluid returns to the reservoir source through reinjection wells. Also, it can be flashed further to produce more steam which used for additional electricity generation. It is knows as double/triple flash process. and eventually returned to the reservoir source through reinjection wells. Double/triple-flashing is used to produce more steam to increase electricity production and efficiency (Anderson & Rezaie, 2019).

Binary power plants work by transferring heat from the geothermal fluid to a secondary working fluid with a lower boiling point than water, contained in a closed loop. The secondary working fluid vaporises and this steam rotates a turbine. This technology gives an opportunity to use geothermal fluids for electricity generation with lower temperatures than flash or dry steam power plants. Current binary cycle technology allows to produce electricity from geothermal fluid with temperatures up to 70-80°C. Binary plants can operate on an organic Rankine cycle (ORC) or a Kalina cycle. Butane or pentane is used in an ORC and a mixture of ammonia and water in a Kalina cycle Binary plants can operate in a fully closed cycle where 100% of extracted geothermal fluid is returned to the reservoir using injection wells. This allows for a zero emission operation and maximises the sustainable use of resources (DiPippo, 2012; Anderson and Rezaie, 2019).

Wellhead generators are modular units of less than 10 MW, usually with a standard design that produces electricity from a single well. Wellhead generators have gained popularity as a viable option because they can speed up return on investment by allowing early revenue generation during a geothermal field's development phase. Wellhead generators have a number of benefits, including the ability to utilise wells waiting to be connected to larger electric power plants, shorter pipeline requirements, quicker installation times, the ability to gather early reservoir behaviour data prior to the startup of larger electric power plants, and the ability to train field operations staff (IRENA, 2020 cited by IRENA and IGA 2023: 17).

3.3 Technologies for heating and cooling from geothermal source

Geothermal resources, which are suitable for heating and cooling, are widespread globally in the form of shallow geothermal resources or deep-seated aquifers hosted in permeable formations in sedimentary basins, and volcanically and tectonically active zones. Geothermal fluids can be extracted from shallow wells that are a few hundred metres deep using GHPs or from deep wells of several kilometres in depth (IRENA and IGA 2023: 18).

The major categories of geothermal heating and cooling applications are **space heating and cooling incl. district heating; agriculture and food processing; industrial process heat; and health, spa and tourism** (IRENA and IGA 2023: 18).

District heating networks supply hot water to residential and commercial buildings for space heating and domestic hot water on a larger scale to multiple buildings (IRENA and IGA 2023: 18). Major components of district heating system are presented in figure 3.3. It consists of two circles – (1) geothermal fluid circle and (2) district heating fluid circle. Heat transfer between two circles occurs in heat exchanger. Geothermal heat generation units in a district heating system, normally, operate in a constant mode and covers a base part of heat load curve. They work in a combination with conventional boilers which are used in a peak load.

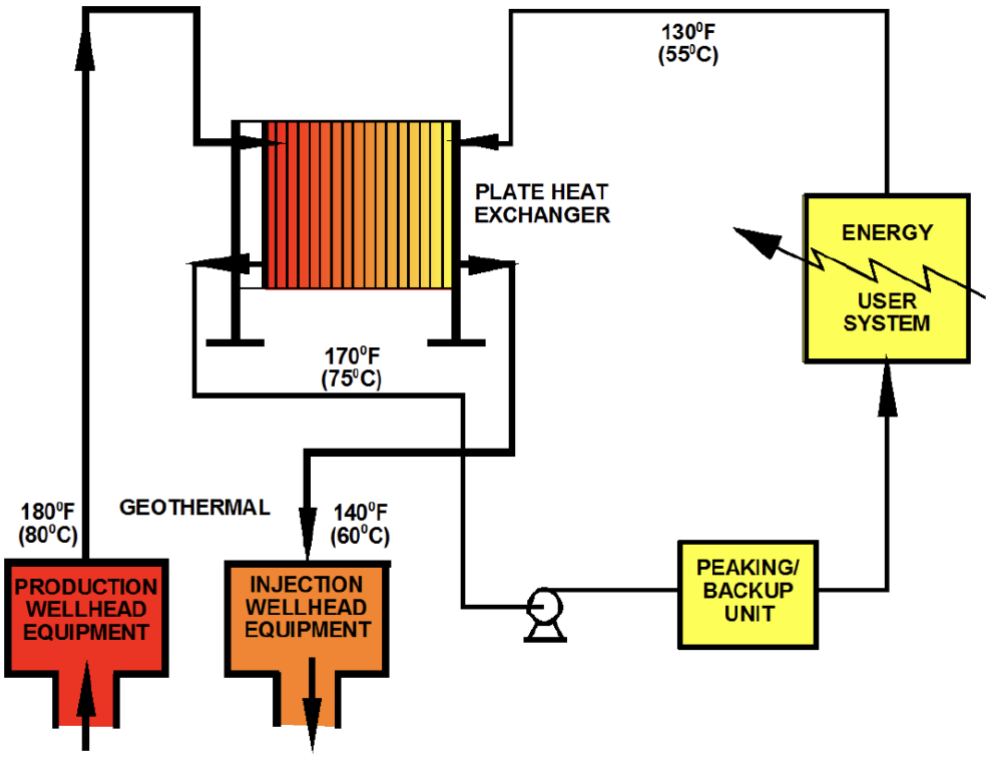

Figure 3.3: Major components of geothermal district heating system (John & Linenau 2009)

The use of geothermal heat in **agricultural and agri-food** is significant and possible at a wide range of temperatures of geothermal fluid. Geothermal greenhouse heating requires temperatures between 40 and 100°C. Aquaculture uses geothermal heat to heat water to a temperature of 20-30°C to provide optimal conditions for algae and fish. In open-field farming, geothermal soil heating is provided by a network of buried pipes with hot water. This increase crop yields and extend the growing period. (IRENA and IGA 2023: 18).

Natural geothermal hot springs have historically been used for bathing, swimming and medicinal purposes. Artesian and pumped geothermal water is used in **swimming pools, saunas and bath** in many countries.

3.4 Innovation technologies in geothermal energy

New technologies that allow usage of geothermal energy from deep-seated resources beyond those mentioned above are being developed through research and demonstration projects and tests of commercial feasibility. These technologies have different levels of maturity and readiness, and not available for commercial implementation. These include:

Enhanced or engineered geothermal systems (EGSs) improve geothermal system permeability through chemical, thermal and hydraulic stimulation. This can be done for geological conditions with high temperatures of the rock, but low permeability and fluid volume that makes these formations not sufficient with conventional technologies. The permeability of the rock can be increased by pumping water or other fluids (such as carbon dioxide), which will fracture the rock and create an artificial reservoir (IRENA and IGA 2023: 15).

Advanced geothermal systems (AGSs) are deep, large, artificial closed-loop circuits in which a working fluid is circulated and heated by sub-surface rocks through conductive heat transfer. AGSs can to be used in almost any locaiton, as it does not require an adequate water reservoir with good permeability. However, as this demand longer wells, to increase the surface of heat transfer, higher drilling costs occurs (IRENA and IGA 2023: 15).

Supercritical Geothermal Systems are characterized by significantly high temperatures and a reservoir that contains fluids in a supercritical state. This means that for pure water the temperature must be at least 374°C and pressure at least 221bar. These supercritical fluids can be found in deep volcanic hydrothermal systems in Iceland, Japan, Kenya, Mexico, and New Zealand. Due to the higher energy content of the fluid, the productivity of these supercritical systems may be much greater than conventional high-temperature systems have (Fridleifsson & Albertsson 2014). The use of these systems have several technical challenges, including the use of corrosive liquids. This technology have been studied in recent years (IRENA and IGA 2023: 15).

4. THE CITY OF SUBOTICA HEATING SUPPLY SYSTEM ANALYSES

4.1 The city of Subotica general information

The city of Subotica is the northernmost city of the Republic of Serbia, the second largest city of the Autonomous Province of Vojvodina and the administrative center of the North Bačka District. The geographical position is determined by 46°5'5'' north latitude and 19°39'47'' east longitude. (Local sustainable development strategy of the city of Subotica 2013-2022: 10).

Figure 4.1: The city of Subotica location (source: https://www.google.com/maps)

Historically and thanks to its geographical location the city of Subotica has become important administrative, industrial, commercial, traffic and cultural center of Severnobacka District. There is the Palic settlement and the Palic Lake (102 meters above sea level) at seven kilometers away from Subotica which is a famous recreation and spa area.

The territory of the city of Subotica has an area of 1,007 km^2. The city has 137,753 inhabitants who live in 19 settlements organized into 37 local communities (Local sustainable development strategy of the city of Subotica 2013-2022: 11).

A constant increase of inhabitant's number was recorded until 1981 in Subotica, while in the period from 1981 to 2011, the opposite tendency is evident, and that is, the total number of the population is decreasing. Migratory movements of the population from the village to the city are noticeable, and the reduction of the total number of inhabitants in smaller settlements is especially pronounced (Energy manager of the City of Subotica 2021).

The transit pan-European road E-75, which connects it with the Republic of Hungary in the north and via Belgrade with Southern Europe in the south passes the city of

Subotica. There are the main roads towards Novi Sad, Sombor, Horgoš and Senta intersect in the city itself. In addition, Subotica is connected to the whole Europe by a railway. The Belgrade-Budapest railway passes through the urban center of the city where it meets with the railway lines towards Sombor, Horgoš, Crvenka and Baja (Local sustainable development strategy of the city of Subotica 2013-2022: 12).

City	Distance from Subotica, km
Belgrade	184
Budapest	203
Zagreb	537
Vienna	440
Bucharest	708

Table 4.1: Distance of Subotica from the main economic centers in the region

Subotica is well connected with three international airports. Belgrade airport is 165 km away, Budapest airport is 190 km away, while Osijek airport is 120 km away. There is a sports airport "Ivan Sarić" in Subotica.

According to the seismic regional map of Serbia, the area of the City of Subotica belongs to the VIII zone of the Mercali-Kankani-Zieberg scale (MCS) due to the intensity of the earthquake. An earthquake of this strength is characterized as strong (IUPCS 2018: 21).

4.2 Climate

The area of the city of Subotica has a moderately continental climate. The average annual air temperature is 10.5^0C, the warmest months are July and August, and the coldest are January and February (IUPCS 2018: 22).

The annual average of sunshine is between 2100-2200 hours. The greatest sunshine is in July and August. The highest daily averages amount to 10-12 hours of sunshine then (IUPCS 2018: 22).

The average annual relative air humidity is 70%. This data shows that Subotica belongs to relatively dry areas (IUPCS 2018: 22).

The highest number of days with precipitation are in May and November, and the lowest number of days with precipitation are in January and October. The annual average of precipitation is 54.16 cm, which characterizes relatively dry regions (IUPCS 2018: 22).

Winds in Subotica blow from the north-west, northeast and southeast directions. The most frequent wind is north-west and it blows in summer. In winter, the northeast wind blows, it is usually a cold and strong wind. (IUPCS 2018: 22).

Climatic figures	Value
Average air temperature in January, ^{0}C	-0.4
Average air temperature in July, ^{0}C	+22.3
Average annual air temperature, ^{0}C	+11.2
Average annual air humidity, %	72
Average annual number of sunny days	71
Average annual number of cloudy days	94
Average annual amount of precipitation, mm	571.1
Average annual number of snow days	23
Average annual number of foggy days	41
Average annual number of days with hail	1

Table 4.2: General climatic characteristics (Local sustainable development strategy of the city of Subotica 2013-2022)

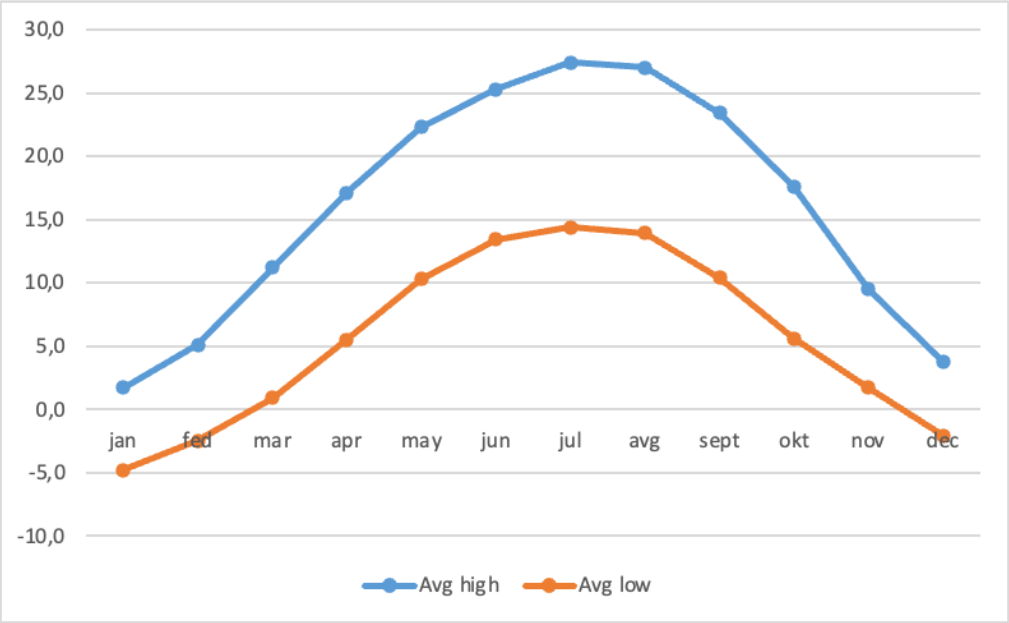

Figure 4.2: Average monthly temperature in Subotica (source: https://en.wikipedia.org/wiki/Subotica)

4.3 Economy

The area around Subotica is mainly farmland, but the city itself is an important industrial and transportation center in Serbia. Due to the surrounding farmlands Subotica has famous food producing industries in the country, including such brands as the confectionery factory "Pionir", "Fidelinka" the cereal manufacturer, "Mlekara Subotica" a milk producer and "Simex" producer of strong alcohol drinks. Also, a few old socialistic industries that survived the transition period in Serbia are in Subotica.

The biggest ones are the chemical fertilizer factory "Azotara" and the rail wagon factory "Bratstvo" (https://en.wikipedia.org/wiki/Subotica).

Subotica is a special customs-extraterritorial zone and free economic zone in Serbia, where business entities from other countries carry out their economic activities, thanks to more liberal business climate. It is regulated by the specific national law which define special customs privileges and simplification of the administrative procedure for business except activities which pose a threat to the national security or environment. Advantages for business are: free import and export of goods and services, exemption from customs and tax duties, business without time limit of customs supervision, exemption from payment of value added tax (VAT), exemption from payment of value added tax (VAT) on energy for production activities etc. (Local sustainable development strategy of the city of Subotica 2013-2022:15).

The main goal of this is to encourage economic activity in Subotica, establish industrial production for export as a comparative advantage and the creation of new jobs. Currently the biggest export industry in town is the "Siemens Subotica" wind generators factory and it is the biggest brownfield investment so far. Also the other foreigner companies came to Subotica as Fornetti, ATB Sever, Masterplast, Dunkermotoren, NORMA Group, Continental Contitech" and "Swarowski". (IUPCS 2018: 25)

Tourism is also important for Subotica as Palic and Palic Lake is traditional recreation and spa zone.

4.4 Heat energy supply system of the city of Subotica

The supply of heat energy to consumers of the city of Subotica, which are in a zone of the existing district heating area, provides PUC "Suboticka Toplana". The founder of PUC "Suboticka Toplana" is the city of Subotica.

PUC "Suboticka Toplana" produces around 100 GWh_{th} of heat energy per heating season. That cover around of 27% of Subotica's households, i.e. ~10,500 apartments and ~335 business consumers, among them are many public, educational, cultural, health and social institutions as well as other economic subjects.

Since the beginning of the 2005/2006 heating season, the PUC "Suboticka Toplana" has been accepting payment only based on the measured real amount of consumed heat. All transfer points of district heating system are equipped with heat meters.

In the period of 2008-2014 overall reconstruction of district heating network was done include water pipelines replacement. The heat distribution network has a full automatic control system that contribute to the optimization of the process on both technical and economic criteria of heat energy production.

The general technical figures of PUC "Suboticka Toplana" are:

- Installed heat power - 124 MW_{th}
- The main fuel is natural gas / back-up fuel is oil
- The length of distribution pipeline network is 53 km
- The length of distribution pipeline network with return lines is 97 km
- 763 heating substations incl. 382 in public residential buildings and 381 in individuals houses

The existing district heating system of city of Subotica is divided into five regions: "Kertvaros", "Novi Grad", "Prozivka", "Center" and "Radialac"/“Zeljeznicko naselje”.

The map of the city of Subotica including district heating system is presented in appendix 1.

As “Suboticka Toplana” covers only around 27% of city’s households, the rest ~40% of households use natural gas for heating and ~33% use other sources to produce heat (electricity, wood and ect.). Aiming to reduce greenhouse gases emission and create sustainable and diversified heat supply system direct use of geothermal heat in the city of Subotica may be considered.

One of potential possibilities could be the connection of new geothermal heat plant to the exist district heating system owned by PUC “Suboticka Toplana” and selling predefined amount of heat to it. Then, it looks reasonable to cover base part of current heat load curve of “Suboticka Toplana” by geothermal source. In this case, it will be operating in a constant mode with a high load factor. This approach widely used in geothermal heating systems (see part 3.3).

Aiming to define the capacity of possible geothermal heat plant, “Suboticka Toplana” heat production plans in last years were carefully analyzed. Annual heat production in 2017-2021 is shown in a figure 4.3. An average outside temperature during the heating period is presented in that figure as well. It was calculated as the arithmetic mean using meteorologic historical data from on-line data base https://sumeteo.info. As we can see the heat production is relatively stable and corelated with outside temperature.

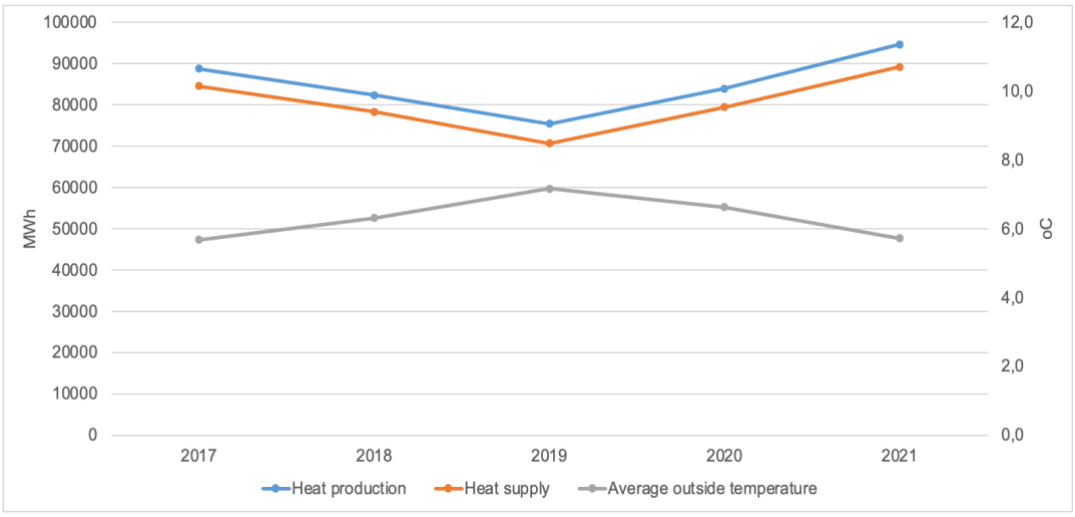

Figure 4.3: Suboticka Toplana heat production and supply 2017-2021
(source: Suboticka Toplana. Business plans 2018-2022. http://www.toplanasubotica.co.rs/en/documents)

The normative heating season lasts from Octobar 15th till April 15th, but the actual length depends on the outside temperature, and it can vary. In a figure 4.4 we can see the correlation between heat production and number of heating days and average outside temperature.

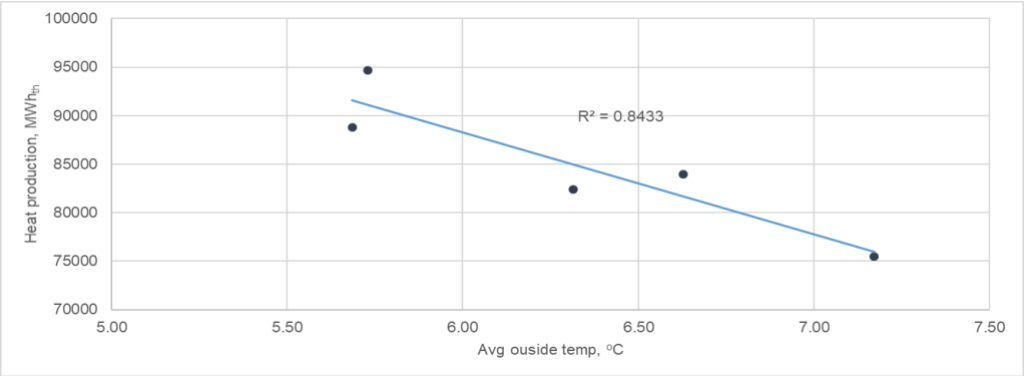

a)

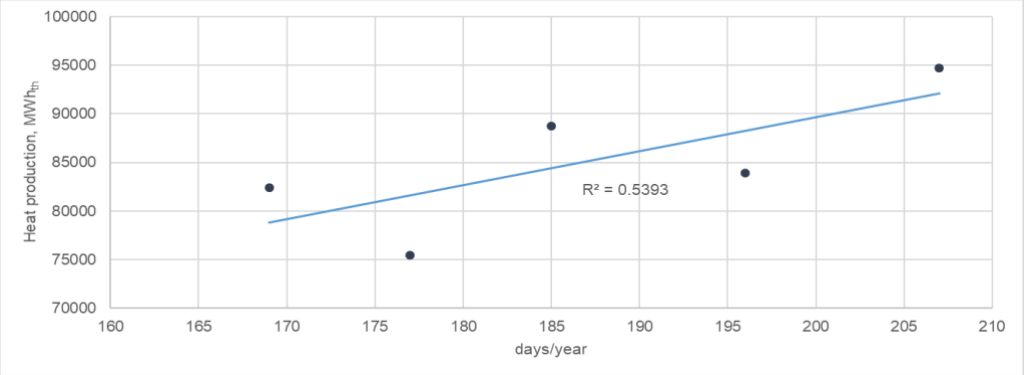

b)

Figure 4.4: Suboticka Toplana heat production vs average outside temperature (a) and number of heating days (b) *(source: Suboticka Toplana. Business plans 2018-2022. http://www.toplanasubotica.co.rs/en/documents)*

Monthly heat production is presents in figure 4.5. Different of heat production from year to year on monthly bases is explained by outside temperature variety which is shown in figure 4.6. Anyway, besides outdoor temperature and heating days there are other climatic factors affecting the heat demand of a given customer base, such as wind and solar radiation.

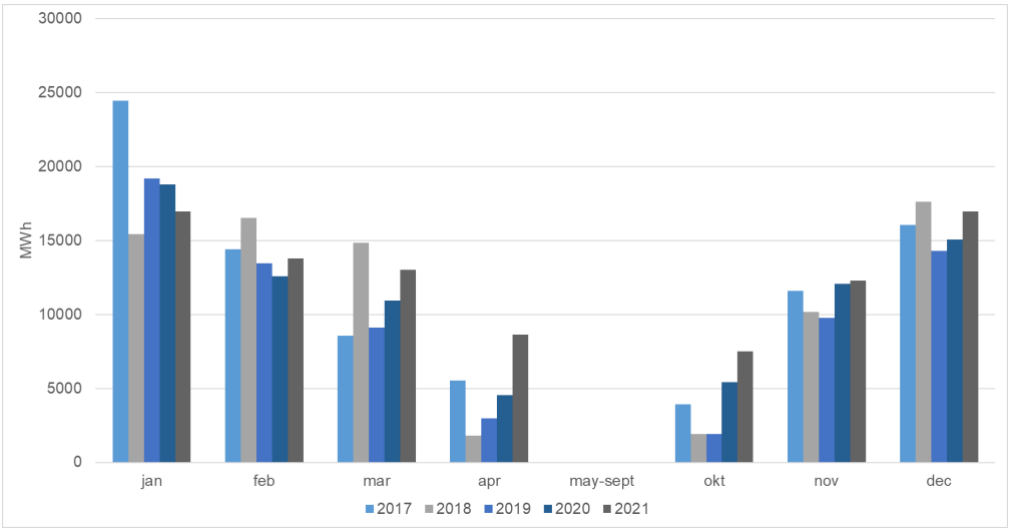

Figure 4.5: Suboticka Toplana monthly heat production 2017-2021 *(source: Suboticka Toplana. Business plans 2018-2022. http://www.toplanasubotica.co.rs/en/documents)*

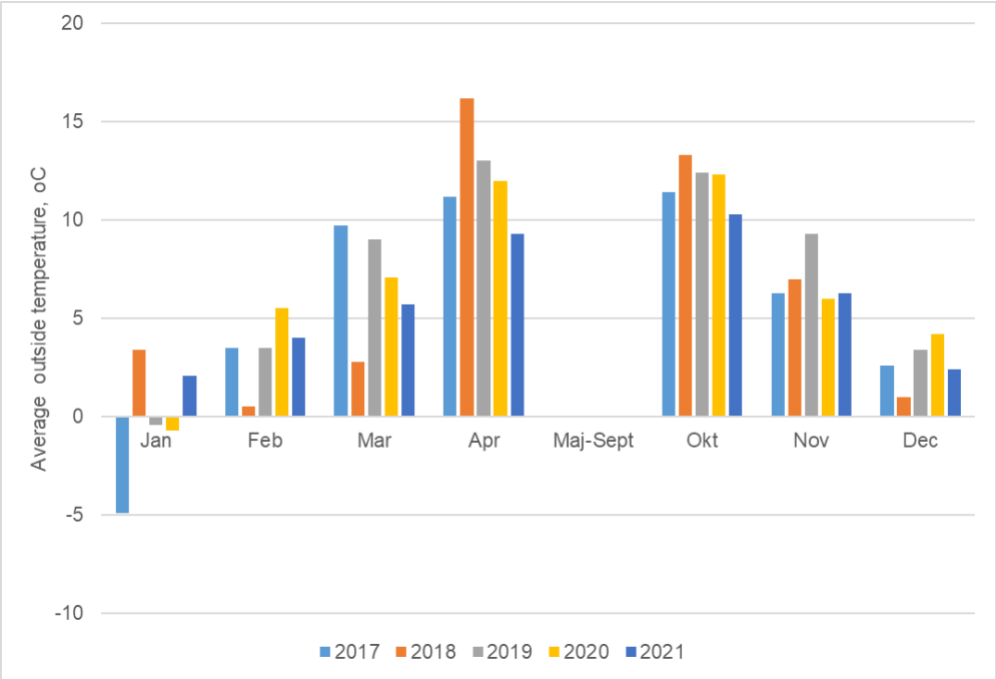

Figure 4.6: Average monthly outside temperature in Subotica 2017-2021*(source: https://sumeteo.info)*

The table 4.3. below shows the breakdown of energy consumption by consumer group. Thera are two groups of consumers – residential and commercial. The total number of residential consumers is slightly increasing (+3,85% in 5 years), while the number of commercial consumers stays almost the same last years.

Consumers	2017	2018	2019	2020	2021	2022
Number of consumers						
residential	10,137	10,134	10,215	10,313	10,527	10,137
commercial	326	332	337	332	325	326
total	10,463	10,466	10,552	10,645	10,852	10,463
Heat Consumption, MWh						
residential	59,221	54,688	46,193	52,116	57,775	59,221
commercial	25,376	23,398	24,477	27,332	31,425	25,376
total	84,597	78,086	70,670	79,448	89,200	84,597
Share in heat consumption						
residential	70.0%	70.0%	65.4%	65.6%	64.8%	70.0%
commercial	30.0%	30.0%	34.6%	34.4%	35.2%	30.0%
total	100.0%	100.0%	100.0%	100.0%	100.0%	100.0%

Table 4.3: Breakdown of energy consumption by consumer group *(source: Suboticka Toplana. Business plans 2018-2022. http://www.toplanasubotica.co.rs/en/documents)*

The share of residential consumer's heat consumption is between 64.8 and 70 % and the rest belongs to commercial consumers group. The figure 4.7 below shows the

heat consumption of two consumer groups in 2017-2022. The shape of this graph is influenced by average outside temperature, heating days and number of consumers.

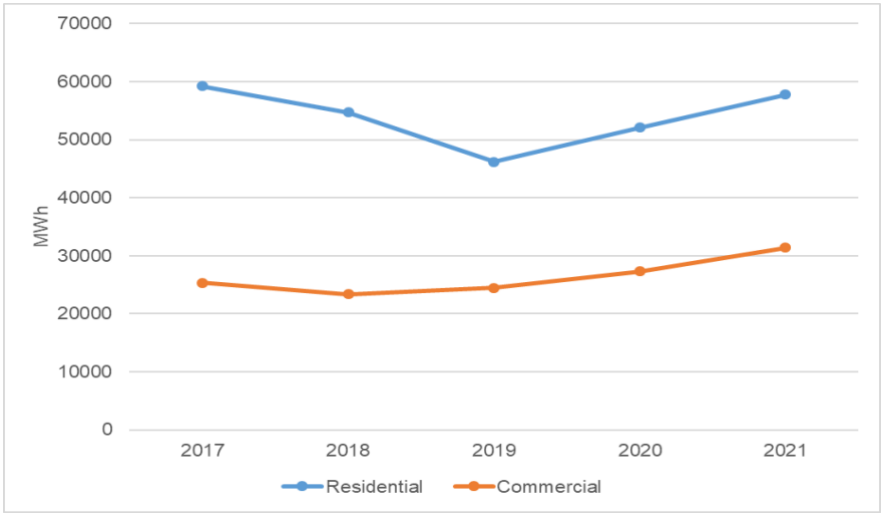

Figure 4.7: Heat consumption of consumer groups in 2017-2022 *(source: Suboticka Toplana. Business plans 2018-2022. http://www.toplanasubotica.co.rs/en/documents)*

It is a common practice to describe DH system operation as load curves, which show the load in dependence of the time. Sorted load curves sort the loads by size, while the unsorted load curve shows the loads by calendar data. Date for load curves was collected from "Suboticka Toplana" reports. The figure below show the load curves for 2019, 2020 and 2021. The curves shapes are very similar over a wide range, but start to differ significantly at the end if the heating season due to different lengths of the heating period.

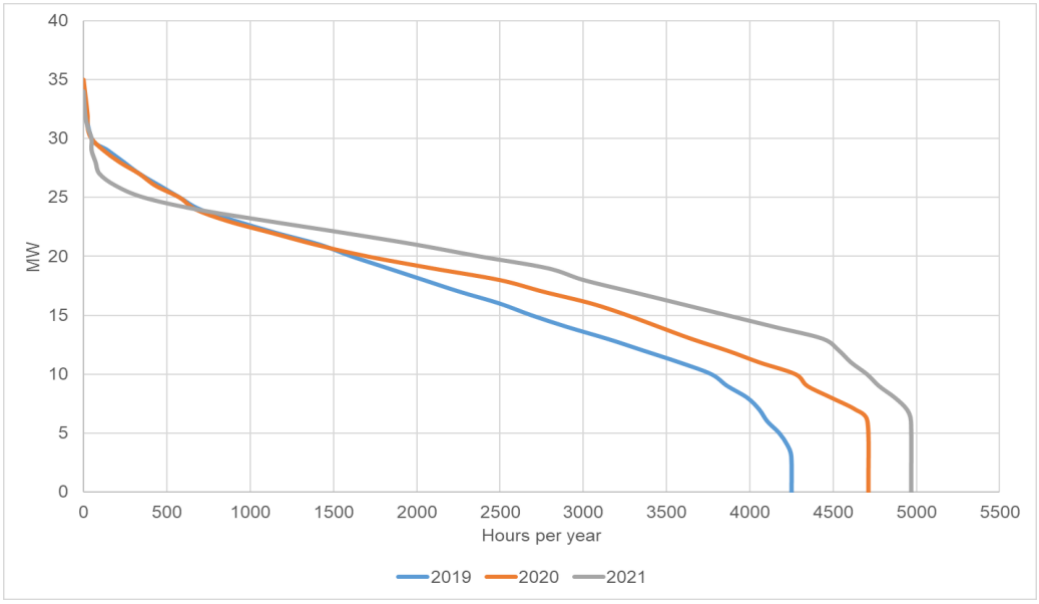

Figure 4.8: Load curves 2019, 2020 and 2021*(source: Suboticka Toplana reports)*

Based on load curves analyses **geothermal heat plant installed capacity 10 MW_{th} and 4000 hours of full load hours are taken for further study.**

The important characteristic of DH system is supply and return temperatures that will influence on geothermal heat plant design. The maximum temperature mode for

Subotica DH is 130/70°C. However, these values are never achievable even in extremely cold days. As an example, during the coldest days in the last 5 years, January 6th-12th of 2017, when the outside temperature dropped below minus 20 Celsius degrees the temperature mode was 95/65°C.

The figure 4.9 shows the available data of supply and return temperatures during the heating season 2009/10. Obviously, "Subotica Toplana" has successfully achieving relatively low supply and return temperatures. Such measure reduces the distribution losses and increases the boiler efficiency.

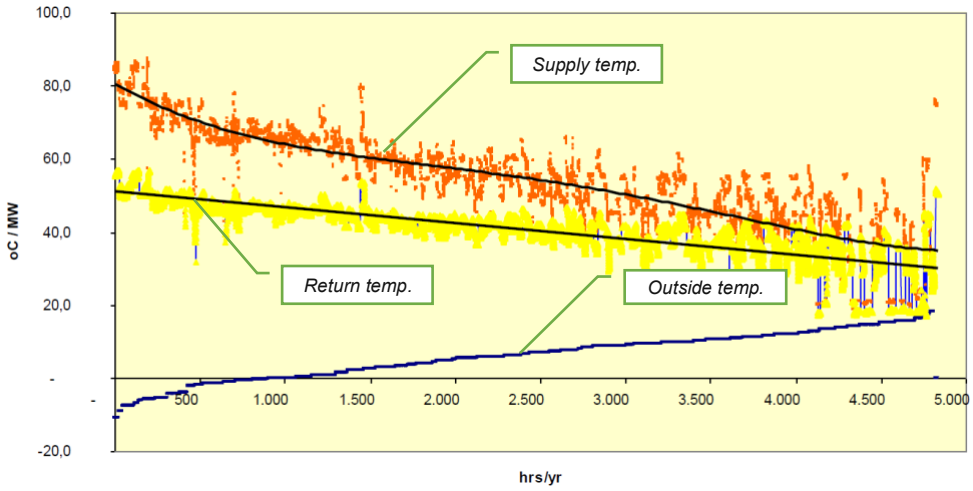

Figure 4.9: Supply, return, and outside temperatures in 2009/2010 *(source: Suboticka Toplana reports)*

As we can see the average supply temperature is around 60^0C than return temperature is around 40^0C. So, **the temperature mode for geothermal heat plant $85/55^0$C is assumed for further study.**

Apart the connection to exist DH there is another option of geothermal heat utilization which will not directly influence on exist business and market for PUC "Suboticka Toplana".

As it was mentioned above, only 27% of households are connected to DH and more than 70% use natural gas and other sources for heating. So, they should produce and consume approximately twice more heat than "Suboticka Toplana" produce i.e. ~100-150GWh$_{th}$ annually (figure 4.7, residential curve).

In addition, according to "General plan of Subotica-Palic area development until 2030", building more than 250,000 square meters of new apartments are projected that will require roughly 25 MW$_{th}$ of installed heat power. At the same time, the exist district heating network expansion and new consumers connection are planed only in areas adjoin with it.

Nevertheless, heat demand forecasts based on urban planning should be interpreted prudently. Visions regarding new building stock and new connections have already existed in the past, but actual development is obviously different. Additional heat demand does not necessarily mean new demand for district heating as it will be affected by various factors:

- New buildings will not automatically be connected to DH. Eventually, the investors will decide about the heating system that shall be installed.

- The competitiveness of DH will play a decisive role. Particularly decentralized gas heating or geothermal local district heating may become a serious competitor. A critical factor for the competitiveness of DH will be the pricing for natural gas.
- Energy savings. With increasing energy prices the incentives to save energy increase and consumers will invest in energy saving measures.

Forecasting the future heat demand is particularly difficult. However, brief analyses of current and projected conditions of heat market shows that potentially exist room for 10MW$_{th}$ geothermal heat plant, which can help to cover growing heat demand and support a transition to "green" heating.

5. PANNONIAN GEOLOGICAL BASIN GEOTHERMAL POTENTIAL OVERVIEW

5.1 Geology of Pannonian basin

The Pannonian Basin is an intraorogenic extensional region floored by a complex system of Alpine orogenic terranes and oceanic suture zones (figure 5.1).

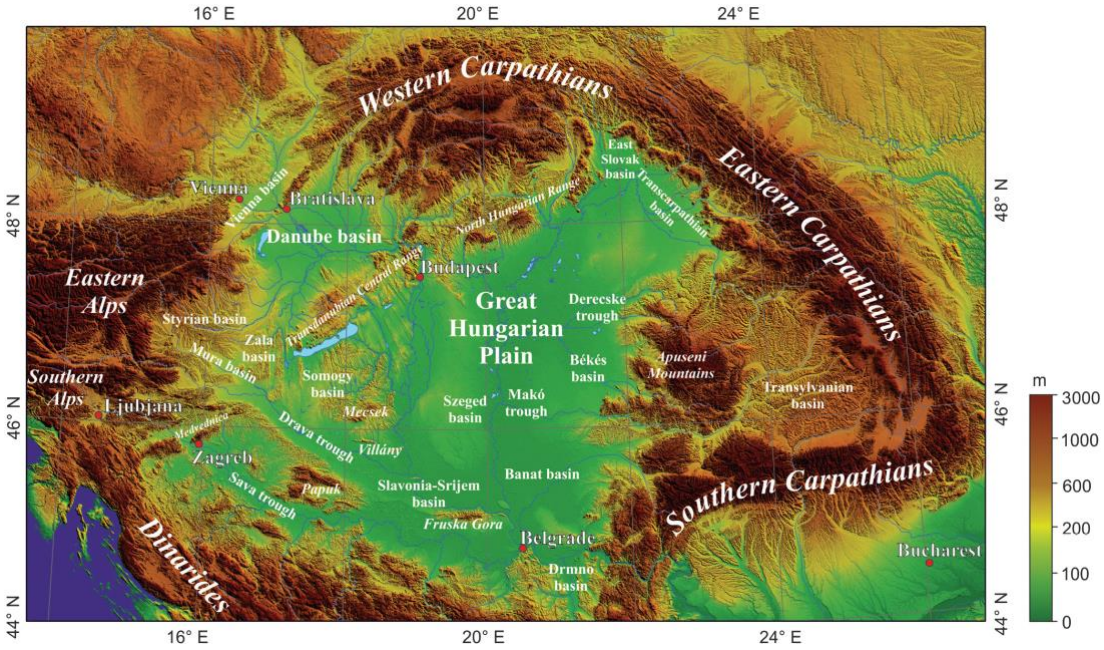

Figure 5.1: Digital terrain model of the Pannonian Basin within the surrounding mountain belts and the location of different subunits (based on Shuttle Radar Topography Mission data by NASA).

When two orogenic terranes were extruded from the East Alpine and Dinaric collision zone towards the Carpathian embayment containing the Magura Ocean, a remnant of the Alpine Tethys, large-scale rifting started in the early Miocene. The Alcapa and Tisza-Dacia megatectonic units, which occupied different palaeogeographical positions and are distinguished by distinct evolutionary histories, are the sources of these terranes. Early and Middle Miocene calc-alkaline magmatism was intense and represents the primary syn-rift phase of basin evolution. The lithosphere thinned out significantly resulting in increased heat flow and temperature gradient values (Dövényi & Horváth 1988; Horváth et al. 2015).

The Pannonian Basin underwent morphological changes during the Miocene era until the present, leading to the formation of a diverse basin structure. This structure is characterized by the presence of deep troughs, ranging from 5 to 8 kilometers in depth, as well as shallower basin areas with depths typically ranging from 1 to 3 kilometers. Additionally, the basin features island mountains, which are exposed sections of the underlying pre-Cenozoic basin floor. The current configuration of the basin system has been shaped by various geological processes, including the formation of syn-rift grabens controlled by normal and transfer faults during the Early and Middle Miocene. This was followed by a period of subsidence in the Late Miocene, as well as regional strike-slip faulting and basin inversion events during the neotectonic phase from the Pliocene through the Quaternary. The basin-fill sedimentary and volcanic rocks can be divided into three tectono-stratigraphic mega

sequences by two regional unconformities (figure 5.2). The lower mega sequence developed during the Early and Middle Miocene, when the initial terrestrial-lacustrine depositional environment was flooded by the Paratethys sea (Horváth et al., 2015). Due to the Paratethys sea level fall and uplift of the surrounding mountains, marine connections were closed and sub areal erosion and/or change of the depositional environments led to the development of the base-Pannonian unconformity. The middle mega sequence developed during the Late Miocene to Early Pliocene, when the large Lake Pannon existed and gradually vanished. Terrestrial deposits from the Late Pliocene and Quaternary, including red clays, loess-paleosol sequences, and alluvial plain deposits, make up the upper mega sequence, which lies above the top-Pannonian regional unconformity. The top-Pannonian unconformity is a manifestation of the neotectonics phase of evolution and is connected to a significant erosional hiatus. The tectonostratigraphic charts in figure 5.2 depict the various lithostratigraphic units and tectonic activity phases in subbasins. (Horváth et al., 2015).

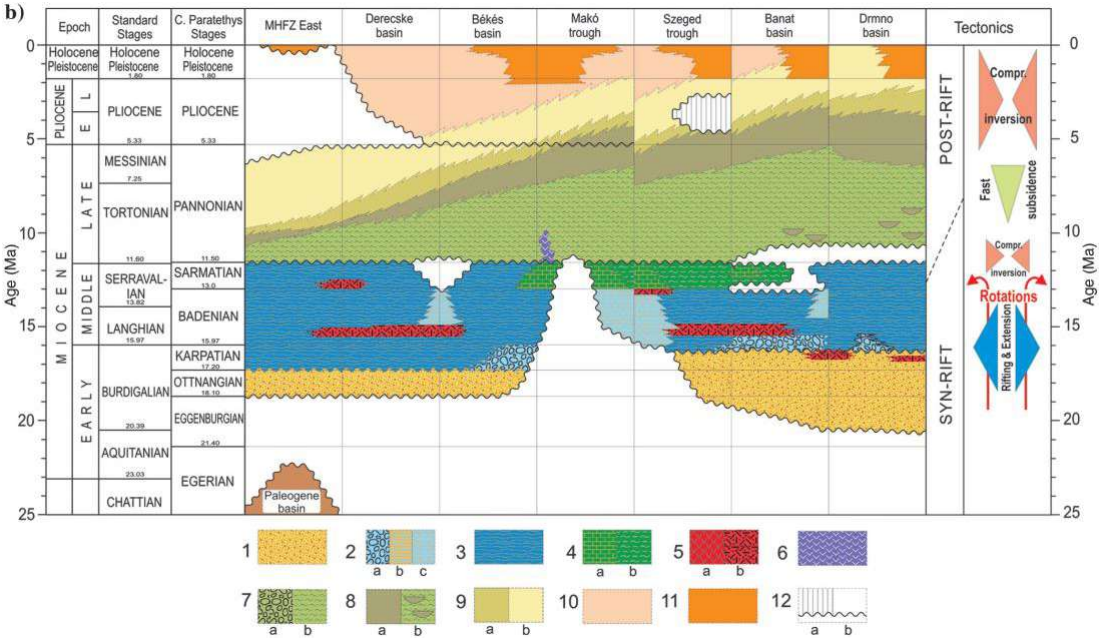

Legend: 1 = basal conglomerate, fluvial-lacustrine clastics; 2 = marine basin margin: (a) gravel, near shore mud, and limestone with (b) lignite and (c) biogenic limestone; 3 = open-marine clay and marl; 4 = brackish water (a) biogenic limestone and (b) offshore marl; 5 = volcanites: (a) andesites, (b) rhyolitic ignimbrites and tuffs; 6 = volcanites: alkali basalts; 7 = lacustrine (a) shoreline conglomerate, and (b) open-water marl; 8 = turbidites from the (a) shelf slope, and (b) local sources; 9 = shelf slope (a), and (b) shelf margin to plain sequence; 10 = alluvial plain deposits; 11 = red clays and loesses with paleosols, windblown sand and silt, river gravel and sand; 12 = unconformity with (a) stratigraphic gap and (b) correlative conformity.

Figure 5.2: Tectonostratigraphic charts of the main syn- and postrift formations in subbasins (Horváth et al. 2015 – modifikovano)

5.2 Geothermal potential of Pannonian basin

High geothermal potential is well known for the Pannonian basin. It is distinguished by a positive geothermal anomaly, with a geothermal gradient of approximately 45°C/km and heat flow densities ranging from 50 to 130 mW/m^2, with a mean value of 90-100 mW/m^2 (Rman et al. 2021). In the Pannonian basin, measurements of heat flow were made in extensive boreholes. The vertical temperature gradient was measured with mercury maximum thermometers or thermistor probes. Since the temperature measurements were taken at great depths (greater than 500m, mostly in the depth range of 1000-2000m), where paleoclimatic and topographic influences are

minimal, they were not taken into account. In a laboratory setting, thermal conductivities of rocks were assessed on core samples (Lenkey et al. 2002). In many boreholes where the lithology of the borehole was known and reliable temperature data were available, heat flow was calculated using the thermal conductivity-depth trends and the thermal conductivities of other rocks derived also from laboratory measurements (figure 5.3) (Lenkey et al. 2002). Groundwater flow, erosion, and sedimentation frequently obstruct the observed heat flow. Sediment thickness in the Pannonian basin ranges from 2-3 km on average for Neogene and Quaternary sediments to 7-8 km in deep troughs. Following the methodology of Lucazeau and Le Douaran (1985), which takes into account the variation in the sedimentation rate and the change in the thermal properties of sediments due to compaction, the thermal effect of sedimentation was calculated using a one-dimensional numerical model. The heat flow that accounts for sedimentation is 10–30% higher than the heat flow that is actually occurring. The peripheral and some internal parts of the basin's late-stage (0–5 Ma) erosion have negligible (5 mW/m^2) effects on the heat flow (Lenkey et al. 2002).

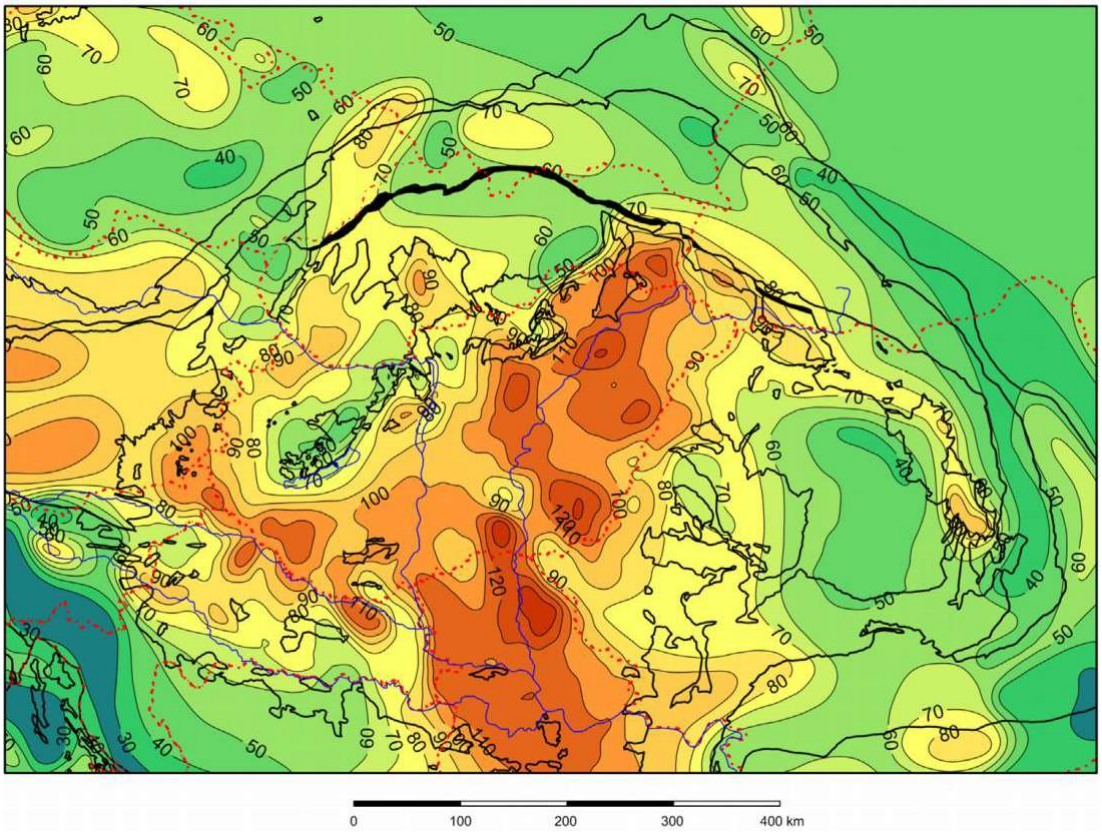

Figure 5.3: Heat flow map of the Pannonian basin and surrounding regions (heat flow values in mW/m^2), corrected for (where appropriate) the cooling effect of fast sedimentation (Lenkey et al. 2002).

The structure and development of the earth's lithosphere are closely related to temperature and heat flow data. This is particularly true for some regions that experience regional subsidence (such as oceanic ridges, passive continental margins, and extensional basins), as these regions' subsidence is largely governed by the structure of the lithosphere's temperature. Temperature conditions are also important in exploration for natural resources, particularly for geothermal prospecting (Dövényi & Horváth 1988). Pannonian crust and lithosphere are much thinner and hotter than an average continental crust, and basin-forming processes that are

responsible for such geological conditions are probably lithospheric stretching and mantle diapirism (Meissner & Stegena 1988).

Both processes, stretching and diapirism, must be intimately connected with each other. Without diapiric movements the high heat flow values in the Pannonian basin cannot be explained. For the modified stretching hypothesis, a very ductile lower crust, heated up by mantle diapirism, is a welcome contribution. The Tertiary volcanism is an additional indication of an extensive heating of the lithosphere and cannot be understood without diapiric processes. Even the reduced crustal thickness can be explained by a diapiric heating and melting of the lower crust, thereby forming granitic melts which enter the upper crust and mafic to ultramafic residues which now have become part of the upper mantle (Meissner & Stegena 1988).

Probably because of its high subsidence rate Pannonian basin is very rich in groundwater, which are “trapped” in different porous rocks.

The first type of geothermal reservoir are deposits of the Upper Miocene to Pliocene siliciclastic sediments which have the several thousand meters thick. These sediments occur at depths to about 4 km in the deepest parts of the basin, where the temperature reaches up to 200°C (Rman et al. 2019)**.**

The second type of geothermal reservoirs is the karstified Paleozoic–Mesozoic carbonates and fractured zones of the crystalline rocks in the basement of the sedimentary basin. They are characterized by the reservoir temperature about 160°C and higher (Rman et al. 2019).

6. GEOTHERMAL RESOURCES ASSESMENT OF CITY OF SUBOTICA AREA

The study of geothermal resources of Subotica area was based on available data of water, oil and gas wells drilled by NIS a.d. in this region in last decades. These data contain temperatures, well test information, geological and petrophysical data incl. results of interpretation and analysis of water. Data was kindly provided by NIS a.d. Wells data is presented in appendixes 2, 3 and 4. Also, hydrothermal well's data from open sources was used.

It is important to mentioned, that despite of large number of wells with temperature measurements (98 wells), only nine wells have detailed geological and petrophysical data.

6.1 Temperature analysis

The Subotica area is covered with a large number of deep wells (500 m and deeper) where temperature data exist. These temperature data have different quality and can classified into three groups - **temperature measurements during hydrodynamic testing of the well (HD), bottom hole temperature measurements (BHT) and temperature data obtained by temperature logging (Tlog).** A total number of temperature measurements is 761 come from 98 wells. The unique database was formed for this study (appendix 2). Number and distribution of measured temperature values by type is shown in figure 6.1.

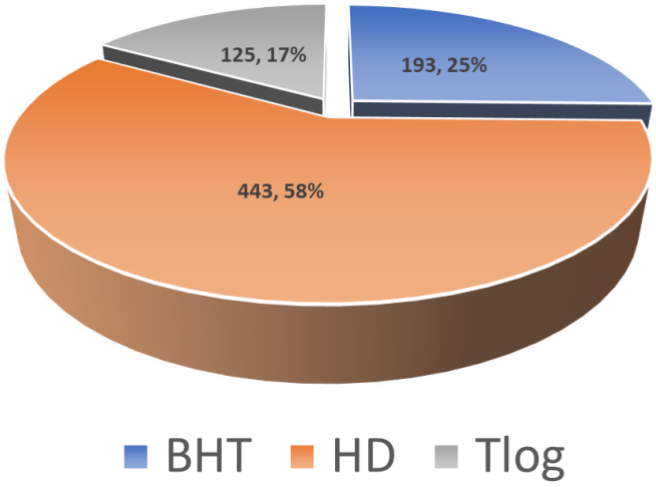

Figure 6.1: Number and distribution of measured temperature values by type

Temperature measurements during hydrodynamic testing (HD) of wells were made mainly in the area of discovered fields and hydrocarbon deposits in different conditions - static, dynamic, before production or during production, during various overhaul operations and ect. Since temperature measurements in the equilibrium condition are needed for the temperature evaluation in the well, the most realistic temperature values are obtained by measuring the temperature in static conditions before production or after closing the well for a long time. HD temperature data was got from 45 wells where 443 measurements were made. Majority of these

measurements were made from the surface to the top of the hydrocarbon production interval, normally on every 100-200 m.

Bottomhole temperature measurements (BT) are available for majority of wells. The database contains 193 bottomhole temperature measurements from 98 wells. The fact that they were also obtained in areas outside the domain of discovered hydrocarbon fields represents their greatest importance, since they allow the temperature to be observed over a wider area. Also, having the temperature measurement at the bottom of the well, gives a possibility to better understand the temperatures at greater depths, below the level of the hydrocarbon production intervals. These measurements are obtained by measuring temperatures during logging, during or immediately after completion of drilling.

Bottomhole temperatures are generally lower than true formation temperatures, since the drilling fluid system is usually not in thermal equilibrium with the formation where the temperature measurements are taken. The time to reach thermal equilibrium depends on a few factors, such as wellbore diameter, mud circulation time, mud composition, and the temperature difference between the formation and the fluid. Several examples of temperature changes at the same depth in the well clearly show dependence on the time passed after the cessation of circulation (figure 6.2). Therefore, it is necessary to make corrections to these measurements.

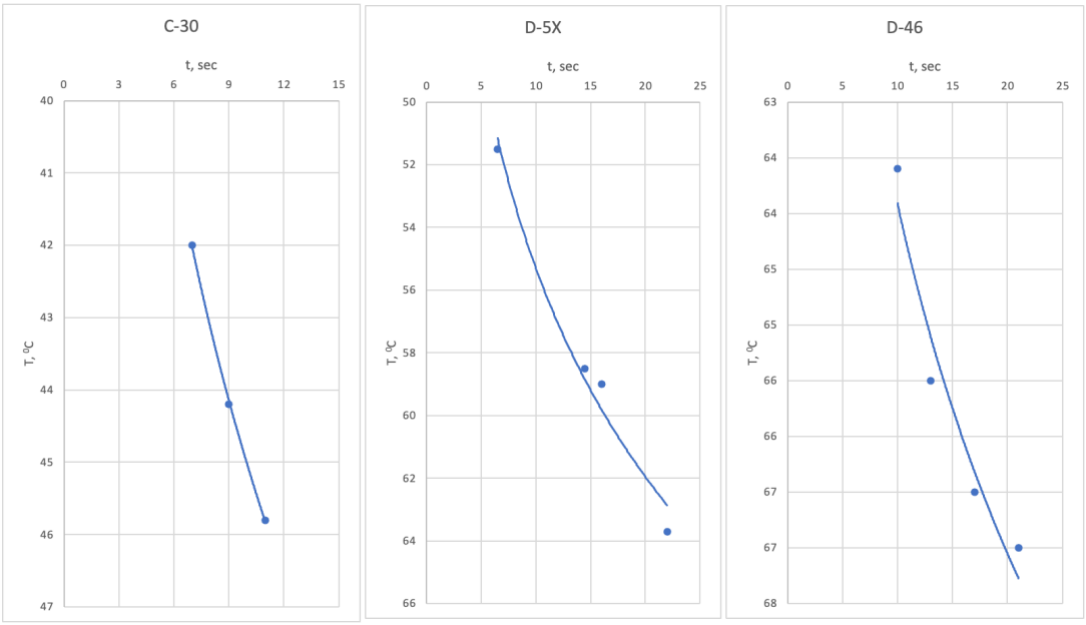

Figure 6.2: Temperature changes in wells C-30, D-5X and D-46 depending on the time passed after the cessation of circulation

There are 85 BTH temperature measurements for 21 wells in database, which also have the data about the time passed after circulation. This is 44% of total number bottomhole temperature measurements. Temperature correction proposed by Waples & Ramly (2001) was applied for these wells. This correction is recommended for measurement depths less than 3500 m, and it uses the following formula:

$$Tc = Ts + f \cdot (Tm - Ts)$$

where:

Tc – corrected temperature, ºC

Ts – surface temperature, ºC

Tm – measured temperature, ºC

f – correction factor, f = (−0.1462*Ln(t_{sc})+1.699) / (0.572*$Z^{0.075}$)

t_{sc} – the time since the cessation of mud circulation, hours

Z – depth, meters

Corrected temperatures were calculated for 85 BTH measurements and presented in the table in appendix 2.

Despite of applied formula performs well under a wide range of geological conditions, it was proposed using data only from the Malay Basin, a young warm basin containing only clastic sediments (Waples et al. 2004). As Subotica area and Pannonian geological basin has another geological condition additional analyses were done. The graph of correlation between temperature and depth for 443 HD measurements and 85 corrected BTH measurements is made and shown in figure 6.3.

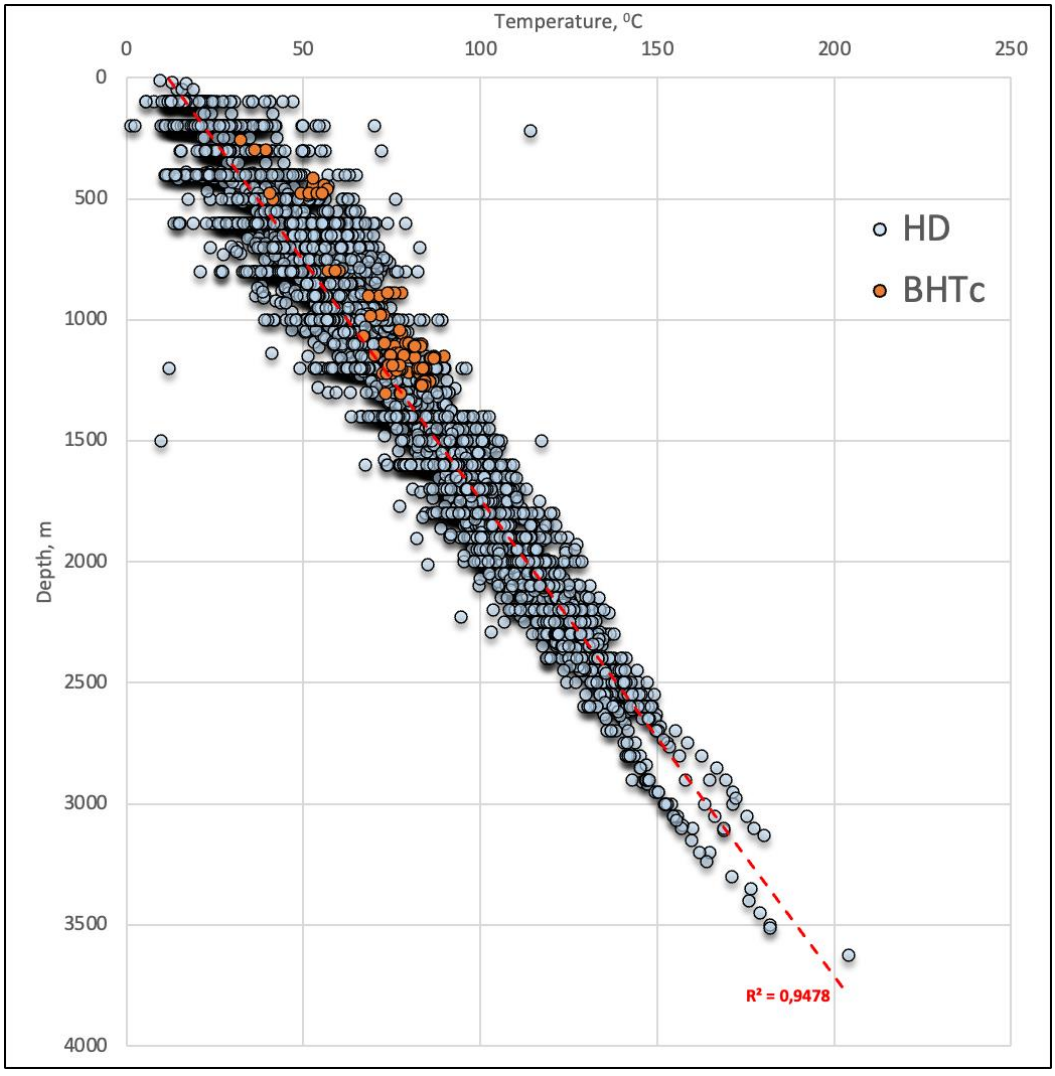

Figure 6.3: Temperatures vs depth plot for all wells in the database.
HD - temperature measurements during hydrodynamic testing, BHTc - corrected bottomhole temperature measurements

The correlation index between the corrected bottomhole temperature measurement and HD temperature measurements is 0.94.

There are only two wells in the database which have HD temperature measurements and BTH temperature measurements including the time passed after circulation at the same time. These two wells we used to validate proposed approach. Correlation graphs, for these two wells, which include HD temperature measurements and corrected BTH temperature measurements was made and shown in figure 6.4. As we can see, the correlation is good.

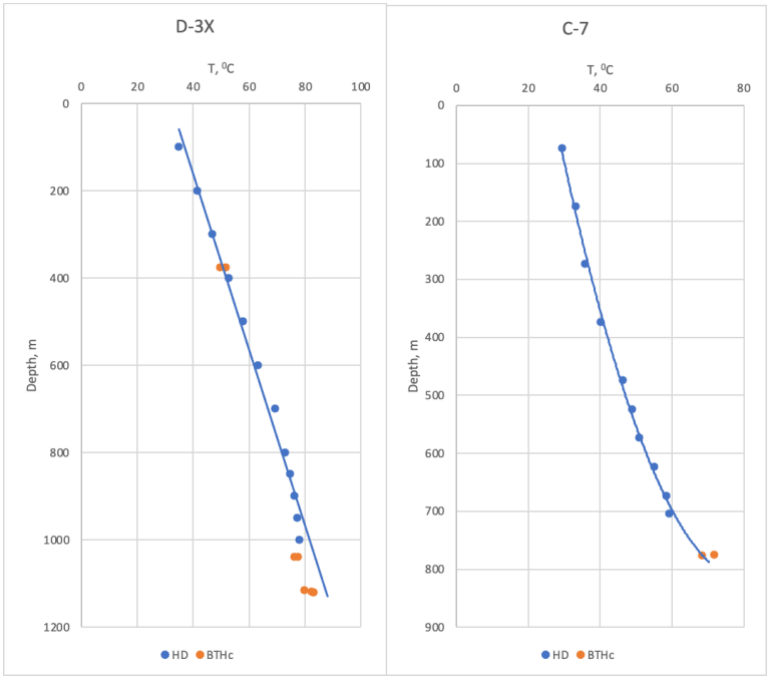

Figure 6.4: Temperature vs depth for D-3X and C-7 wells.

As mentioned above, only 44% of measured bottomhole temperature values can be corrected as they have data about the time passed after circulation. The data of remaining 108 bottomhole temperature measurements, which mostly are from older boreholes and without required data of circulation time, cannot be used directly. So, it is necessary to perform this data that would enable the use it.

Using 85 BTH temperature measurements with available data of the time passed after circulation, a correlation diagram of measured bottomhole temperature values and calculated corrected temperature values was made. It is shown in figure 6.5. The correlation between these two values shows a certain curvature with increasing of depth.

As a result, in order to correct temperature data where we do not have circulation data, the next formula is defined:

$$T_{cor} = -0.0095 \cdot T^2 + 2.084 \cdot T - 13.046$$

where:

T_{cor} - temperature after correction, ^0C

T - measured temperature, ^0C

As we can see in figure 6.5 the correlation coefficient is 0.98, that is acceptable.

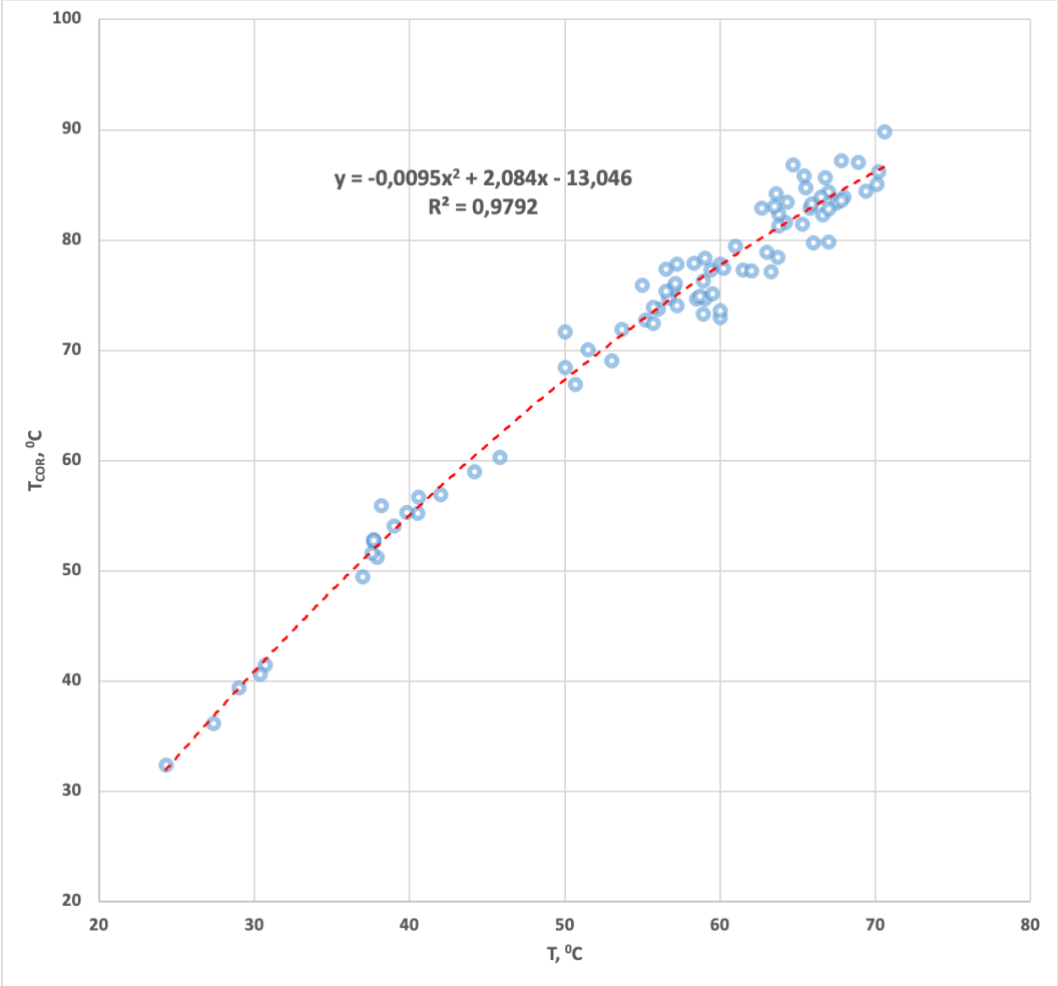

Figure 6.5. Correlation of measured temperature values (T) and corrected temperature values (T_{cor})

To validate this formula the correlation between corrected BTH temperature measurements, which do not have data of circulation, and HD temperature measurements for three wells was made (figure 6.6). As we can see the correlation is good.

Considering the high level of positive correlation, temperature measurements without circulation data were also used for the geothermal assessment. The above-mentioned correction was applied to them.

The data of 125 temperature measurements obtained by **logging measurements** were also used. This type of measurement belongs to the group of production logging measurements and is performed every 10 cm, normally in a few hundred meters of the hydrocarbon reservoir zone. These measurements usually do not contain data of the time elapsed since circulation and it is necessary to correlate them with other types of measurements. The main problems related to this type of temperature measurement are the limited number of boreholes with these measurements, the relatively narrow vertical range of measurements, and often the insufficient amount of data for calculation of correction.

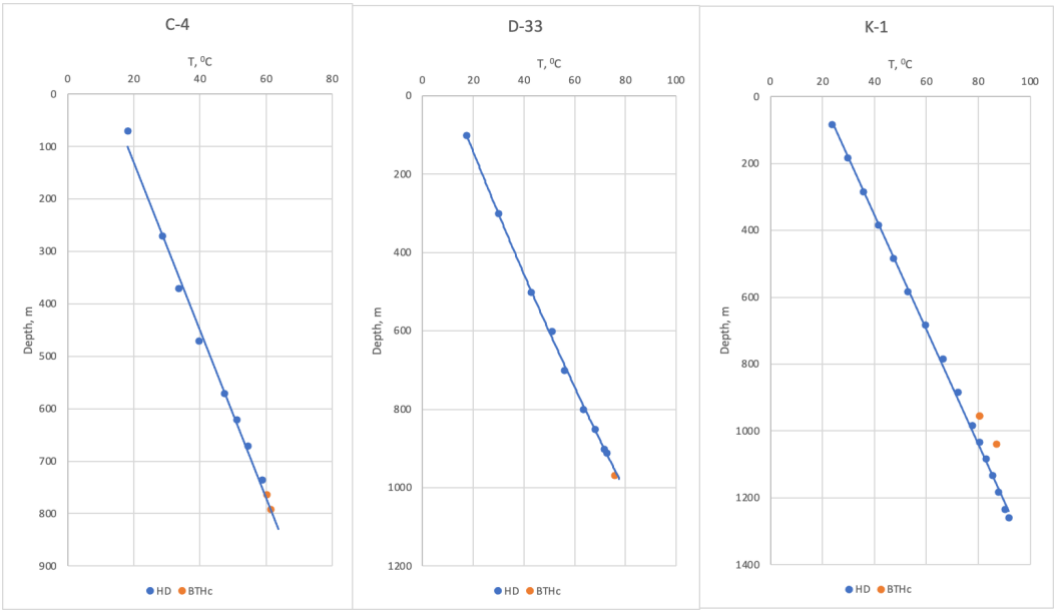

Figure 6.6: Correlation of HD temperature measurements and corrected BTH temperatures measurements for wells C-4, D-33 and K-1

443 calculations of the geothermal gradient, obtained on the basis of temperature measurements during hydrodynamic testing of wells, were made. A mean value of the geothermal gradient of 0.0569 was obtained, i.e. a temperature increases by 5.69^{0}C per each 100 m in this part of the Pannonian Basin (figure 6.7).

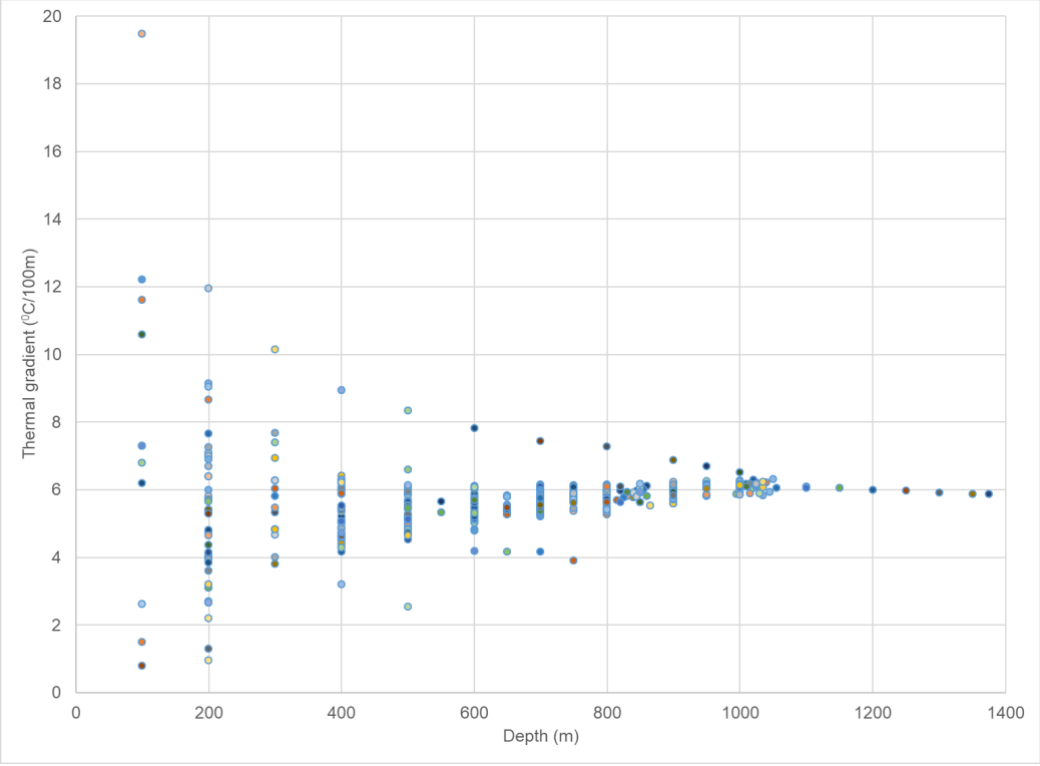

Figure 6.7: Variation of the geothermal gradient with depth in the Subotica area

The diagram clearly shows the disruption of the geothermal gradient in depths less than 500 m, which occurs due to a change in the heat transfer method. At greater

depths, with low porosity and a reduced amount of fluid in the pore space, heat is transferred predominantly by conduction, while at shallower depths, in rock material at a lower level of diagenesis with increased pore space and an increased presence of fluid, the dominant mode of heat transfer takes place. Convection allows for more efficient heat transfer using fluid motion than pure conduction where heat is transferred by the vibrations of a crystal lattice of solids.

Using the available data of temperature measurements and required temperature correction calculations, 9 isothermal maps were created for absolute depth of 500, 750, 1000, 1250, 1500, 1750, 2000, 2500 and 3000 meters (appendix 5). An example of a map for depth 1000 m is presented in figure 6.8. All maps were made using the method of convergent interpolation of point data with a resolution of 50x50 meters in Petrel software from Schlumberger company. Maps were created in cooperation with Scientific and Technological Center of NIS a.d.

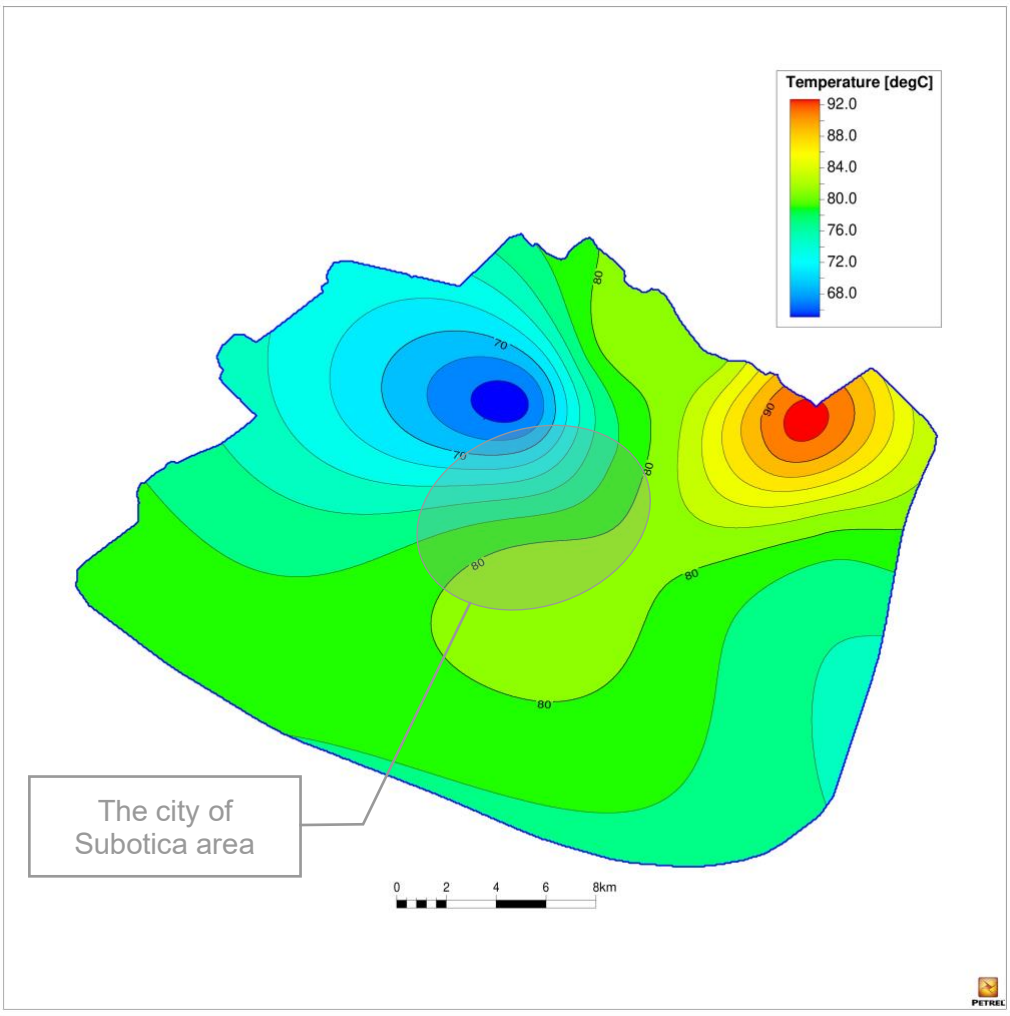

Figure 6.8. Isothermal map at an absolute depth of 1000 m

6.2 Water stability

Water stability represents the degree of potential of water to form deposits of poorly soluble salts or corrosion along production streams and plant elements. Water contains various ions, elements and compounds, and their concentrations and mutual relationships determine whether during the change in temperature and pressure there will be precipitate separation or a negative effect on metal surfaces in the form of corrosion.

The consequences of the formation of deposits and the appearance of corrosion can lead to serious damage to the geothermal system and have a significant economic loss. That is why the prevention of deposits and corrosion is very important, and as part of that, it is necessary to predict the type and extent of potential negative effects of water.

Depending on the temperature of the deposit and the chosen process of using geothermal energy, the deposits can be divided into four groups: (1) carbonates such as calcium and strontium carbonate; (2) silica (SiO_2) and other silicate materials; (3) heavy metal sulfides; (4) different types of chlorides. However, calcium carbonate and silica are by far the most common deposits, which is a common problem in the exploitation of most geothermal plants (figure 6.9).

Figure 6.9: Scaled geothermal pipes (left: calcite, right: mixture of SiO_2 and sulfide) (Andritsos et al. 2014)

The amount and location of the precipitate depends on various parameters, such as degree of supersaturation, kinetics, pH value, chemical composition, CO_2 content, temperature and pressure. Deposits can form in the well itself, in the production layer, and in all parts of the geothermal flow (pipelines, pumps, heat exchangers).

Geothermal fluids also contain compounds that in high enough concentrations can be extremely corrosive. These compounds include Cl^-, H_2S/HS^-, SO_4^{2-}, and in addition, the presence of O_2, H^+ and F^- contribute to the corrosion of geothermal installations. The extent of corrosion, in addition to the chemical composition, is also influenced by temperature and fluid flow. Knowing the corrosion phenomena that can occur is a key factor when selecting the process and designing the entire geothermal energy plant.

The potential of water to form deposits and corrosion can be predicted based on its chemical composition and other characteristics. For this purpose, different indexes have been developed that primarily tell us about the probability of calcium carbonate deposits and the aggressiveness of water towards metal surfaces. The most commonly used are Langelier Saturation Index (LSI), Stiff and Davis Stability Index

(S&DSI), Ryznar Stability Index (RI) and Larson-Skold Index. Calculations of LSI and RI indexes were done that to get general understanding about geothermal water stability in Subotica area.

Total 79 samples from 51 wells had a sufficient set of chemical analyzes for the calculation of water stability indices (appendix 3).

The Langelier Saturation Index (LSI) is an index based on the theoretical concept of saturation and is an indicator of the degree of water saturation with calcium carbonate. At the core of the concept is the crucial influence of the pH value on the solubility balance.

The interpretation of the LSI value with regard to the separation of $CaCO_3$ precipitates is given in table 6.1. It is suitable for waters with a TDS (Total Dissolved Solids) value below 10,000 mg/l.

LSI	Interpretation
< 0	The water is unsaturated with respect to calcium carbonate. Unsaturated water tends to remove the existing protective layer of $CaCO_3$ in pipes and equipment.
= 0	Water is neutral. Deposits are neither formed nor decomposed.
> 0	The water is oversaturated with respect to CaCO3, deposits may form.

Table 6.1: Interpretation of LSI values (Tchobanoglous et al. 2003)

LSI values were calculated using the next formula:

$$LSI = pH - pHs$$

where:

pH - the measured water pH

pHs - the pH at saturation in calcite or calcium carbonate and is defined as:

$$pHs = (9.3 + A + B) - (C + D)$$

where:

A = (Log10 (TDS) – 1) / 10, where TDS is the total dissolved solids, mg/l

B = -13.12 x Log10 (t + 273) + 34.55, where *t* is the temperature of the water, °C

C = Log10 (H) – 0.4, where H is the calcium hardness, mg/l Ca^{2+} as $CaCO_3$

D = Log10 (A), where A is the alkalinity, mg/l as $CaCO_3$

Based on the interpretation of the LSI values, 80% of the tested samples are oversaturated in terms of $CaCO_3$ concentration, which can lead to the formation of deposits (figure 6.10).

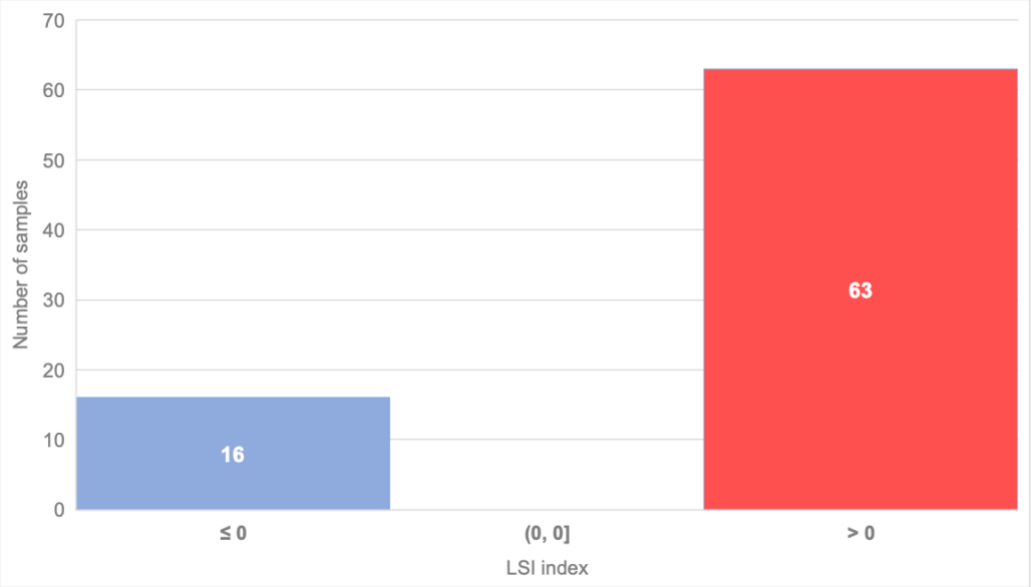

Figure 6.10: Distribution of LSI values in tested samples

The Ryznar Index (RI) is an alternative method of determining the potential for deposit formation. Similar to LSI it is based on the significant effect of pH on equilibrium. The interpretation of the values is given in table 6.2.

RI	Interpretation
< 5.5	Significant formation of deposits
5.5 … 6.2	Formation of deposits
6.2 … 6.8	No problem
6.8 … 8.5	Water is aggressive
> 8.5	Water is extremely aggressive

Table 6.2: Interpretation of Ryznar index (Tchobanoglous et al. 2003)

RI values were calculated using the next formula:

$$RSI = 2(pHs) - pH$$

where:

pH - the measured water pH

pHs - the pH at saturation in calcite or calcium carbonate

By analyzing the Ryznar index in the tested samples, almost 27% have the potential for significant deposit formation, less than 19% of them have no difficulty with deposit formation and aggressiveness, while 11% of the samples of water are extremely aggressive (figure 6.11).

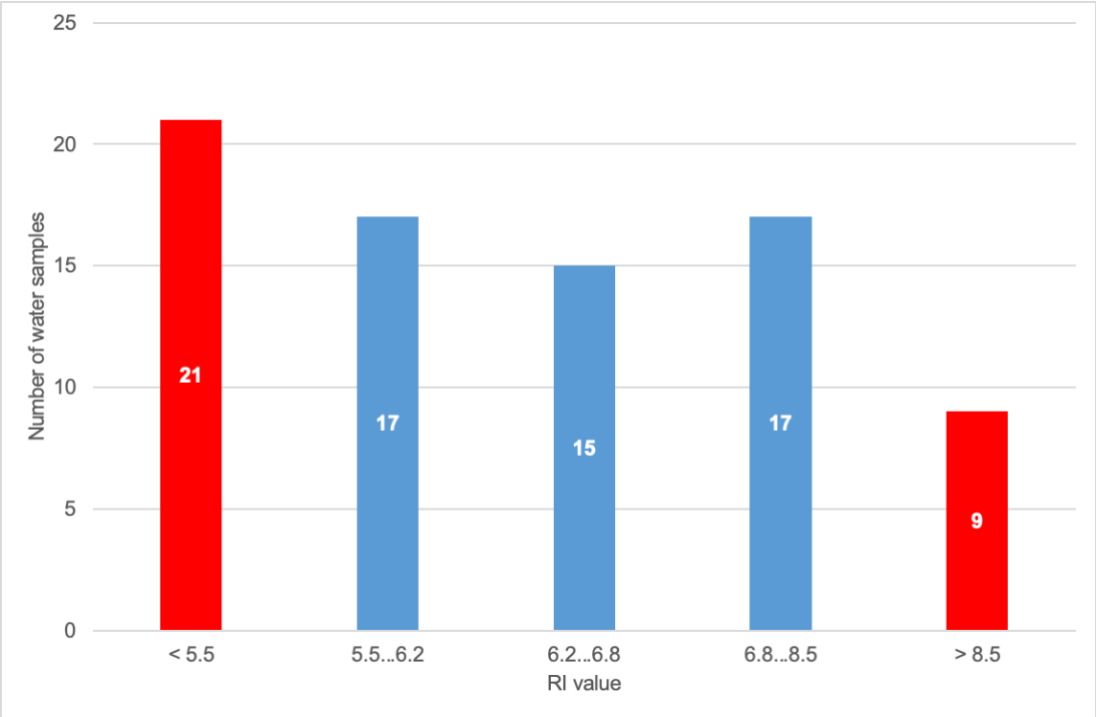

Figure 6.11: Distribution of Ryznar index in the tested water samples

Based on the analysis of tested water samples and using two different stability indexes, a conclusion can be made, that **majority of the samples have the potential to create deposits.** Also, **distinct amount the water samples are potentially corrosive.** Therefore, in order to reduce the formation of deposits and avoid corrosion, especially in heat exchangers and the system of injection wells, various chemical inhibitors and temperature adjustment has to be applied. Physical and chemical fluid monitoring should be implemented as well.

5.3 Energy potential calculation of geothermal recourses

As we are focused on creation of sustainable business case, two factors are important for us. The first, the temperature of reservoir. This topic was carefully analyzed in a part 6.1 and as temperature reaches 155^0C on the depth of 3000 m we have a geothermal potential from this point of view. The second, water availability and amount of water which presents in reservoir and can be pumped up on the surface. It is highly important to define the second factor and connect it with the first one. This would give us a possibility to define the geothermal potential and potential hot spots for further design.

Water saturation of reservoir and its availability is important parameter which can be defined only in wells with specific set of data. There are nine wells (C-22, G-2, G-2H, J-1, J-2, K-2, K-3, L-1, U-1) with a full collection of geological data, including petrophysical interpretation of geophysical logs, in database provided by NIS a.d. (appendix 4). 701 water-saturated layers in nine wells, proven by petrophysical interpretation of geophysical logs, were defined.

Based on these data, distribution of geological layers with water saturation over stratigraphic horizons was made and presented in figure 6.12. As we can see, about

80% of water saturated layers are in the youngest and the shallowest stratigraphic horizons - Pontian, Pliocene and the Quaternary (Pt, Pl and Q). The reasons for this distribution are certainly insufficient diagenetic alteration of these sediments, which enables the existence of a large pore space filled with fluids. Also, exist the possibility, at least partly, of the existence of an open hydrodynamic system which can be replenished by atmospheric precipitation.

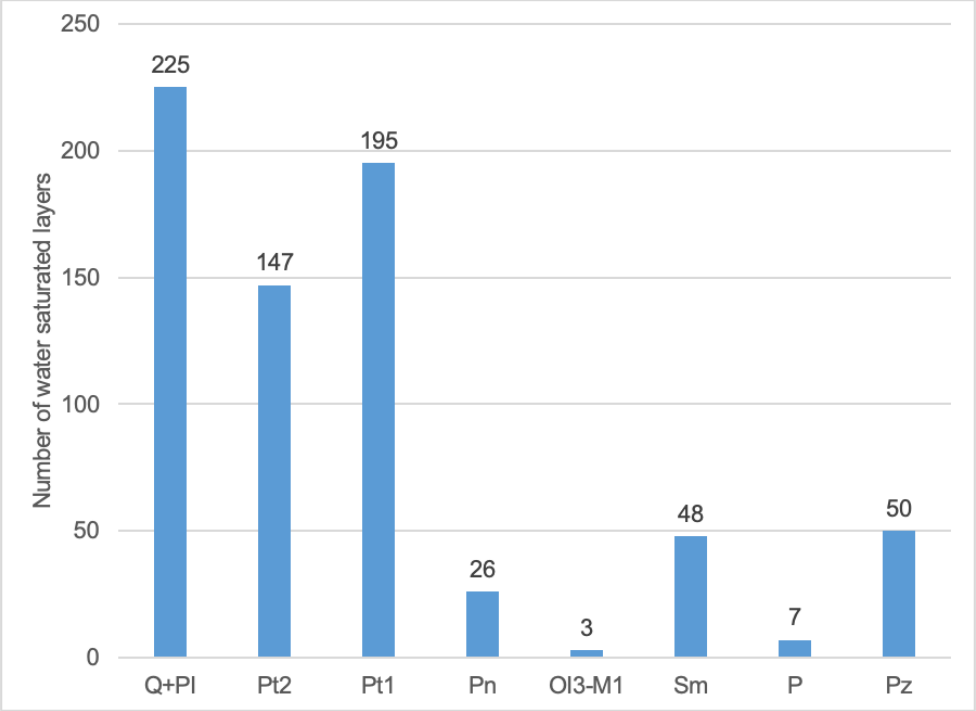

Figure 6.12: Distribution of water saturated intervals based on stratigraphy

The heat energy of the hydrothermal resource is used for a geothermal potential evaluation as integrated parameter, which meets requirements mentioned in a first paragraph of this part. The heat energy of the hydrothermal resource includes temperature in reservoir, volume of the water, which exist in reservoir, and specific heat of water. It can be calculated as:

$$E = (4.19 \times M \times \Delta T)/3{,}6$$

where:

E – heat energy, MWh_{th}

4.19 - specific heat of water (kJ/kg×K)

M – the amount of water that is heated in reservoir, kg

ΔT – temperature difference between the aquifer temperature and the reference temperature of 20°C.

The calculation of amount of water was performed using the volumetric method, with the following parameters taken as a starting point: area and thickness of geological layers saturated with water, effective porosity, and water saturation.

Area was assumed as single value of 2500 m^2 for all layers since this is a cell size in geological resource model in Petrel software. Thickness of geological layers, effective porosity, and water saturation were taken from wells data, which include petrophysical interpretation results of geophysical logs, provided by NIS a.d. (appendix 4). The thus

obtained value of the volume of the collector with water was reduced by the values of effective porosity and water saturation.

$$M = 2500 \times t \times P_t \times S_w \times 1000$$

where:

2500 - area of water horizon, m^2

t – layer thickness, m

P_t – porosity, %

S_w – water saturation, %

1000 – water density, kg/m^3

The heat energy for a cell 50x50 m was calculated for each of 701 water-saturated layers of nine wells proven by petrophysical interpretation of geophysical logs.

An example of the calculation of heat energy value of a geothermal resource in one well is shown in figure 6.13. All calculations results are presented in appendix 4.

Well	Stratigraphy	Top m	Bottom m	Top abs m	Bottom abs m	Thickness, m	Porosity, %	Effective Porosity, %	Gamma ray, GAPI	Density log, g/cm	Rt, Ohmm	A µW/m	Water saturation %	Permeability, mD	Shaliness %	Saturation	T	ΔT	M, t	E MWh	Litologija
G-2	Pt2	750.10	757.80	643.90	651.60	7.70	24.3	22.3			6.5		100.0		4.80	Water	50.41	30.4	4292.8	152.27658	Peščar
G-2	Pt2	760.30	763.50	654.10	657.30	3.20	25.3	19.2			5.3		100.0		12.68	Water	50.96	31.0	1536.0	55.47351	Glinoviti peščar
G-2	Pt2	766.90	768.50	660.70	662.30	1.60	25.4	18.4			5.3		100.0		11.27	Water	51.31	31.3	736.0	26.887086	Glinoviti peščar
G-2	Pt2	774.70	788.00	668.50	681.80	13.30	25.3	22.9			6.3		100.0		3.14	Water	51.73	31.7	7614.3	281.9006	Peščar
G-2	Pt1	788.00	788.10	681.80	681.90	0.10	28.7	18.9			4.5		86.3		19.92	Water	52.45	32.5	40.8	1.5438349	Glinoviti peščar
G-2	Pt1	912.80	917.40	806.60	811.20	4.60	21.5	16.2			5.7		92.1		13.45	Water	63.32	43.3	1715.8	84.725702	Glinoviti peščar
G-2	Pt1	918.00	919.00	811.80	812.80	1.00	25.6	19.7			5.8		82.5		13.36	Water	63.74	43.7	406.3	20.734127	Glinoviti peščar
G-2	Pt1	919.90	920.80	813.70	814.60	0.90	22.6	20.5			6.8		85.7		7.02	Water	63.89	43.9	395.3	20.241811	Glinoviti peščar
G-2	Pt1	924.20	930.80	818.00	824.60	6.60	19.9	16.2			6.8		96.8		7.63	Water	64.24	44.2	2587.5	133.53557	Laporoviti peščar
G-2	Pt1	931.70	932.60	825.50	826.40	0.90	18.0	14.9			6.2		100.0		10.09	Water	64.84	44.8	335.3	17.536481	Laporoviti peščar
G-2	Pt1	939.90	943.20	833.70	837.00	3.30	21.7	16.3			5.3		97.0		16.73	Water	65.49	45.5	1304.4	69.230124	Laporoviti peščar
G-2	Pt1	946.40	948.10	840.20	841.90	1.70	18.8	14.8			5.6		100.0		14.27	Water	66.01	46.0	629.0	33.765139	Laporoviti peščar
G-2	Pt1	963.80	965.50	857.60	859.30	1.70	19.7	16.0			6.5		100.0		8.52	Water	67.21	47.2	680.0	37.453901	Laporac
G-2	Pt1	969.20	970.00	863.00	863.80	0.80	18.4	15.8			6.3		100.0		9.68	Water	67.57	47.6	316.0	17.536441	Laporac
G-2	Pt1	971.70	972.90	865.50	866.70	1.20	18.4	15.7			6.7		100.0		7.30	Water	67.73	47.7	471.0	26.228844	Laporac
G-2	Pt1	973.50	974.50	867.30	868.30	1.00	18.1	15.7			6.4		100.0		8.83	Water	67.85	47.9	392.5	21.91177	Laporac
G-2	Pt1	976.00	977.40	869.80	871.20	1.40	19.3	16.0			6.5		100.0		8.74	Water	68.02	48.0	560.0	31.370453	Laporac
G-2	Pt1	978.60	979.50	872.40	873.30	0.90	16.5	14.3			6.3		100.0		8.21	Water	68.19	48.2	321.8	18.08842	Laporac
G-2	Pt1	979.90	980.80	873.70	874.60	0.90	20.0	16.0			6.3		100.0		9.64	Water	68.27	48.3	360.0	20.274828	Laporac
G-2	Pt1	1040.90	1047.60	934.70	941.40	6.70	14.3	13.3			8.5		100.0		1.69	Water	76.28	56.3	2227.8	146.27927	Peskoviti laporac
G-2	Pt1	1048.90	1058.20	942.70	952.00	9.30	15.3	14.6			8.9		100.0		1.35	Water	76.73	56.7	3394.5	224.68259	Peskoviti laporac
G-2	Pt1	1063.90	1068.40	957.70	962.20	4.50	17.0	16.6			7.2		100.0		0.61	Water	77.58	57.6	1867.5	125.45847	Peskoviti laporac
G-2	Pt1	1069.10	1074.00	962.90	967.80	4.90	17.0	16.6			6.7		100.0		1.63	Water	77.88	57.9	2033.5	137.30803	Peskoviti laporac
G-2	Pt1	1079.80	1086.40	973.60	980.20	6.60	14.5	14.3			7.5		100.0		0.68	Water	78.48	58.5	2359.5	160.38633	Peskoviti laporac
G-2	Pt1	1087.00	1097.60	980.80	991.40	10.60	14.5	13.7			7.7		100.0		2.89	Water	78.89	58.9	3630.5	249.4301	Laporac
G-2	Pt1	1098.30	1105.40	992.10	999.20	7.10	15.0	14.1			7.1		100.0		2.90	Water	79.53	59.5	2502.8	173.81511	Laporac
G-2	Pt1	1110.00	1114.80	1003.80	1008.60	4.80	14.0	11.9			7.3		100.0		8.98	Water	80.19	60.2	1428.0	100.27648	Laporac
G-2	Pt1	1127.00	1133.90	1020.80	1027.70	6.90	13.3	11.6			8.5		100.0		5.42	Water	81.15	61.2	2001.0	142.75795	Laporac
G-2	Pt1	1138.20	1143.80	1032.00	1037.60	5.60	13.2	12.1			7.9		100.0		4.00	Water	81.78	61.8	1694.0	122.1074	Laporac
G-2	Pt1	1146.20	1147.90	1040.00	1041.70	1.70	12.3	9.0			7.9		100.0		12.81	Water	82.24	62.2	382.5	27.773379	Laporac
G-2	Pt1	1173.50	1176.60	1067.30	1070.40	3.10	13.6	9.7			8.0		100.0		14.93	Water	83.78	63.8	751.8	55.938788	Laporac
G-2	Pt1	1185.00	1186.10	1078.80	1079.90	1.10	11.3	8.0			8.2		100.0		14.65	Water	84.43	64.4	220.0	16.537445	Laporac
G-2	Pt1	1189.50	1190.60	1083.30	1084.40	1.10	12.2	8.6			8.6		100.0		14.43	Water	84.69	64.7	236.5	17.847974	Laporac
G-2	Pt1	1193.70	1195.20	1087.50	1089.00	1.50	11.4	9.8			9.3		100.0		7.68	Water	84.92	64.9	367.5	27.836009	Laporac
G-2	Pn	1212.40	1214.40	1106.20	1108.20	2.00	14.8	12.4			7.2		100.0		5.76	Water	85.98	66.0	620.0	47.726414	Laporac
G-2	Pn	1229.80	1230.80	1123.60	1124.60	1.00	11.0	7.9			7.6		100.0		9.41	Water	86.97	67.0	197.5	15.429916	Laporac
G-2	Pn	1232.40	1233.50	1126.20	1127.30	1.10	10.1	7.6			7.2		100.0		11.49	Water	87.11	67.1	209.0	16.364221	Laporac
G-2	Pz	1268.40	1278.00	1162.20	1171.80	9.60	4.4	3.8			18.4		100.0		3.17	Water	89.15	69.1	912.0	78.573799	Green schist (tectonized)
G-2	Pz	1278.80	1279.80	1172.60	1173.60	1.00	4.3	3.8			22.4		100.0		1.65	Water	89.74	69.7	95.0	7.7291267	Green schist (tectonized)
G-2	Pz	1280.60	1285.60	1174.40	1179.40	5.00	6.0	4.9			17.6		100.0		3.49	Water	89.84	69.8	612.5	49.905272	Green schist (tectonized)
G-2	Pz	1286.50	1288.90	1180.30	1182.70	2.40	9.7	7.5			13.6		100.0		5.69	Water	90.17	70.2	450.0	36.840277	Green schist (tectonized)
G-2	Pz	1290.80	1294.20	1184.60	1188.00	3.40	5.7	5.0			20.1		100.0		2.42	Water	90.42	70.4	425.0	34.914175	Green schist (tectonized)
G-2	Pz	1300.90	1307.00	1194.70	1200.80	6.10	7.2	6.3			16.1		100.0		4.22	Water	90.99	71.0	960.8	79.566826	Green schist (tectonized)
G-2	Pz	1309.50	1310.70	1203.30	1204.50	1.20	10.2	7.7			14.0		100.0		5.26	Water	91.47	71.5	231.0	19.2619	Green schist (tectonized)

Figure 6.13: Heat energy values of a geothermal resource for G-2 well

Based on heat energy calculations in nine wells, a 3D model, which contains energy values of geothermal resources in research area expressed in kWh_{th}, was created. The total area included in this study is 574 km^2. The model extends vertically from 200 meters above sea level to an absolute depth of 3000 meters. The algorithm of convergent interpolation was used to spread calculated heat energy in nine wells to whole 3D cube. The single heat energy values of the geothermal resource within the 3D model range from 0 to 1160 MWh_{th}.

The model was made in cooperation with Scientific and technological center of NIS Company in Petrel software.

Based on 3D model, nine geothermal isoenergetic maps of 500-, 750-, 1000-, 1250-, 1500-, 1750-, 2000-, 2500- and 3000-meters depth were created (appendix 6). Examples of geothermal resource energy maps at an absolute depth of 1000 and 1500 m are shown in figures 6.14 and 6.15.

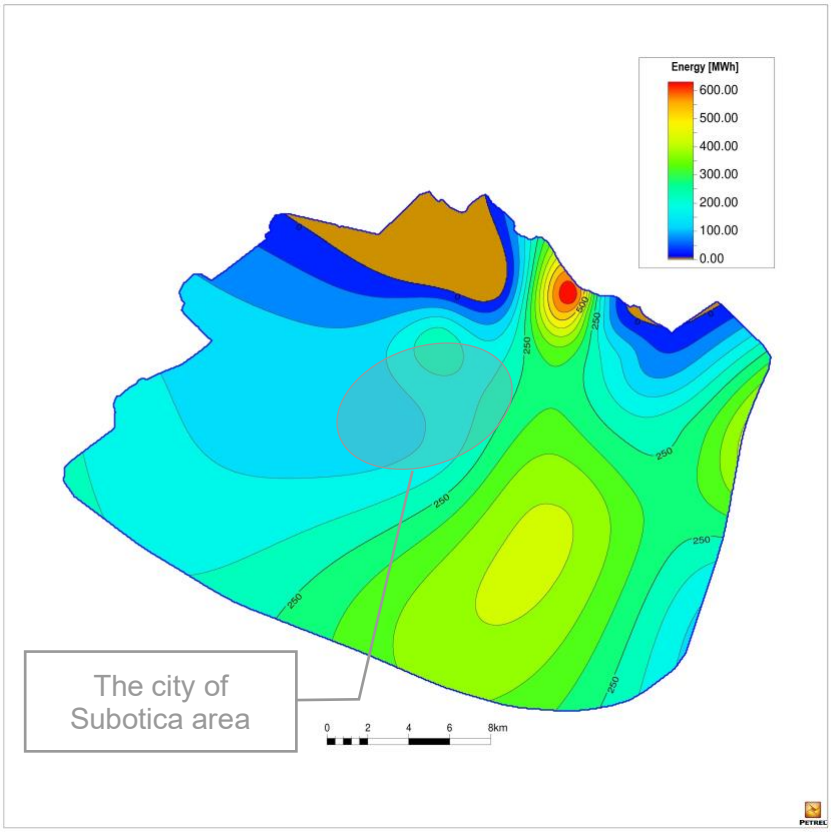

Figure 6.14: Isoenergetic map of geothermal resource at an absolute depth of 1000m

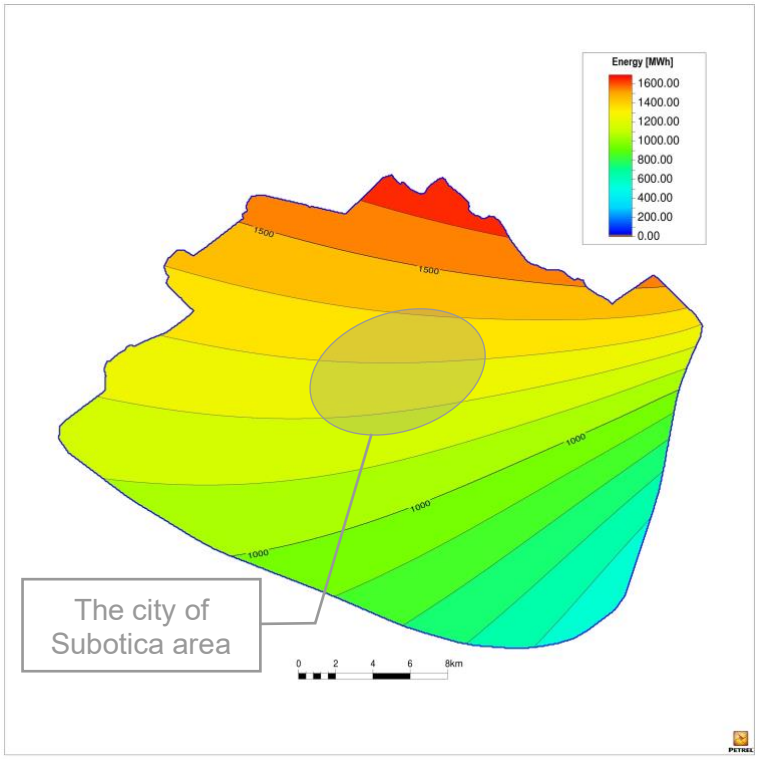

Figure 6.15: Isoenergetic map of geothermal resource at an absolute depth of 1500m

According to input parameters, the calculated heat energy can be interpreted as the ratio between the amount of water in the reservoir and the temperature. This ratio changes with depth. Trying to simplify we can say, there is larger amount of water (see figure 6.12) with lower temperature in shallower intervals, whereas there is smaller amount of water with higher temperatures in deeper parts. However, the real picture is much complex as there are a lot of influenced factors.

The total heat energy belongs to researched area of 574 km^2 was calculated based on 3D model. The distribution of this heat energy in depth and reservoir temperature are shown in figure 6.16. As we can see 46% of total heat energy is concentrated in layers at the depth of 1500 m, where Paleozoic formations present.

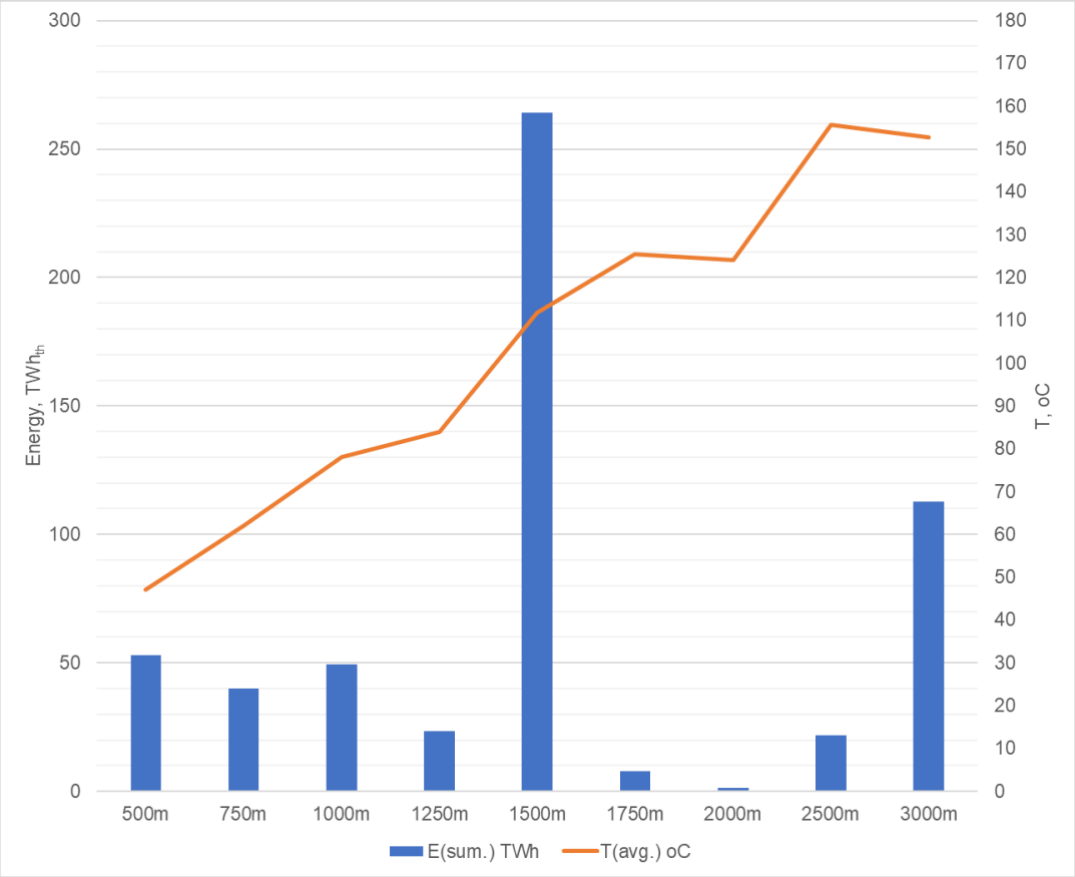

Figure 6.16: Distribution of heat energy and temperature by depth

The total amount of geothermal heat energy of research area is 573 TWh_{th}. This number represents the theoretical amount of heat of the geothermal resource obtained using the available data for the study and the practical use of this energy is possible only in a small part of it.

6.4 Conclusion

According to geological assessment of the city of Subotica area, **the 1500 m depth layers are nominated as priority for further DH geothermal system study and design.** The temperature of geothermal water on this depth is ~115^{0}C that is corresponds to DH temperature regime requirements. Furthermore, geothermal potential on this depth looks promising (figure 6.16).

Also important characteristics of geothermal reservoir which must be define on this stage are permeability and water saturated layers thickness or aquifer thickness.

Permeability is the capacity of a rock layer to transmit water or other fluids, such as oil. The standard unit for permeability is the Darcy (D) or, more commonly, the millidarcy (mD).

The exact value of permeability can be defined in laboratory doing rock samples specific experiment or calculated based on a fluid production data. In our case it is not enough data for 1500 m depth of Subotica area to precisely define the permeability value. That brings significant geological uncertainty of the project.

As Paleozoic geological formation is spreaded in whole Pannonia basin where NIS a.d. has more the 850 oil and gas production wells NIS Geological Department was asked for assist to solve this issue.

86 wells, which produce oil from similar geological formations as in Subotica area, were identifid in NIS database. Using this data permeability calculation for all these wells were done. Calculated permeability values were also validated using laboratory analyses of rock samples, which exist in a very limited amount. All this data is confidential and cannot be fully presented in this paper.

Base on this calculations and analytics the following permeability values are defined:

- minimum value of permeability is 0.08 mD
- mean value of permeability is 46 mD
- maximum value of permeability is 964 mD

Wide range of permeability is consequence of fractured reservoir where there is no equal distribution of characteristic, but more chaotic and probability distribution take place.

Using created 3D geological model and NIS a.d. database of 86 wells aquifer thickness was defined. It was assumed, that water production can be organized from few isolated water saturated layers at the same time. So, the sum of thicknesses of this layers was defined. The following values were taken for further calculations:

- minimum aquifer thickness is 15 m
- mean aquifer thickness is 50 m
- maximum aquifer thickness is 220 m

7. TECHNOLOGICAL AND ENERGETIC DESIGN OF THE GEOTHERMAL HEAT PLANT

7.1. Method of approach

The goal of technical evaluation is to create feasible technological scheme of 10 MW heat power production and distribution system. All results and conclusions are based on technical calculation, reliable and proven data.

Technological and energetic design of the geothermal heat power plant was done in a few steps with a goal to substantiate and define important technical data on each of them.

- **Geothermal wells design.** Here we must define production and injection wells construction and calculate required distance between them. Also, it is important to choose electrical submersible pump (ESP) as it is critical equipment which consume a lot of electricity.
- **Process flow diagram** development with a goal to give general overview how heat power production will be organized and working on. Also, critical elements and equipment should be defined for further special attention on them.
- **Heat exchanger design.** Here we must calculate water and heat flows, temperature regime and choose the number, power, and type of heat exchanger.
- **Geothermal heat production system modeling** and calculations (including subsurface and surface parts) by specifying the key reservoir parameters, well casing scheme, pump details, and heat exchanger temperature regime. As an output of the modeling, feasibility of proposed scheme should be proved, and main technical characteristics of geothermal heat production system will be defined.

The effective exploration and utilization of geothermal resources necessitates a comprehensive and cohesive assessment of all factors influencing the final value of a venture. Project evaluation must take into account the anticipated reservoir performance in the context of energy generation strategies and well performance. When confronted with strategic choices that entail substantial capital investment, it is imperative to conduct a comprehensive evaluation of the level of uncertainty associated with all variables that can substantially impact the ultimate economic result of a particular undertaking (Jorge A. Acuna et al. 2002). As we have significant geological uncertainties, probabilistic approach was chosen for further calculations as common tool for such cases.

As it was mentioned in a part 6.4, we have a wide range of basic reservoir characteristics in Paleozoic formations, which are crucial for further study. In our case, the key uncertainties relate to the permeability of the reservoir and thickness of aquifers (water-saturated layers). As we have a big number of temperature measurements in this area (more than 760 measurements, see part 6.1), we can surely assume that the temperature of reservoir is 110^0C.

Having wide range of permeability and thickness of aquifers in a different wells in Paleozoic formation (see part 6.4), alternative numerical simulation models are created (most likely, pessimistic and optimistic), in order to represent the uncertainty range of geothermal power production and water flow.

Entire model of doublet geothermal system was done using special software tool DoubletCalc 1.4. This tool supports probabilistic approach.

The three values that define as "most likely" (P50), "pessimistic" (P10), and "optimistic" (P90) are used to describe the uncertainty about the possible range for each relevant parameter in the models that were developed and used for the project evaluation. By definition, there is a 50% chance that the actual value of an uncertain parameter will be either equal to or less than the P50 value. The likelihood that the actual value will be equal to or lower than the P10 value is only 10%. With a 90% probability that the actual value does not exceed that limit (i.e., there is only a 10% chance that the real value is higher than that), the P90 value represents the other extreme. According to this methodology, the expected reservoir performance (reservoir permeability and aquifer thickness) were defined in terms of "most likely", "pessimistic", and "optimistic" (Jorge A. Acuna et al. 2002).

Different technological scenarios were applied with a goal to achieve required fluid flow and geothermal energy production. Besides conventional vertical drilling, in addition two technologies are applied, as horizontal drilling and hydraulic fracturing. These technologies are widely used to stimulate production from low-permeability and tiny layer reservoir. As it was mentioned in a part 3.4 this approach allow to improve geothermal system.

Four technological scenarios were analyzed: (1) vertical well, (2) vertical well with hydraulic fracturing, (3) horizontal well, (4) horizontal well with hydraulic fracturing. Investment cost increase from 1 to 4 scenario.

As a result of the modeling, for each technological scenario three different versions of the model are available that would result in the required P50, P10 and P90 performance forecast. **It was decided, to move forward with economical evaluation of the project with a scenario which will give us not less than 10 MW of heat power with P50 ("most likely") probability.**

7.2 Geothermal wells design

Geothermal water normally cannot be used directly in a district heating system due to dissolved chemicals components and necessity to have a flexible system with sustainable work of subsurface part. According to a geothermal energy best practices, a doublet scheme was chosen. A doublet system is made up of two wells: one production well and one injection well (figure 7.1). The conceptual scheme of usage of the geothermal energy looks like, the hot geothermal water must be pumped out the production well, utilized at the surface and then returned into the reservoir through the injection well. Geothermal fluid reinjection keeps water mass balance in the reservoir and prevent pressure drop in it. In addition, circulated cooled geothermal water heat back up from hot deep rocks before being pumped out back to the surface through the production well. Such scheme provides a sustainable and reliable geothermal system.

However, because of cooled water injection, the geological reservoir inevitably cools over time. As a result, the thermal power reduce. Normally, there are 2 phases of doublet system operation. The first phase, outlet geothermal water the temperature is close to the initial temperature of the reservoir. The second phase begins when the outlet geothermal water temperature becomes lower than the initial reservoir temperature and ends when it becomes close to the inlet geothermal water temperature. After that, further operation of the system becomes impossible.

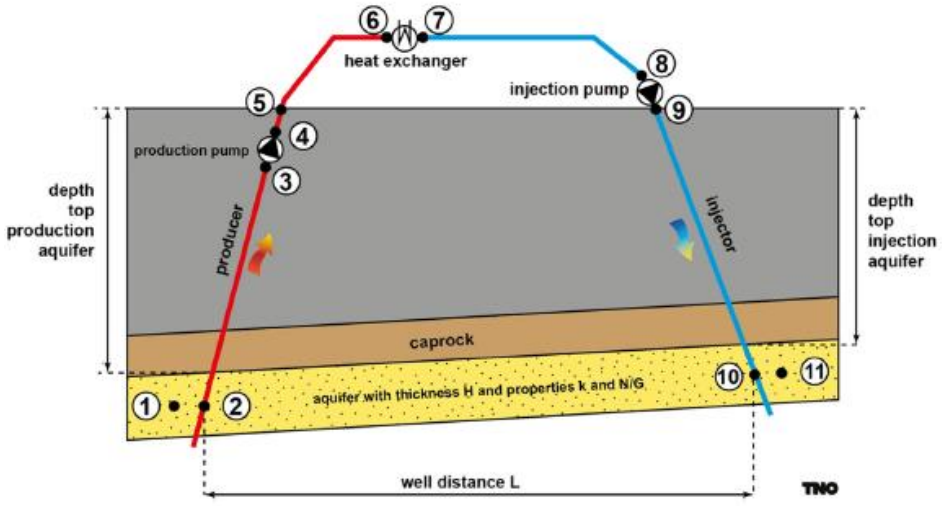

Figure 7.1: Schematic of a doublet system (Mijnlieff 2020).

1,11 – the aquifer and geothermal source; 2 – mid-aquifer in the production well; 3- inlet production pump; 4- outlet production pump; 5-top production well; 6- inlet heat exchanger; 7- outlet heat exchanger; 8 - inlet injection pump; 9- outlet injection pump; 10 - mid-aquifer in the injection well

The operating time can be calculated using the formula:

$$t = \frac{\pi \times C_0 \times \rho_H \times h \times R^2}{3 \times C_B \times m}$$

where,

t – time, s;

C_0 - specific heat capacity of rocks, kJ/kg^{0}C;

ρ_H – geothermal fluid density, kg/m^3;

h – thickness of geological layer, m;

R - distance between production and injection wells, m;

C_B - specific heat capacity of geothermal water, kJ/kg^{0}C;

m – mass flow, kg/s.

The precise design of a geothermal doublet system depends on the geological environment. On the current phase, production and injection is decided to organize in the same geological layer (Paleozoic formation).

As we have a range of water saturated layer thickness in Paleozoic (see part 6.4), calculations of operating time for median thickness and different distance between production and injection wells were done. Results are presented in figure 7.2.

Distance of 2000 m between production and injection wells with operation time 29 years is chosen for further study.

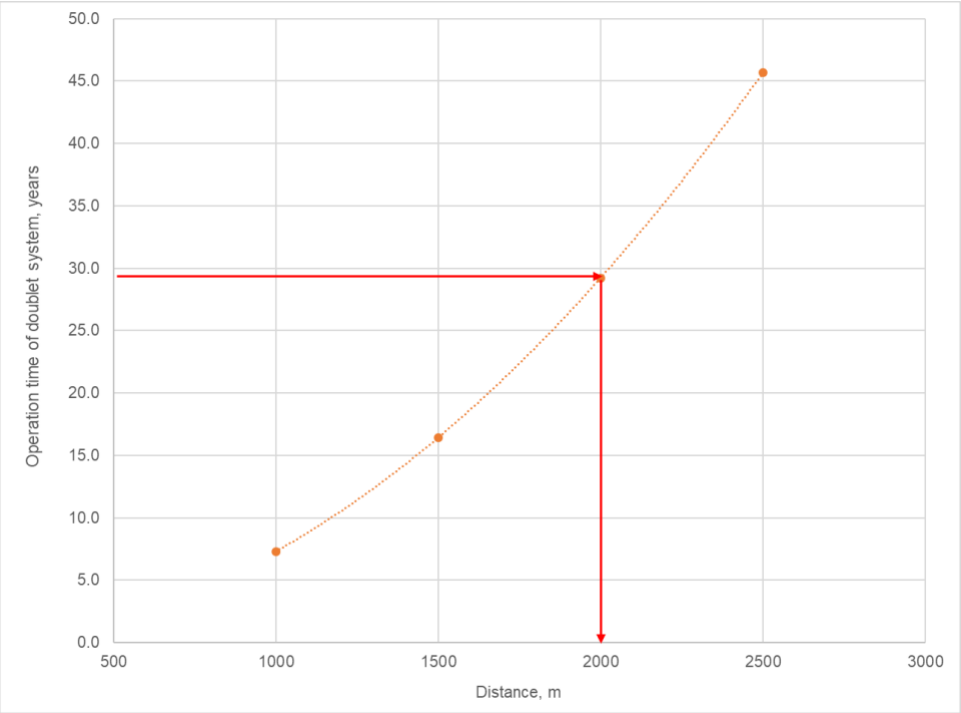

Figure 7.2: Distance between production and injection wells

Well design is a complex process and it must take into account geological conditions, the formation pressures, hole depth, formation temperature and other factors. Well design includes the casing design, what consists of selecting the casing sizes, weight, grades and setting depths. This is done by calculating the burst, collapse, and axial loads affecting the casing during drilling of the well and while the well is in production. The casing design is of utmost importance for the success and the cost of the well, and influence on hydraulic regime of the well (Moumin 2013).

Well design is out of scope of this study, but different papers (Aydin & Merey 2021, Moumin 2015, Hagen 2008, Moumin 2013) were review and NIS a.d. experience in drilling in Serbia was investigated. Base on that conceptual design of vertical well incl. casing scheme is proposed and shown in figure 7.3.

As it was mentioned above, two technologies for reservoir stimulation are proposed – horizontal drilling and hydraulic fracking.

Horizontal drilling is a process of directing a bit to drill along a horizontal path oriented approximately 85 to 95° from a vertical direction (figure 7.4).

Natural fractured reservoirs, low permeability reservoirs (less than 1 md), and economically unreachable reservoirs (a possibility to reduce the number of wells on a field) are potential candidates for horizontal drilling application.

The reservoir rocks which are potential candidates for horizontal drilling application include the following: naturally fractured reservoirs, low permeability reservoir (<1 md) and economically inaccessible reservoirs (ability to reduce the number of wells in the development of a whole field). All these indicators belong to Paleozoic reservoir, which we have on a depth of 1500 m in research area.

Additional advantage what we have it is ability to orient the borehole to across parallel or orthogonal fractures of reservoir and involve them in production. That can give significant growth of permeability and production rate. However, it requires deep

exploration works to define natural fracks direction and required orientation of horizontal part of the well.

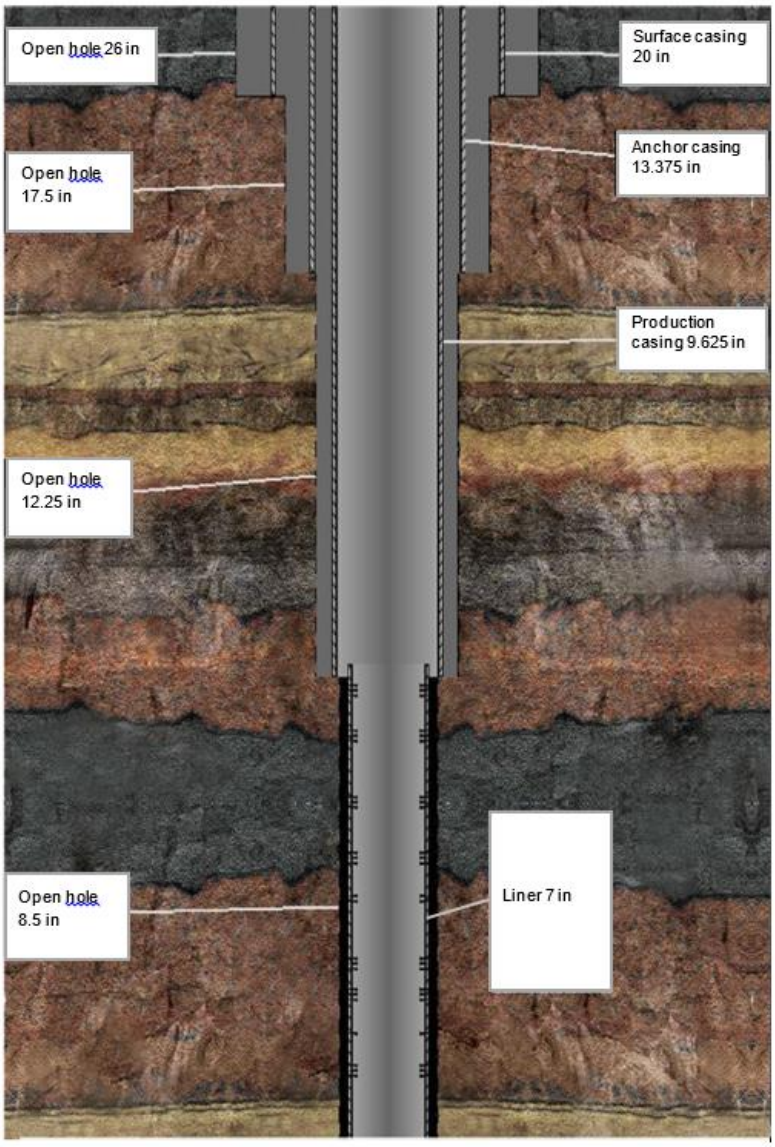

Figure 7.3: Vertical wellbore schematic (Moumin 2013)

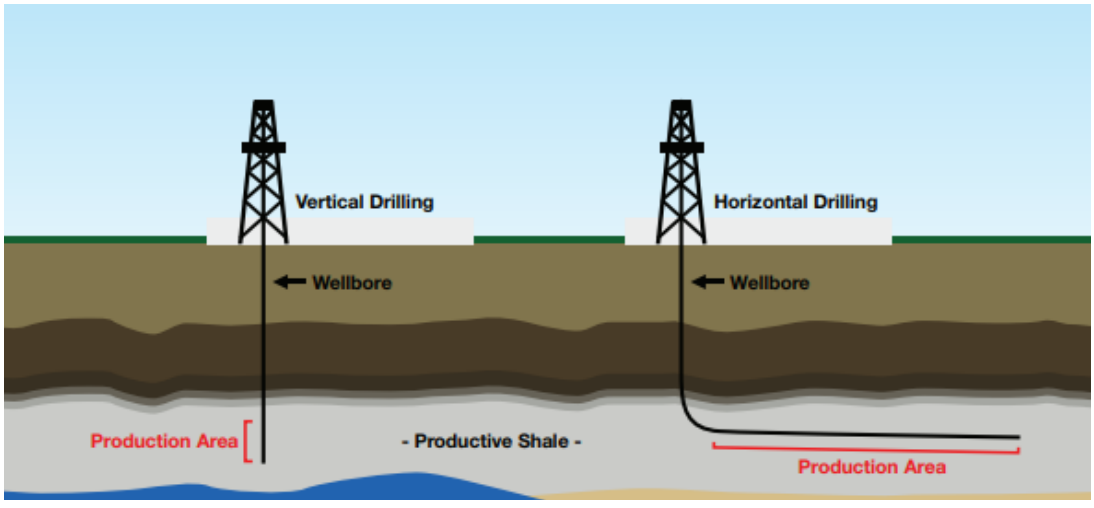

Figure 7.4: Vertical vs horizontal drilling (source: https://www2.uregina.ca/projectday/wp-content/uploads/2021/04/PSE-Group-5-poster.pdf)

According to NIS experience in horizontal drilling in Paleozoic formations in Pannonian basin, it increases production efficiency that can be expressed as permeability growth from 2 up to 4 times. This correlation uses further for modeling doublet system with horizontal well.

Horizontal well with 500 m horizontal part and 900 angle is chosen for further analyses. Casing scheme of horizontal well is similar to vertical one.

Fracking (also known as hydraulic fracturing, hydrofracturing, or hydrofracking) is a well stimulation technique involving the fracturing of bedrock formations by a pressurized liquid. The process involves the high-pressure injection of "fracking fluid" (primarily water, containing sand or other proppants suspended with the aid of thickening agents) into a wellbore to create cracks in the deep-rock formations through which natural gas, petroleum, or water will flow more freely. When the hydraulic pressure is removed from the well, small grains of hydraulic fracturing proppants (either sand or aluminum oxide) hold the fractures open. (https://en.wikipedia.org/wiki/Fracking).

Fracking can be applied in the vertical well and in horizontal one as well. Technically, it is more complex and demanding operation in the horizontal well. Normally one fracking operation fulfill in a vertical well, but multi-fracking in a horizontal one take place. Few fracking operations doing along the horizontal part of the well one by one (see figure 7.5).

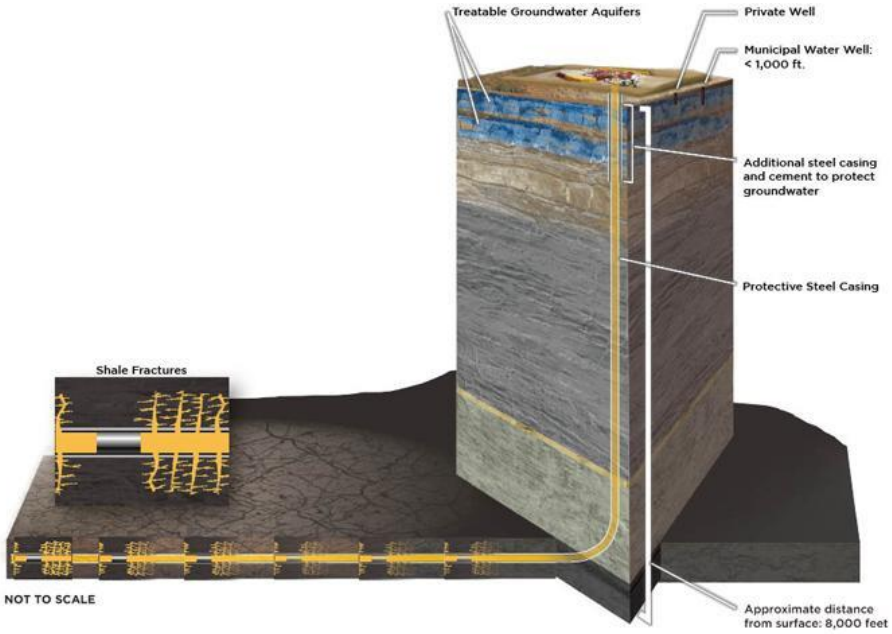

Figure 7.5: Horizontal well with fracking schematic (source: https://www.energy.virginia.gov/gas-oil/HydraulicFracturing.shtml)

Five fracking operations, every 100 m, in horizontal well is chosen for further analyses.

That to estimate influence of fracking on the doublet geothermal system model the value of skin factor (S) is assumed as - 4.5. Skin factor is a dimensionless factor calculated to determine the production efficiency of a well by comparing actual conditions with theoretical or ideal conditions. A positive skin value indicates some

damage or influences that are impairing well productivity. A negative skin value indicates enhanced productivity, typically resulting from stimulation, fracking for example.

Fracking is used by NIS to stimulate oil and gas production on exist oil fields in Serbia. It is mature technology and service companies, which can do it, present on Serbian market.

Key characteristics of horizontal wells and hydraulic fracturing (length, angle, number of fracks and ect.) were chosen preliminary based on available data from oil&gas and service companies operating Pannonian basin. Horizontal drilling and hydraulic fracturing are very complex technical operations that must be designed and executed experienced service companies. Only carful all available data analyses, especially geological ones, and precise design can define exact parameters of horizontal well and fracking.

After drilling wellheads must be installed. Wellheads include different equipment. The most important is the master valve which is aimed to isolate the well. The wellhead should be designed according to the practice codes ANSI, API, ASME and ect. (Hagen 2008: 7). A typical wellhead is presented in figure 7.6.

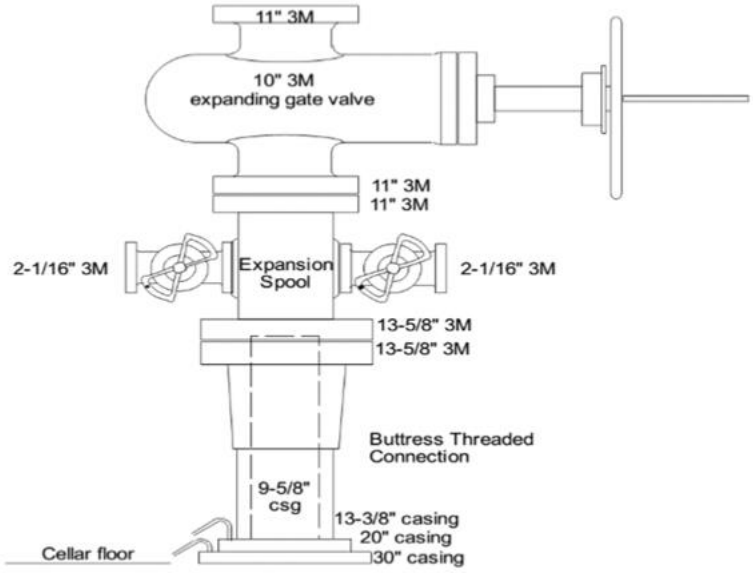

Figure 7.6: Typical complete wellhead (Hagen 2008: 7).

7.3. Electrical submersible pump

That to pump up required amount of geothermal water on a surface the electrical submersible pump, typically called an ESP, is used. The ESP is an efficient and reliable artificial-lift method for lifting moderate to high volumes of fluids from wellbores. The ESP's main components include:

- Multistage centrifugal pump
- Three-phase induction motor

- Seal-chamber section
- Power cable
- Surface controls

The components are normally tubing hung from the wellhead with the pump on top and the motor attached below.

One of the world leaders in ESP manufacturing is Schlumberger Company (www.slb.com). Schlumberger's REDA ESP system with high-efficiency pump was chosen. This ESP can handle production rates from 26 to 12,712 m^3/d with boost pressures of up to 400 bar. In addition to typical applications in oil, water, and brine production, REDA pumps are used for direct fluid injection, that is important for our use case. (https://www.slb.com/-/media/files/al/product-sheet/high-efficiency-pumps-ps.ashx).

These submersible pumps are multistage centrifugal pumps. Each stage consists of a rotating impeller and a stationary diffuser. Corrosion-resistant coatings and stainless steel construction are available for H_2S, CO_2 and other corrosive environments (https://www.slb.com/-/media/files/al/product-sheet/high-efficiency-pumps-ps.ashx).

Base on a list of available ESPs from Schlumberger (figure 7.7) pump H series was chosen as it corresponds to required flow (4320 m^3/d) and casing diameter (7 inches).

High-Efficiency Pumps

Pump Capacity Ranges

Series	OD, in [mm]	Min. Casing, in [mm]	60-Hz Min. Flow, bbl/d	60-Hz Max. Flow, bbl/d	50-Hz Min. Flow, m^3/d	50-Hz Max. Flow, m^3/d
A	3.380 [85.9]	4.500 [114.3]	400	3,400	53	450
D	4.000 [101.6]	5.500 [139.7]	200	7,000	26	927
G	5.130 [130.3]	6.625 [168.3]	800	12,000	106	1,590
S	5.380 [136.7]	7.000 [177.8]	1,600	16,500	210	2,186
H	5.630 [143.0]	7.000 [177.8]	5,000	36,000	660	4,770
J	6.750 [171.5]	8.625 [219.1]	4,500	25,000	596	3,313
M	8.630 [219.2]	10.750 [273.1]	12,000	32,500	1,590	4,306
N (950)	9.500 [241.3]	11.750 [298.5]	24,000	47,500	3,180	6,293
N (1000)	10.000 [254]	11.750 [298.5]	10,000	59,000	1,325	7,817
P	11.250 [285.8]	13.625 [346.1]	53,600	96,000	7,102	12,718
L	7.250 [184.2]	8.625 [219.1]	11,000	54,000	1,450	7,150

Enhanced stability configuration of a REDA system abrasion-resistant ESP.

Figure 7.7: Schlumberger high-efficiency pumps list (source: www.slb.com)

7.4. Process flow diagram of geothermal power plant

The sustainability and efficiency of the heat production system depends on the selected thermal scheme and process flow diagram of the plant. It reflects on the entire technological process of converting geothermal heat to district heating. Only the main equipment and main pipelines are indicated, without fittings and secondary devices are shown on process flow diagram.

Next important income points were considered for process flow diagram design:

- geothermal water can contain some sand and dissolved gases;
- geothermal water usually has potential to form deposits and corrosion;
- outlet thermal power must be easy regulated;
- entire process should be flexible and allow easy switching between different equipment;
- crucial equipment must be fully or partly duplicated.

Designed process flow diagram is presented in figure 7.8.

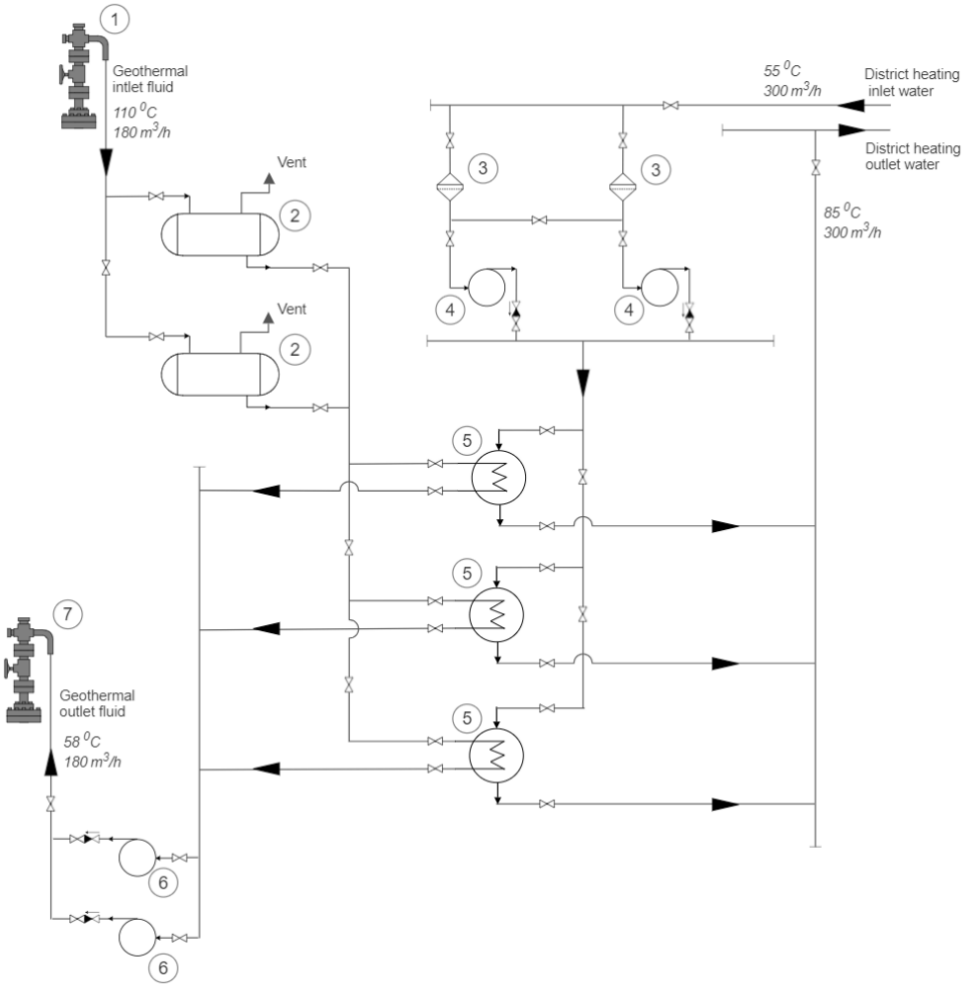

Figure 7.8: Process flow diagram of the heat plant

(1 – production well; 2 - separators; 3 - filters; 4 - district heating pumps; 5- plate heat exchangers; 6 – high-pressure pumps; 7 –injection well).

There are two independence circles – geothermal water circle and district heating circle. Heat transfer from geothermal working fluid to heating water occurs in heat exchangers which are the main equipment of the heat plant.

As the total heat power is 10 MW, 3 (three) plate heat exchanger were chosen, 5 MW each. Two of them are primary and one is back-up. Heat exchanger calculation is presented in a part 7.5.

Geothermal water from the well enters the separator, where mechanical impurities are trapped and gases dissolved in water are released due to pressure drop. There are two separators, one primary and one back-up. Further, geothermal water enters the plate heat exchangers, where the heat transfer from geothermal to heating water. After heat exchangers, geothermal water is pumped by high-pressure pumps through a two kilometers length pipeline to the injection well.

District heating water temperature of 55^0C enters the filters, which aim to trap possible mechanical impurities, and is pumped to the heat exchangers by district heating pump. There are two filters and two district heating pumps, one primary and one back-up. After the heat exchangers, district heating water temperature of 85^0C is let to district heating system.

7.5. Heat exchangers design

Alfa Laval plate heat exchanger was chosen for installation on the site. Alfa Laval is a leading global provider of specialized products and engineered solutions. The technical data was collected on manufacturer web-site (https://www.alfalaval.com).

A plate heat exchanger is a type of heat exchanger that uses metal plates to transfer heat between two fluids. This has a major advantage over a conventional heat exchanger in that the fluids are exposed to a much larger surface area because the fluids are spread out over the plates. This facilitates the transfer of heat, and greatly increases the speed of the temperature change (figure 7.9).

The plate heat exchanger consists of a pack of corrugated metal plates with portholes for the input and output of the two separate fluids. The heat transfer between the two fluids takes place through the plates. The plate pack is assembled between a frame plate and a pressure plate and compressed by tightening bolts. The plates are fitted with a gasket which seals the channel and directs the fluids into alternate channels. (Gasketed plate heat exchangers. Instruction Manual 2023: 20).

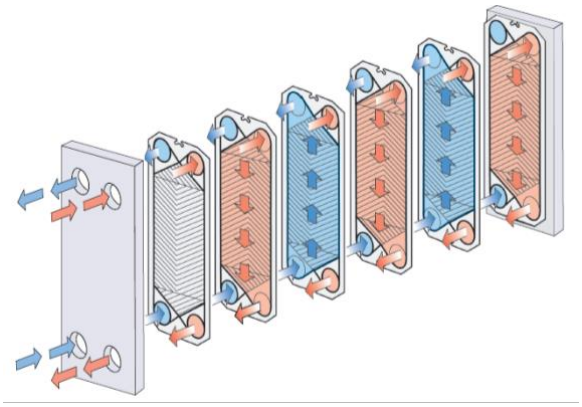

Figure 7.9: Plate heat exchanger schematic (source: Gasketed plate heat exchangers. Instruction Manual 2023: 20).

Heat exchanger calculations aiming to define heat load, working fluids parameters, mass flow and choose heat exchanger type were done. The following equations of heat transfer theory were used.

Transferred quantity oh heat (heat supply) of mass flow calculations:

$$Q = 4.19 \times m \times \Delta T$$

where:

Q - transferred quantity oh heat, W

4.19 - specific heat capacity of water, kJ/kg^{0}C

m – water mass flow rate, kg/h

ΔT – inlet and outlet temperature difference, ^{0}C

Heat exchanger heat load and LMTD calculation:

$$Q = k \times A \times LMTD$$

where:

Q - heat load, W

k - heat transfer coefficient, W/m^2 x °C

A - heat transfer area, m^2

LMTD - logarifmic mean temperature difference, °C

Heat transfer coefficient defines by the equation:

$$\frac{1}{k} = \frac{1}{\alpha_1} + \frac{1}{\alpha_2} + \frac{\delta}{\lambda} + R_f$$

α_1 - the heat transfer coefficient between the warm medium and the heat transfer surface, W/m^2 x °C

α_2 - the heat transfer coefficient between the heat transfer surface and the cold medium, W/m^2 x °C

λ - the thermal conductivity of the material separating the medias, W/m^2 x °C

δ - the thickness of the heat transfer surface, m

R_f - the fouling factor, m^2 x °C / W

Logarifmic mean temperature difference (LMTD) can be calculated by using the following formula:

$$LMTD = \frac{\Delta T1 - \Delta T2}{ln\frac{\Delta T1}{\Delta T2}}$$

Where:

ΔT1 = T1–T4 and ΔT2 = T2–T3

T1 - temperature inlet – hot side, °C

T2 - temperature outlet – hot side, °C

T3 - temperature inlet – cold side, °C

T4 - temperature outlet – cold side, °C

The temperature program of heat exchanger is shown in the figure 7.10.

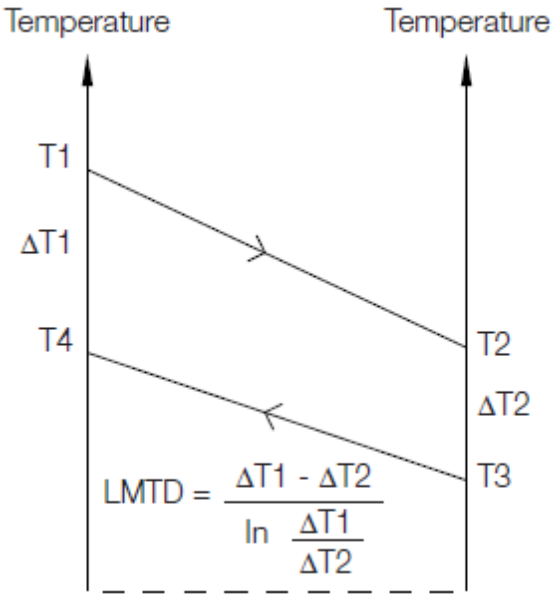

Figure 7.10: Heat exchanger temperature program (source: The theory behind heat transfer. Plate heat exchangers 2004)

To calculate a heat exchanger and solve a thermal problem, we must know several parameters. Further data can then be determined. The six most important parameters are as follows:

- the amount of heat to be transferred (heat load);
- the inlet and outlet temperatures on the primary and secondary sides;
- the flowrate on the primary and secondary sides;
- the maximum allowable pressure drop on the primary and secondary sides;
- the maximum operating temperature;
- the maximum operating pressure.

The maximum allowed temperature and pressure influence the cost of the heat exchanger. As a general rule, the lower the maximum temperature and maximum pressure are, the lower the cost of the heat exchanger will be. However, last three bullets are predefined by district heating network regime and geothermal fluid.

We have predefined the total heat load (10MW), inlet and outlet temperature for district heating network (85/55 ^{0}C), inlet geothermal water temperature (110^{0}C). So,

required flow of geothermal water, outlet geothermal water temperature must be calculated.

First, we must calculate mass flow of district heating working fluid and choose heat exchanger type prior to final heat exchanger calculation. Required mass flow of working fluid for supplying 10 MW of heat to the district heating network was calculated using above-mentioned equation:

$$Q = 4.19 \times m \times \Delta T$$

then,

$$m = 3600 \text{ x}10{,}000 / 4.19 \text{ x } (85 - 55) = 286{,}396 \text{ kg/h}$$

Single heat exchanger has heat load is 5 MW (see part 7.4) and two of them will provide required heat supply of 10 MW. So, water mass flow for single heat exchanger is:

m = 3600 x 5,000 / 4.19 x (85-55) = 143,198 kg/h

The values of water mass flow of 300 m^3/h and 150 m^3/h are taken for further calculations.

As we know heat load (5MW), max water temperature (110^0C), chloride content in geothermal water (see appendix 3) and max flow rate (150 m^3/h) Alfa Laval M15 heat exchanger was chosen (figures 7.11, table 7.1). Suitable for heating and cooling in a wide range of applications, this model is available with a wide selection of plate and gasket types.

Main benefits of it are:

- high energy efficiency – low operating cost;
- flexible configuration – heat transfer area can be modified;
- easy to install – compact design;
- high serviceability – easy to open for inspection and cleaning and easy to clean by CIP.

The heat load and flowrate of plate heat exchanger are defined by a number of plates, which can be installed in available dimension. For Alfa Laval M15 this dimension is max 3,700 mm. As required mass flow is 150 m^3/h and max flowrate for this type of heat exchanger is 388 m^3/h, we can assume that approximately a half of maximum number of plates will be needed. However, this type of calculations and design is not a scope of this study and must be done authorized company.

The choice of materials does not normally influence the efficiency, only the strength and corrosion properties of the unit. According to producer recommendations, as chloride content in geothermal water is up to 2000 ppm and temperature is110^0C/230^0F titanium plates were chosen.

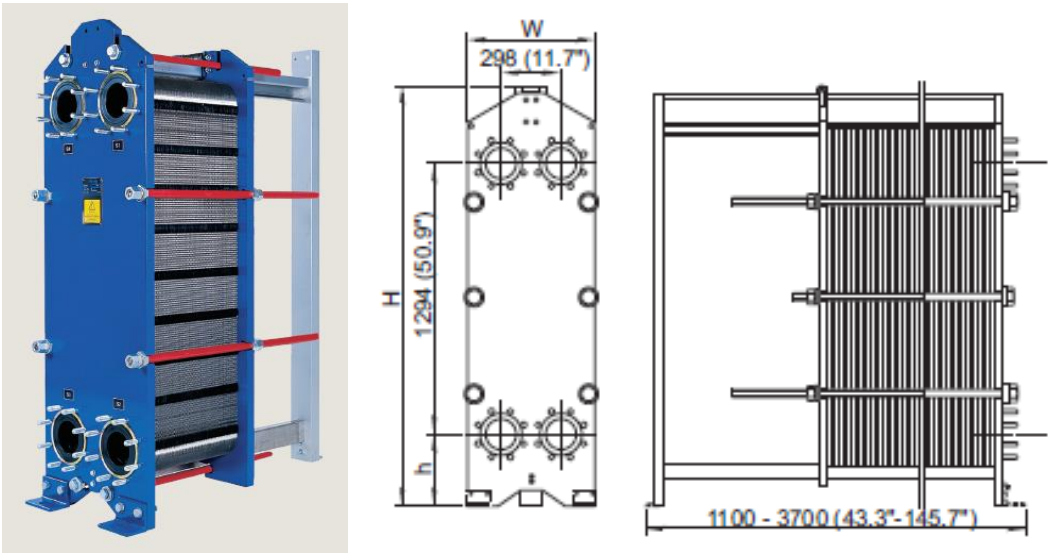

Figure 7.11: Alfa Laval M15 Heat exchanger (source: https://www.alfalaval.com)

Max flowrate, m3/h	388
Max design pressure, bar	30
Max design temperature, 0C	180
Heat transfer plates materials	304/304L, 316/316L, 904L, 254, C-276, C-2000, 825, Ni, Ti, TiPd
Gaskets materials	NBR, EPDM, FKM, Q
Flange connections (lined) materials	stainless steel, titanium
Frame and pressure plate materials	carbon steel, epoxy painted
Connection standards	Port size: 150 mm EN 1092-1 DN150 PN10 EN 1092-1 DN150 PN16 EN 1092-1 DN200 PN25 ASME B16.5 Class 150 NPS 6 ASME B16.5 Class 300 NPS 6

Table 7.1: Alfa Laval M15 Heat exchanger specification (source: https://www.alfalaval.com)

Thermal calculation of heat exchanger was done in on-line tool (https://tlk-energy.de/en/tools/heat-exchanger-calculator-online#learn-more-benefits) and results are presented in figures 7.12 and table 7.2.

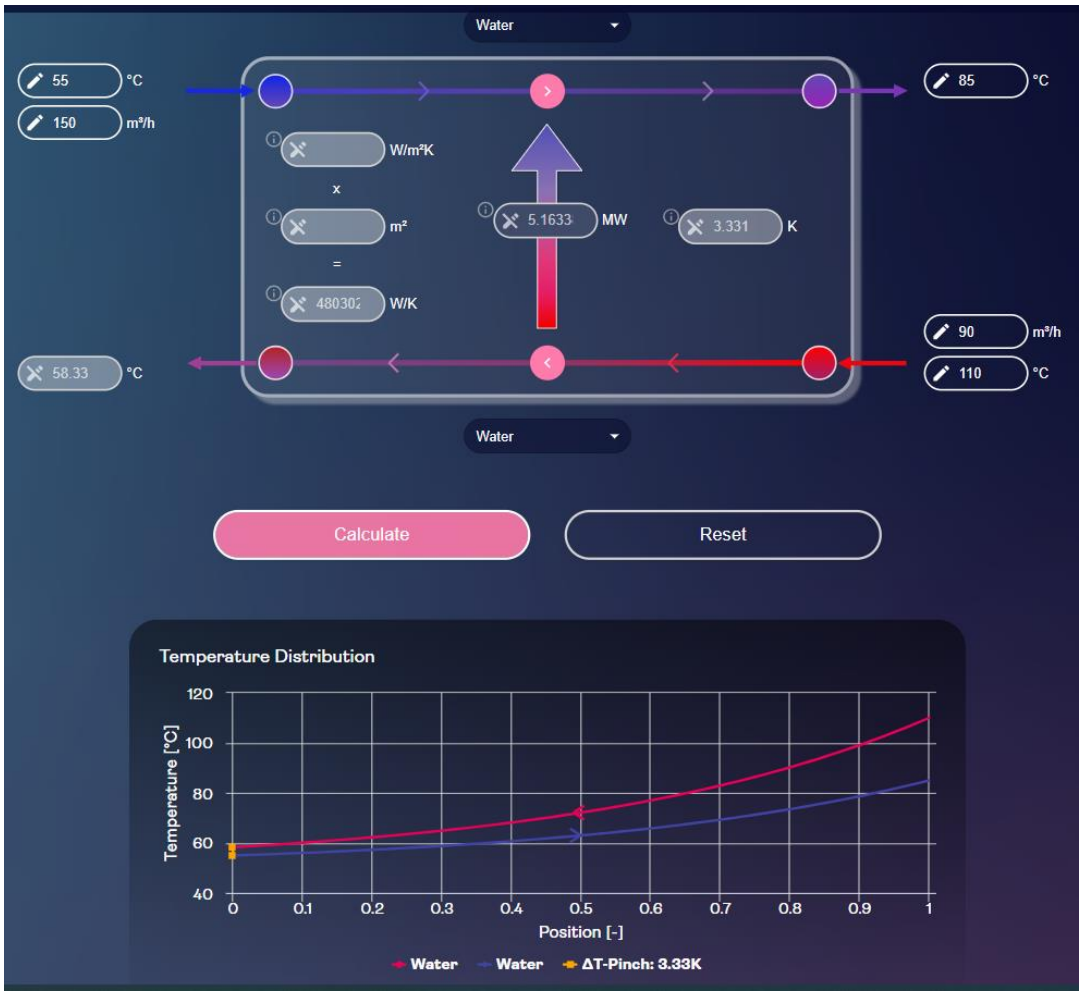

Figure 7.12: Heat exchanger calculations results (screen shot from https://tlk-energy.de/en/tools/heat-exchanger-calculator-online#learn-more-benefits)

	Geothermal water	DH working fluid (water)
Heat load, MW	5.16	
Volume floe rate, m^3/h	90	150
Temperature inlet, ^0C	110	85
Temperature outlet, ^0C	58.33	55
Temperature difference, ^0C	51.67	30
LMTD, ^0C	10.75	

Table 7.2: Heat exchanger calculations results

As we can see, proposed heat exchanger is feasible, give us required amount of heat and has an acceptable temperature program. Important information is that required flow rate of geothermal water to secure 10MW of thermal power must be 90x2=180m^3/h.

7.6. Geothermal heat production system modeling and design

As it mentioned above (see part 7.1) doublet geothermal system modeling was done in DoubletCalc v1.4.3 software. DoubletCalc v1.4.3 is a software tool that was developed by TNO. It enables to calculate a pre-drill indicative geothermal power of a future geothermal system by specifying the key reservoir parameters, the casing scheme, the pump details and heat exchanger temperature regime. This tool supports probabilistic approach which considers uncertainties in the geological reservoir characteristics (Mijnlieff et al. 2014).

As it was mentioned above in a part 7.1, four technological scenarios were analyzed. There is the list of parameters that are required for chosen scenarios modeling in following tables 7.3 and 7.4

Parameters	Units	Vertical well	Vertical well with a frack	Horizontal well	Horizontal well with a frack
Input geological parameters					
Permeability[1] (min/medium/max)	mD	0.08 / 46 / 964		0.35 / 162 / 2410	
Aquifer thickness (min/medium/max)	m	15 / 50 / 220			
Brine salinity (total dissolved solids, NaCl equivalent) (min/medium/max)	ppm	2000 / 4000 / 6000			
Depth top aquifer at production well (medium)	m	1500			
Depth top aquifer at injection well (medium)	m	1500			
Aquifer temperature	°C	110			
Average surface temperature	°C	20,0			
k_h/k_v ratio of the aquifer (anisotropy)	-	1			
Input for pump and doublet					
Injection temperature	°C	58			
Distance between production and injection well at aquifer level	m	2000			
Pump efficiency	%	61			
Pump depth in production well	m	800			
Pump pressure difference	bar	60			

Table 7.3: List of income parameters for chosen scenarios modeling (1).
(1- permeability values assumed according to parts 6.4 and 7.2)

Parameters	Units	Vertical well	Vertical well with a frack	Horizontal well	Horizontal well with a frack
Production well specification input					
Outlet diameter of the producer	inch	7	7	7	7
Production casing inner diameter	inch	9 5/8	9 5/8	9 5/8	9 5/8
Production casing base vertical depth	m	1000	1000	1000	1000
Production casing section length along hole	m	1000	1000	1000	1000
Absolute roughness production casing		1.2	1.2	1.2	1.2
Borehole casing inner diameter	inch	7	7	7	7
Borehole casing base vertical depth	m	1500	1500	1500	1500
Borehole casing section length along hole	m	1500	1500	1800	1800
Absolute roughness production casing		1.2	1.2	1.2	1.2
Skin production well		- 2	-4.5	- 2	-4.5
Inclination between production well trajectory and reservoir	deg	0	0	90	90
Injection well specification input					
Inlet diameter of the injector	inch	7	7	7	7
Production casing inner diameter	inch	9 5/8	9 5/8	9 5/8	9 5/8
Production casing base vertical depth	m	1000	1000	1000	1000
Production casing section length along hole	m	1000	1000	1000	1000
Absolute roughness production casing		1.2	1.2	1.2	1.2
Borehole casing inner diameter	inch	7	7	7	7
Borehole casing base vertical depth	m	1500	1500	1500	1500
Borehole casing section length along hole	m	1500	1500	1800	1800
Absolute roughness production casing		1.2	1.2	1.2	1.2
Skin injection well		2	-4.5	2	-4.5
Inclination between injection well trajectory and reservoir	deg	0	0	90	90

Table 7.4: List of income parameters for chosen scenarios modeling (2)

The calculation of the geothermal power takes the following into account (Mijnlieff et al. 2014):

- pressure loss caused by flow in the aquifer to the production well and from the injection well;
- pressure loss around production and / or injection well caused by 'skin';
- pressure loss in the production and injection wells as a result of friction by flow;
- pressure difference caused by gravity;
- pressure difference caused by the pump in the production well;
- heat loss in the production and injection wells as a result of the release of heat to the environment.

A theoretical description of the calculation and equations, which are behind the model, are presented in DoubletCalc 1.4 manual (Mijnlieff et al. 2014).

Doublet Calculator 1.4.3 Result Table

probabilistic plots | fingerprinting | export base case details

file: \\sns06cfsh01\homefolderr\zalevskii.nv\desktop\doubletcalc\ww_last.xml

Geotechnics (Input)

Property	min	median	max
aquifer permeability (mD)	0.0	46.0	964.0
aquifer net to gross (-)	0.75	0.8	0.85
aquifer gross thickness (m)	15.0	50.0	220.0
aquifer top at producer (m TVD)	1350.0	1500.0	1650.0
aquifer top at injector (m TVD)	1350.0	1500.0	1650.0
aquifer water salinity (ppm)	2000.0	4000.0	6000.0

Property	value
number of simulation runs (-)	1000.0
aquifer kh/kv ratio (-)	1.0
surface temperature (°C)	20.0
geothermal gradient (°C/m)	0.059
[mid aquifer temperature producer (°C)]	110.0
inital aquifer pressure at producer (bar)]	0.0
[initial aquifer pressure at injector (bar)]	0.0
exit temperature heat exchanger (°C)	58.0
distance wells at aquifer level (m)	2000.0
pump system efficiency (-)	0.61
production pump depth (m)	800.0
pump pressure difference (bar)	60.0
outer diameter producer (inch)	7.0
skin producer (-)	-2.0
skin due to penetration angle p (-)	0.0
pipe segment sections p (m AH)	800.0,1000.0,1500.0
pipe segment depth p (m TVD)	800.0,1000.0,1500.0
pipe inner diameter p (inch)	7.0,9.62,7.0
pipe roughness p (milli-inch)	1.2,1.2,1.2
outer diameter injector (inch)	7.0
skin injector (-)	2.0
skin due to penetration angle i (-)	0.0
pipe segment sections i (m AH)	50.0,1000.0,1500.0
pipe segment depth i (m TVD)	50.0,1000.0,1500.0
pipe inner diameter i (inch)	7.0,9.62,7.0
pipe roughness i (milli-inch)	1.2,1.2,1.2

Geotechnics (Output)

Monte Carlo cases (stochastic inputs)	P90	P50	P10
aquifer kH net (Dm)	0.76	4.01	31.77
mass flow (kg/s)	3.87	19.65	113.15
pump volume flow (m³/h)	14.5	73.6	424.5
required pump power (kW)	39.6	201.0	1159.8
geothermal power (MW)	0.58	4.08	24.96
COP (kW/kW)	14.7	19.6	22.8

aquifer pressure at producer (bar)	137.9	145.77	153.66
aquifer pressure at injector (bar)	137.98	145.8	153.69
pressure difference at producer (bar)	12.65	16.83	17.72
pressure difference at injector (bar)	34.77	46.31	47.75
aquifer temperature at producer * (°C)	105.28	110.7	115.7
temperature at heat exchanger (°C)	93.85	105.69	113.56

base case (median value inputs)	value
aquifer kH net (Dm)	1.84
mass flow (kg/s)	9.13
pump volume flow (m³/h)	34.2
required pump power (kW)	93.4
geothermal power (MW)	1.73
COP (kW/kW)	18.5

aquifer pressure at producer (bar)	145.79
aquifer pressure at injector (bar)	145.79
pressure difference at producer (bar)	17.14
pressure difference at injector (bar)	47.21
aquifer temperature at producer * (°C)	110.0
temperature at heat exchanger (°C)	103.11
pressure at heat exchanger (bar)	47.03

* @ mid aquifer depth

Figure 7.13: Results of doublet geothermal system modeling with vertical well (screen shot from DoubletCalc v.1.4.3)

The premises for the calculation of the geothermal energy, given the reservoir, wells and heat exchanger characteristics are mass balance, impulse balance and energy balance (Mijnlieff et al. 2014).

Results of 4 scenarios modeling are presented in appendix 7. Example of output results (output mask of DoubletCalc v1.4.3) of vertical well scenario is shown in figure 7.13.

As an important result of modeling, probabilistic plots of geothermal power for four scenarios are presented in figure 7.14**.** The scenario with outlet thermal power of 10 MW and probability not less than P50 is selected. So, **the doublet geothermal system with horizontal well is defined for further study.**

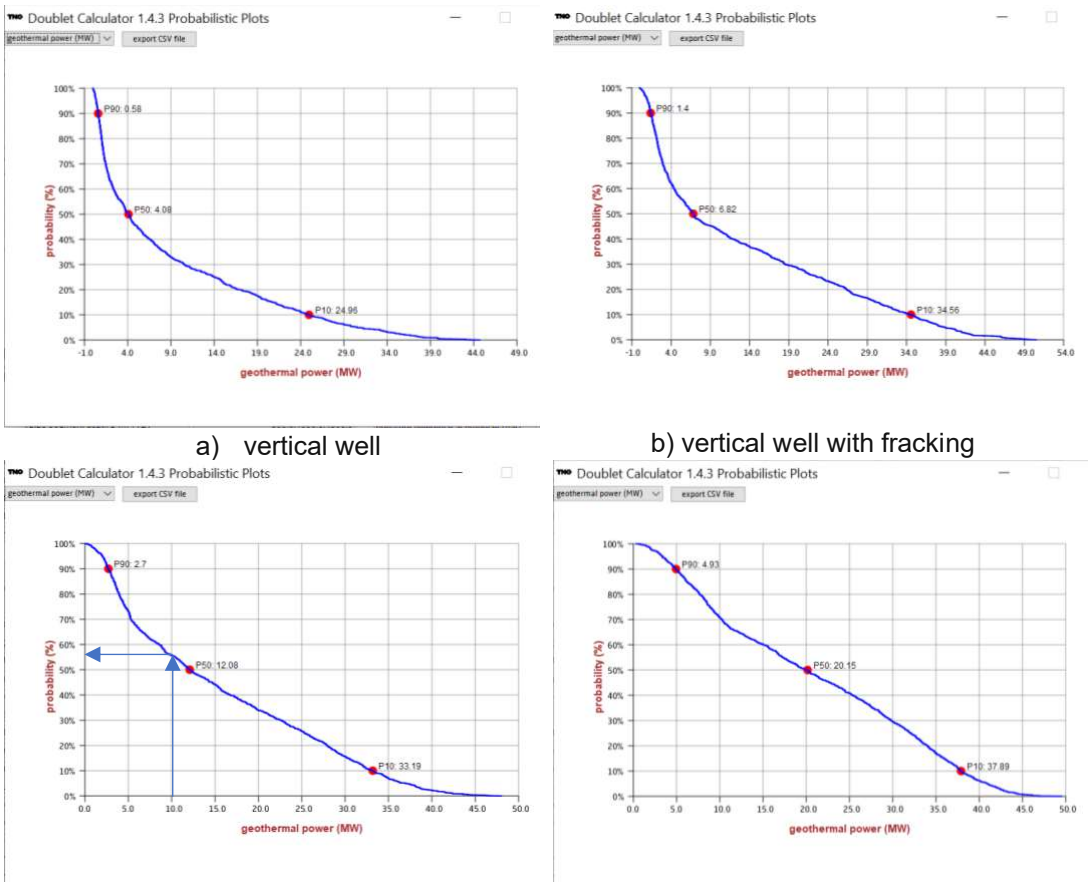

a) vertical well

b) vertical well with fracking

c) horizontal well

d) horizontal well with fracking

Figure 7.14: Results of doublet geothermal system modeling. Probabilistic plots of geothermal power (DoubletCalc v.1.4.3)

7.7. Conclusions

Overall technical analyses and design of geothermal thermal power plant was done in the part 7 of this study. Variety of data was used that to design feasible and reliable technological scheme. Huge massive of geological data, technical specifications of equipment, different scientific papers and local oil & gas companies' available

experience were used. As we have significant geological uncertainties probabilistic approach was applied.

As a result, 10 MW thermal power doublet geothermal system with two horizontal wells (one production and one injection) and two plate exchangers, 5 MW each, was chosen. The main technical data and parameters are presented in a table 7.5.

Parameter	Units	Value
Thermal power	MW	10
Full load hours	h	4000
Thermal power production	GWh	40
DH system water flow	m^3/h	300
DH system outlet temperature	^0C	85
DH system inlet temperature	^0C	55
Number of production wells	-	1
Depth of aquifer	m	1500
Type of production well		horizontal well, 500 m horizontal part length
Number of injection wells		1
Depth of aquifer		1500
Type of injection well		horizontal well, 500 m horizontal part length
Geothermal fluid flow	m^3/h	180
Outlet geothermal water temperature (surface)	^0C	110
Inlet geothermal water temperature (sutface)	^0C	58
Distance between production and injection wells	m	2000
ESP type		Schlumberger high-efficiency pump H series
ESP depth	m	800
Electric power of ESP	kW	550
Type heat exchanger		Alfa Laval M15; 5 MWx3; Titanium

Table 7.5: Geothermal doublet system specification.

8. ECONOMIC EVALUATION OF THE PROJECT

Economic evaluation of projects aims to determinate the profitability and feasibility of an investment. One of the most common methods used for this purpose is Net Present Value (NPV) and Profitability Index (PI).

Net Present Value is a fundamental financial metric that measures the profitability of an investment or project. It calculates the difference between the present value of cash inflows generated by the project and the total initial investment cost. The aim is to identify whether the project will generate a positive return after considering the time value of money. NPV is the sum of all the discounted future cash flows. A positive NPV results in profit, while a negative NPV results in a loss.

The profitability index is calculated as the ratio between the present value of future expected cash flows and the initial amount invested in the project. A higher PI means that a project will be considered more attractive.

A profitability index of 1.0 is logically the lowest acceptable measure on the index, as any value lower than that number would indicate that the project's present value is less than the initial investment. As the value of the profitability index increases, so does the financial attractiveness of the proposed project.

All input parameters to the calculation were carefully researched and updated with the most recent available data.

Firstly, investment costs were analyzed. Specific investment cost were calculated for current period of time using CPI=3% than it is necessary. Investment costs include the following:

1. **Well drilling and completion costs** are assumed as 2.95 mln.euro per well based on data provided by NIS a.d as the only company in Serbia which has experience in horizontal wells drilling.
2. **Pipelines construction costs.** There are two pipelines: high-pressure 2 km length pipeline from heat plant to injection well and district heating network connection pipelines 1 km total length. According to available market data cost of pipeline constriction assumed as 70 euro/m/inch.
3. **Heat plant construction costs**. Different sources gives approximately the same specific cost of heat plant 100 euro/kW (Beckers & Young 2017; Mattson & Neupane G 2017; U.S. Department of Energy 2016).
4. **Project development costs**, assumed as 5% of total investment.
5. **Unexpected costs,** which can occur during drilling and construction phase, assumed as 2% of total investment.

The total investment is 8,589,420 euro. Capital share structure for investment costs is presented in the table 9.1. It is assumed that investor is going to invest 2,576,826 (30% of whole investment) of its own capital. The rest of investment $6,012,594 (70%) will be borrowed from the bank for 20 years. Investment period is assumed as 20 years. Project development and construction works will take 2,5 years. Investment distribution by years is assumed as 30%, 50% and 20%. Start of operating is planed from the October of the second year, when heating season will start.

	Bank	Equity
Loan	€ 6,012,594	€ 2,576,826
% of total investment	70%	30%
Interest rate	5%	N/A
Loan period	20 years	N/A
Annual repayment	€ 181,836	N/A
Total repayment with interest rate	€ 9,166,856	N/A
repayment	€ 5,553,102	N/A
interest rate	€ 3,613,753	N/A

Table 8.1: Detailed capital share, interest rates and loan period.

According to Trading Economics econometric models (figure 9.1, https://tradingeconomics.com/euro-area/interest-rate) interest rate in EU is projected to trend around 4.50 percent in 2024. Base on that, bank interest rate is assumed as 5.0 %.

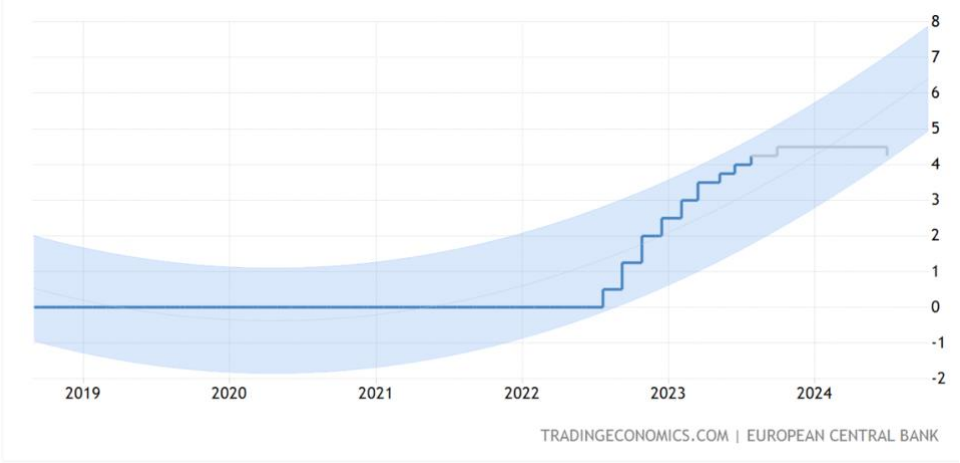

Figure 8.1: Interest Rate in Euro Area forecast (https://tradingeconomics.com/euro-area/interest-rate)

After 10 years of operation heat plant repair works cost of 300,000 euro are planned. Wells workover operation cost of 250,000 euro are planed every 5 years.

The term of depreciation is assumed as 15 years.

Secondly, all cost as maintenance, electricity, labor, land and ect. were analyzed with specific focus on available data for Serbia and the local market. They include the followings:

1. **Land costs.** Required land area for wells site and heat plant is assumed as 7.2 ha. Easy access to wells and workover operations possibility must be considered. Due to that, well site area is defined accounting with workover operation requirements and workover rig functioning. In addition, access roads are included in the total required area. The annual price of a rent was taken as 2000 euro per hectare per year in accordance with current market data.

2. **Maintenance costs.** The annual maintenance costs were assumed as 1.5% of investment for subsurface part and 1.0% of investment for surface part (Beckers & Young 2017; Mattson & Neupane G 2017; U.S. Department of Energy 2016).
3. **Electricity costs.** Electricity tariff was taken as 135 euro/MWh in accordance with public data from EPS Company (www.eps.rs), whish a single electricity distributor in Serbia (https://www.eps.rs/cir/snabdevanje/Documents/20230317_Odluka%20o%20regulisanoj%20ceni.pdf).
4. **Labor costs** are calculated as gross annual salary multiply number of employees. Gross annual salary is assumed 25,000 euro based on local labor market data. Number of employees with permanent contract is 6 as we have 24/7 schedule of operations.
5. **Insurance expenses** are assumed as 0.75% of asset value at the end of the period.
6. **Selling general and administrative (SG&A) expenses** comprise all direct and indirect selling costs, operational overhead costs, and administrative expenses unrelated to production and sales. SG&A costs are assumed as 0.5% of turnover.
7. **Other operating expenses**, also known as overhead expenses, is the amount which generally does not depend on sales or production quantities. Other operating expenses are assumed as 1.0% of total operational costs.

Thirdly, following important data was considered as well.

1. **Heat price.** It is assumed that we are going to sell heat to central district heating system whose owner and the main supplier Subotickia Toplana. It produces heat by gas boilers. Another option is to compete with decentralized heating systems, which use gas as well. Due to that heat price was calculated as:

$$T_{heat} = P_{gas} / \eta,$$

W\here,

P_{gas} – gas price on the Serbian market, 2.7 euro/MWh (https://www.srbijagas.com/wp-content/uploads/2022/10/Cene-prirodnog-gasa-za-javno-snabdevanje-od-01.10.2022-a.pdf);

η - boiler efficiency, 85%

T_{heat} = 2.7/0.85 = 3.2 euro/MWh

2. **CO_2 price.** According to Trading Economics econometric models (figure 8.2, https://tradingeconomics.com/euro-area/interest-rate) EU Carbon Permits is expected to trade at 90.82 euro per ton by the end of 3Q2023 and around 95 euro in 2024. Base on that, CO_2 price is assumed as 90 euro per ton.

Figure 8.2: EU Carbon Permits price forecast, euro per ton (https://tradingeconomics.com/)

3. **Corporate tax** rate value is 15%.
4. **Property tax** rate is 0.4% of asset value at the end of the period.
5. **Consumer Price Index** (CPI) is assumed 3% according to National bank of Serbia forecast (figure 8.3).

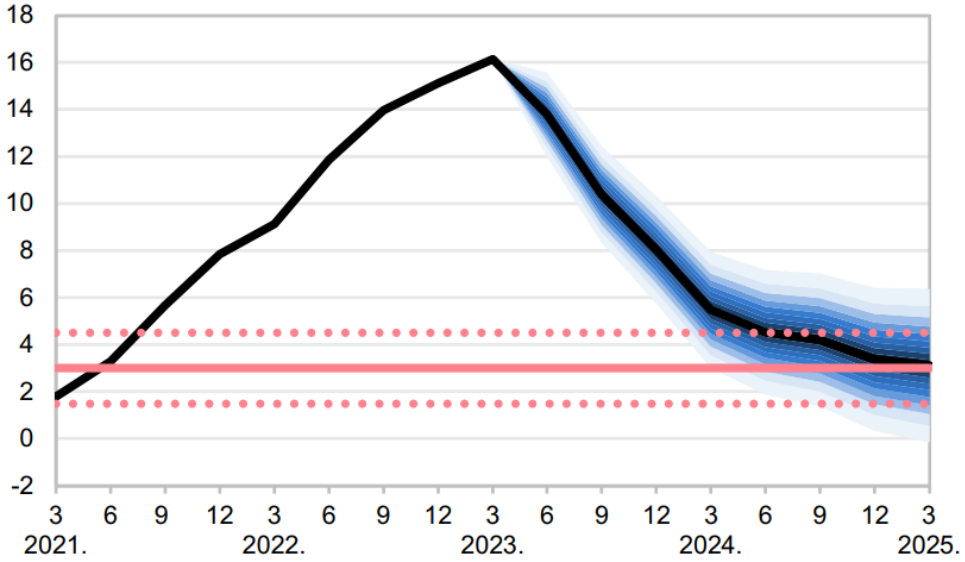

Figure 8.3: Inflation forecast in Serbia (source: National bank of Serbia 2023)

6. **Weighted average cost of capital** (WACC) is assumed 5% according with IEA study (IEA 2021).

Results of calculations are presented in tables 9.2, 9.3 and 9.4. Two scenarios are calculated: with and without CO_2 trading.

Technical figures		
Heat Power	**MW_{th}**	**10**
Full Load hours	h	4,000
Production	**GWh/y**	**40.0**
Production wells		1
Injection wells		1
Pipeline to the DH network	m	1000
Distance between production and injection wells	m	2000
CO2 emission	kg/kWh	0.198
CO2 emission	t/y	7920
Investment figures		
Well cost	EUR/well	2,950,000
Wells cost	EUR	5,900,000
Pipelines cost	EUR	1,120,000
GT heat power plant cost	EUR/kW	100
Project development (% of investment)	%	5
Unplanned costs (% of investment)	%	2
Total investment	**EUR**	**8,589,420**
Equity	%	30%
	EUR	2,576,826
Bank Loan	%	70%
	EUR	6,012,594
Bank loan period	y	20
Bank interest rate	%	5%
Wells workover (every 5 years)	EUR	250,000
Infrastructure repair (10 years)	EUR	300,000
Investment horizon	y	20
Term of depreciation	y	15
Construction period	y	2.5
Tax rate	%	15.0
CPI	%	3.0
Discount rate / cost of capital	%	5.0
Price of energy recourses and CO2		
Electricity price	EUR/kWh	0.135
CO2 price	EUR/t	90
Gas price	EUR/kWh	0.027
Heat price	EUR/kWh	0.032
Operational costs		
Cost of land (rent)	**EUR/y**	**14,300**
Required land	ha	7.2
Cost of land (rent)	EUR/ha/y	2,000
Electricity costs	**EUR/y**	**655,600**
Electricity consumption (production and injection)	kWh/y	5,600,000
Electricity consumption (DH pumps)	kWh/y	360,000
Maintenance cost	**EUR/y**	**109,700**
Cost for subsurface (1,5% of investment)	EUR/y	88,500
Cost for surface (1% of investment)	EUR/y	21,200
Property tax	**%**	**0.4**
SG&A (% of turnover)	**%**	**0.5**
Insurance	**%**	**0.75**
Other operation costs (% of total operational costs)	**%**	**1**
Labor cost	**EUR/y**	**150,000**
Headcount	person	6
Headcount cost	EUR/person/year	25,000

Table 8.2: Geothermal heat plant economical model input data

Year	Discounted CF	Nominal CF	Investment, Replacement& Residual Value	Revenue			Income / bank loan	Bank loan payment		Depreciation	O&M costs							Tax	Nominal Costs	Discounted Costst
				Total	Heat Sales	CO2 Sales		Payment of bank loan	Interest rate		*Labor cost*	*Land costs*	*Electricity costs*	*Maintenance*	*Proprety tax*	*Other costs (SG&A, insurance and ect.)*	TOTAL incl. add costs			
0	(2,576,826)	(2,576,826)	(2,576,826)																(2,576,826)	(2,576,826)
1	0	0	(4,294,710)				4,294,710												(4,294,710)	(4,090,200)
2	(451,221)	(497,471)	(1,717,884)	674,197	674,197	0	1,717,884	(181,836)	(300,630)	(286,314)	*(79,568)*	*(15,171)*	*(426,800)*	*(58,190)*	*(33,212)*	*(69,437)*	(689,202)	0	(2,889,552)	(2,620,909)
3	(333,662)	(386,255)		1,388,846	1,388,846	0		(190,928)	(291,538)	(572,628)	*(163,909)*	*(15,626)*	*(879,208)*	*(119,872)*	*(30,922)*	*(70,299)*	(1,292,635)	0	(1,775,101)	(1,533,399)
4	(308,708)	(375,236)		1,430,511	1,430,511	0		(200,475)	(281,991)	(572,628)	*(168,826)*	*(16,095)*	*(905,584)*	*(123,468)*	*(28,631)*	*(67,574)*	(1,323,281)	0	(1,805,747)	(1,485,593)
5	(285,055)	(363,810)		1,473,426	1,473,426	0		(210,498)	(271,968)	(572,628)	*(173,891)*	*(16,578)*	*(932,752)*	*(127,172)*	*(26,341)*	*(64,623)*	(1,354,770)	0	(1,837,236)	(1,439,523)
6	(262,638)	(351,959)		1,517,629	1,517,629	0		(221,023)	(261,443)	(572,628)	*(179,108)*	*(17,075)*	*(960,734)*	*(130,988)*	*(24,050)*	*(61,433)*	(1,387,122)	0	(1,869,588)	(1,395,116)
7	(459,907)	(647,136)	(307,468)	1,563,158	1,563,158	0		(232,074)	(250,392)	(572,628)	*(184,481)*	*(17,587)*	*(989,557)*	*(134,917)*	*(21,760)*	*(57,994)*	(1,420,359)	0	(2,210,294)	(1,570,814)
8	(221,269)	(326,916)		1,610,053	1,610,053	0		(243,678)	(238,788)	(572,628)	*(190,016)*	*(18,115)*	*(1,019,243)*	*(138,965)*	*(19,469)*	*(54,294)*	(1,454,502)	0	(1,936,968)	(1,311,016)
9	(202,205)	(313,686)		1,658,354	1,658,354	0		(255,862)	(226,604)	(572,628)	*(195,716)*	*(18,658)*	*(1,049,821)*	*(143,134)*	*(17,179)*	*(50,319)*	(1,489,574)	0	(1,972,040)	(1,271,195)
10	(184,149)	(299,959)		1,708,105	1,708,105	0		(268,655)	(213,811)	(572,628)	*(201,587)*	*(19,218)*	*(1,081,315)*	*(147,428)*	*(14,888)*	*(46,057)*	(1,525,598)	0	(2,008,064)	(1,232,777)
11	(167,052)	(285,715)		1,759,348	1,759,348	0		(282,088)	(200,378)	(572,628)	*(207,635)*	*(19,795)*	*(1,113,755)*	*(151,850)*	*(12,598)*	*(41,494)*	(1,562,597)	0	(2,045,063)	(1,195,706)
12	(587,520)	(1,055,102)	(784,168)	1,812,128	1,812,128	0		(296,192)	(186,274)	(572,628)	*(213,864)*	*(20,388)*	*(1,147,167)*	*(156,406)*	*(10,307)*	*(36,615)*	(1,600,596)	0	(2,867,230)	(1,596,581)
13	(135,546)	(255,592)		1,866,492	1,866,492	0		(311,002)	(171,464)	(572,628)	*(220,280)*	*(21,000)*	*(1,181,582)*	*(161,098)*	*(8,017)*	*(31,407)*	(1,639,618)	0	(2,122,084)	(1,125,386)
14	(121,049)	(239,668)		1,922,487	1,922,487	0		(326,552)	(155,914)	(572,628)	*(226,888)*	*(21,630)*	*(1,217,030)*	*(165,931)*	*(5,726)*	*(25,853)*	(1,679,689)	0	(2,162,155)	(1,092,035)
15	(107,334)	(223,139)		1,980,162	1,980,162	0		(342,880)	(139,586)	(572,628)	*(233,695)*	*(22,279)*	*(1,253,541)*	*(170,909)*	*(3,436)*	*(19,937)*	(1,720,835)	0	(2,203,301)	(1,059,825)
16	(94,362)	(205,981)		2,039,567	2,039,567	0		(360,024)	(122,442)	(572,628)	*(240,706)*	*(22,947)*	*(1,291,147)*	*(176,036)*	*(1,145)*	*(13,644)*	(1,763,082)	0	(2,245,548)	(1,028,711)
17	(264,449)	(606,122)	(413,212)	2,100,754	2,100,754	0		(378,025)	(104,441)	(286,314)	*(247,927)*	*(23,636)*	*(1,329,881)*	*(181,317)*		*(10,504)*	(1,811,198)	0	(2,706,876)	(1,181,001)
18	(89,806)	(216,129)		2,163,776	2,163,776	0		(396,926)	(85,540)		*(255,365)*	*(24,345)*	*(1,369,778)*	*(186,757)*		*(10,819)*	(1,865,534)	(31,905)	(2,379,905)	(988,900)
19	(83,698)	(211,501)		2,228,689	2,228,689	0		(416,772)	(65,694)		*(263,026)*	*(25,075)*	*(1,410,871)*	*(192,360)*		*(11,143)*	(1,921,500)	(36,224)	(2,440,190)	(965,666)
20	(77,938)	(206,793)		2,295,550	2,295,550	0		(437,611)	(44,855)		*(270,917)*	*(25,827)*	*(1,453,197)*	*(198,130)*		*(11,478)*	(1,979,145)	(40,733)	(2,502,343)	(943,107)
21	(126,323)	(351,932)		1,182,208	1,182,208	0		(459,492)	(22,975)		*(139,522)*	*(26,602)*	*(748,397)*	*(102,037)*		*(5,911)*	(1,032,694)	(18,981)	(1,534,141)	(550,668)
NPV, EUR	***(7,140,717)***																***NPV of Costs, EUR***			***(32,254,955)***
PI	***0.17***																***Annuity of Costs, EUR***			***(2,588,221)***
IRR	***#NUM!***																***LRGC (incl. Cost Escal.), EUR/MWh***			***(64.7)***
Annuity, EUR	***(572,990)***																			

Table 8.3: Geothermal heat plant economical model. Without $C0_2$ trading.

				Revenue				Bank loan payment			O&M costs									
Year	Discounted CF	Nominal CF	Investment, Replacement& Residual Value	Total	Heat Sales	CO2 Sales	Income / bank loan	Payment of bank loan	Interest rate	Depreciation	*Labor cost*	*Land costs*	*Electricity costs*	*Maintenance*	*Proprety tax*	*Other costs (SG&A, insurance and ect.)*	TOTAL incl. add costs	Tax	Nominal Costs	Discounted Coststs
0	(2,576,826)	(2,576,826)	(2,576,826)																(2,576,826)	(2,576,826)
1	0	0	(4,294,710)				4,294,710												(4,294,710)	(4,090,200)
2	(110,001)	(121,276)	(1,717,884)	1,052,302	674,197	378,105	1,717,884	(181,836)	(300,630)	(286,314)	*(79,568)*	*(15,171)*	*(426,800)*	*(58,190)*	*(33,212)*	*(71,327)*	(691,111)	0	(2,891,461)	(2,622,641)
3	334,872	387,656		2,167,741	1,388,846	778,896		(190,928)	(291,538)	(572,628)	*(163,909)*	*(15,626)*	*(879,208)*	*(119,872)*	*(30,922)*	*(74,193)*	(1,296,568)	(1,051)	(1,780,085)	(1,537,705)
4	341,711	415,352		2,232,774	1,430,511	802,263		(200,475)	(281,991)	(572,628)	*(168,826)*	*(16,095)*	*(905,584)*	*(123,468)*	*(28,631)*	*(71,586)*	(1,327,333)	(7,623)	(1,817,422)	(1,495,198)
5	347,819	443,915		2,299,757	1,473,426	826,331		(210,498)	(271,968)	(572,628)	*(173,891)*	*(16,578)*	*(932,752)*	*(127,172)*	*(26,341)*	*(68,754)*	(1,358,943)	(14,433)	(1,855,842)	(1,454,101)
6	353,239	473,374		2,368,750	1,517,629	851,120		(221,023)	(261,443)	(572,628)	*(179,108)*	*(17,075)*	*(960,734)*	*(130,988)*	*(24,050)*	*(65,689)*	(1,391,421)	(21,489)	(1,895,375)	(1,414,358)
7	139,500	196,290	(307,468)	2,439,812	1,563,158	876,654		(232,074)	(250,392)	(572,628)	*(184,481)*	*(17,587)*	*(989,557)*	*(134,917)*	*(21,760)*	*(62,378)*	(1,424,786)	(28,801)	(2,243,522)	(1,594,429)
8	362,176	535,099		2,513,006	1,610,053	902,954		(243,678)	(238,788)	(572,628)	*(190,016)*	*(18,115)*	*(1,019,243)*	*(138,965)*	*(19,469)*	*(58,809)*	(1,459,062)	(36,379)	(1,977,908)	(1,338,726)
9	365,767	567,425		2,588,397	1,658,354	930,042		(255,862)	(226,604)	(572,628)	*(195,716)*	*(18,658)*	*(1,049,821)*	*(143,134)*	*(17,179)*	*(54,969)*	(1,494,271)	(44,234)	(2,020,971)	(1,302,736)
10	368,821	600,770		2,666,048	1,708,105	957,944		(268,655)	(213,811)	(572,628)	*(201,587)*	*(19,218)*	*(1,081,315)*	*(147,428)*	*(14,888)*	*(50,846)*	(1,530,436)	(52,376)	(2,065,278)	(1,267,902)
11	371,369	635,167		2,746,030	1,759,348	986,682		(282,088)	(200,378)	(572,628)	*(207,635)*	*(19,795)*	*(1,113,755)*	*(151,850)*	*(12,598)*	*(46,427)*	(1,567,580)	(60,817)	(2,110,863)	(1,234,178)
12	(63,212)	(113,519)	(784,168)	2,828,411	1,812,128	1,016,282		(296,192)	(186,274)	(572,628)	*(213,864)*	*(20,388)*	*(1,147,167)*	*(156,406)*	*(10,307)*	*(41,697)*	(1,605,728)	(69,567)	(2,941,930)	(1,638,177)
13	375,071	707,253		2,913,263	1,866,492	1,046,771		(311,002)	(171,464)	(572,628)	*(220,280)*	*(21,000)*	*(1,181,582)*	*(161,098)*	*(8,017)*	*(36,641)*	(1,644,904)	(78,640)	(2,206,010)	(1,169,894)
14	376,282	745,013		3,000,661	1,922,487	1,078,174		(326,552)	(155,914)	(572,628)	*(226,888)*	*(21,630)*	*(1,217,030)*	*(165,931)*	*(5,726)*	*(31,244)*	(1,685,134)	(88,048)	(2,255,648)	(1,139,255)
15	377,102	783,968		3,090,681	1,980,162	1,110,519		(342,880)	(139,586)	(572,628)	*(233,695)*	*(22,279)*	*(1,253,541)*	*(170,909)*	*(3,436)*	*(25,490)*	(1,726,443)	(97,804)	(2,306,712)	(1,109,568)
16	377,556	824,156		3,183,401	2,039,567	1,143,835		(360,024)	(122,442)	(572,628)	*(240,706)*	*(22,947)*	*(1,291,147)*	*(176,036)*	*(1,145)*	*(19,363)*	(1,768,858)	(107,921)	(2,359,245)	(1,080,797)
17	176,887	405,428	(413,212)	3,278,903	2,100,754	1,178,150		(378,025)	(104,441)	(286,314)	*(247,927)*	*(23,636)*	*(1,329,881)*	*(181,317)*		*(16,395)*	(1,817,148)	(160,650)	(2,873,476)	(1,253,688)
18	336,627	810,132		3,377,270	2,163,776	1,213,494		(396,926)	(85,540)		*(255,365)*	*(24,345)*	*(1,369,778)*	*(186,757)*		*(16,886)*	(1,871,662)	(213,010)	(2,567,138)	(1,066,699)
19	334,612	845,548		3,478,589	2,228,689	1,249,899		(416,772)	(65,694)		*(263,026)*	*(25,075)*	*(1,410,871)*	*(192,360)*		*(17,393)*	(1,927,812)	(222,762)	(2,633,040)	(1,041,983)
20	332,404	881,967		3,582,946	2,295,550	1,287,396		(437,611)	(44,855)		*(270,917)*	*(25,827)*	*(1,453,197)*	*(198,130)*		*(17,915)*	(1,985,646)	(232,867)	(2,700,979)	(1,017,971)
21	74,940	208,779		1,845,217	1,182,208	663,009		(459,492)	(22,975)		*(139,522)*	*(26,602)*	*(748,397)*	*(102,037)*		*(9,226)*	(1,036,042)	(117,930)	(1,636,438)	(587,387)
NPV, EUR	***2,996,717***																***NPV of Costs, EUR***			***(33,034,417)***
PI	***1.35***																***Annuity of Costs, EUR***			***(2,650,767)***
IRR	***12.8%***																***LRGC (incl. Cost Escal.), EUR/MWh***			***(66.3)***
Annuity, EUR	***240,464***																			

Table 8.4: Geothermal heat plant economical model. With $C0_2$ trading.

According with calculations project without CO_2 trading has deeply negative NPV minus 7,140,717 euro and Profitability Index PI = 0.17. (table 9.3). So, this scenario is not acceptable and eliminated.

The scenario with CO_2 trading has positive NPV 2,996,717 euro and Profitability Index PI = 1.35 (table 9.4). Starting from year 3 project will be having annual positive nominal cash flow except year 12 than repair works have to be executed and required investment are planned. Planned break even time is foreseen after 8 years, as we can see in the figure 8.4.

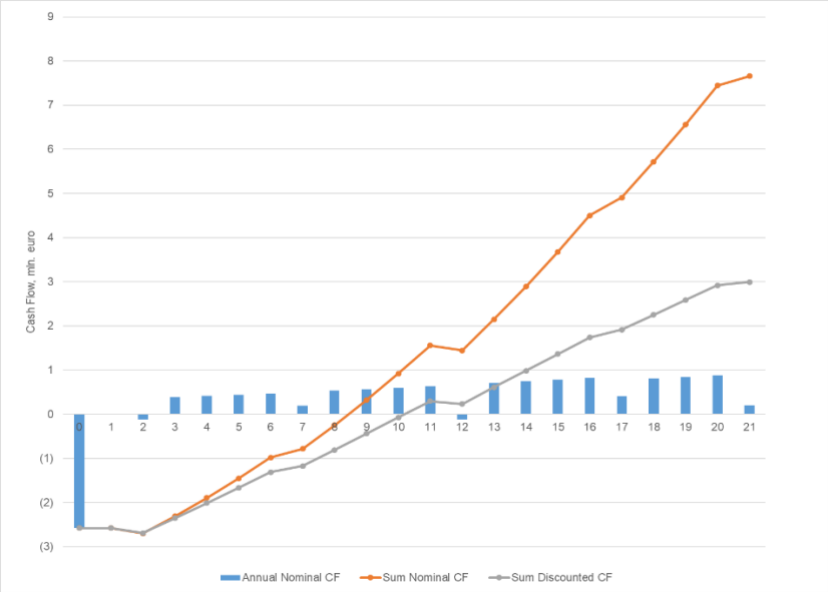

Figure 8.4: Nominal and discounted CF

Sensitivity analyses (figure 8.5) shows that project is stable and even investment increase by 40% won't make NPV negative. Gas price has crucial impact on the project, but it not expected its drop. Gas price decrease by 20% makes project inexpedient. As, electricity consumption is significant its price crustily influence on the project stability. Electricity price growth more than 29% makes NPV negative.

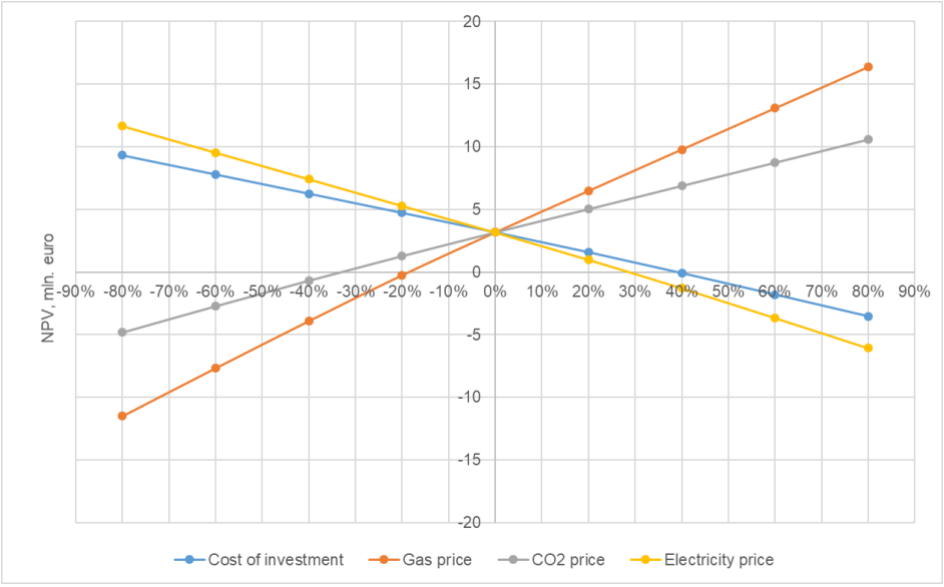

Figure 8.5: Sensitivity analysis for NPV

CO_2 trading is not a regular business in Serbia and as Serbia is not a member of EU there is no sustainable mechanisms and legal base to manage this. On the other hand, significant amount of electricity, almost 6 GWh annually, is required to operate geothermal heat plant. We should take into account, that around than 70% of electricity generation in Serbia comes from coal burning power plants (see part 1). Only consumption of "green" electricity will make this project renewable. Also important factor, that price of electricity has a crucial impact on the whole project efficiency.

This dilemma should be carefully analyzed and can be a theme for another research.

From the geographical point of view, Serbia looks attractive for PV power and we can observe a rise of interest to PV power projects on a local market nowadays.

Based on above mentioned facts, the next assumption is done. Set up of PV power plant and Geothermal heat plant together (GeoT-PV system), as one energy asset, will create additional new value of the project, makes it attractive and sustainable. Concept of proposed system is presented in figure 8.6

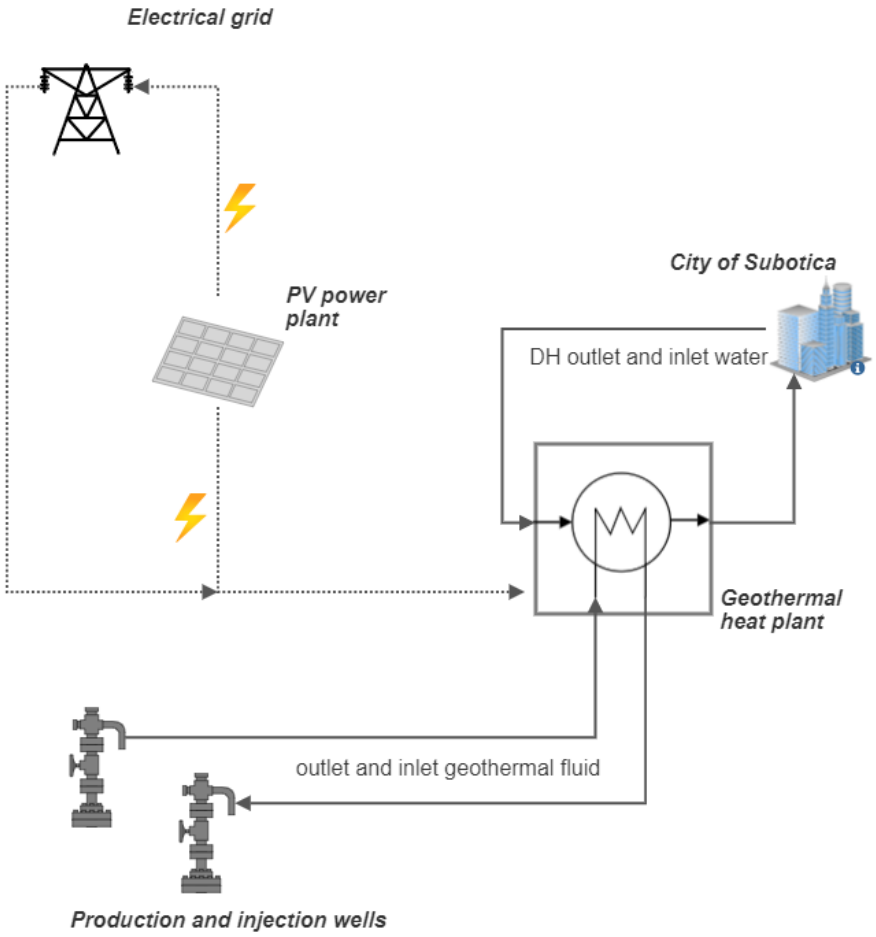

Figure 8.6: Concept of GeoT-PV system

PV plant must cover annual electricity demand of geothermal heat plant. It is obvious that outlet power curve of PV plant and demand curve of electric power of geothermal plant will not concur. It is assumed that it will be agreed with electrical grid provider (EPS) that annual electric power balance will be "zero". This means, that annual

electricity production of PV power will be equal to electricity consumption of geothermal heat plant and electricity costs will be zero.

Required power of PV plant can be calculated as:

$$P = \frac{E}{H \times r}$$

where,

P - power of PV plant, kW

E - annual electricity production/consumption, 5.96×10^6 kWh

H - annual radiation, 1,590 kWh/m^2/a (Photovoltaic Geographical Information System, www.re.jrc.europa.eu).

r - performance ratio of PV system, 0.77 (Zalevskii 2022).

$$P = \frac{5.96 \times 10^6}{1590 \times 0.77} \sim 5\ MW$$

Majority of the data and PV plant conceptual design were taken from (Zalevskii 2022) where similar PV plant for Serbia was described and calculated. The following new assumption and changes in input data, comparing to above analyzed scenarios, for economical appraisal of GeoT-PV system were made:

1. There is no CO_2 trading.
2. Project was divided for two phases. PV plant development and construction could be done faster than geothermal one as last has subsurface part and required geological exploration. PV plant will be finished one and a half year earlier and start operation. This is an opportunity to start selling electricity earlier into a grid and provide additional revenue. Due to that, investment distribution by years was changed to 40%, 40% and 20% respectively.
3. Electricity selling price was assumed as 110 euro/MWh in accordance with current public data from EPS Company (https://www.eps.rs) and available market information from independent electricity producers in Serbia.
4. Unplanned costs were decreased to 1% as total investment increased.
5. After 10 years of operation the additional PV plant repair works are planed. The total cost of repair works is 750,000 euro.
6. Based on IRENA 2021 report and considering current local market data trends, 600 euro/kW is taken as specific investment cost for PV plant.
7. PV plants require a significant area of a land for installation. The specific value 27,500 m^2 per MW (Zalevskii 2022) was taken and required area of land was added into the model.
8. The annual maintenance costs of the PV plant was assumed as 12 euro/kW based on reports IRENA 2021, IRENA 2012, Electric Power Research Institute 2015, Keating et al. 2015 and the local market data.
9. Addition headcount for PV plant, plus two positions, was added.

Results of calculations are presented in tables 9.5 and 9.6.

Technical figures		
Power	**MW_{th}**	**10**
Full Load hours	h	4,000
Heat production	**GWh_{th}/y**	**40.0**
Electricity production	**GWh_e/y**	**6.0**
Annual radiation	$kWh/m^2/a$	1,590
Performance ratio		0.77
Power of PV	**MW_e**	**5.0**
Production wells		1
Injection wells		1
Pipeline to the DH network	m	1000
Distance between production and injection wells	m	2000
Investment figures		
Well cost	EUR/well	2,950,000
Wells cost	EUR	5,900,000
Pipelines cost	EUR	1,120,000
GT heat power plant cost	EUR/kW	100
Specific investment cost for PV	EUR/kW	600
Project development (% of investment)	%	5
Unplanned costs (% of investment)	%	1
Total investment	**EUR**	**11,686,710**
Equity	%	30%
	EUR	3,506,013
Bank Loan	%	70%
	EUR	8,180,697
Bank loan period	y	20
Bank interest rate	%	5%
Wells workover (every 5 years)	EUR	250,000
Infrastructure repair (10 years)	EUR	750,000
Investment horizon	y	20
Term of depreciation	y	15
Construction period for PV	y	1
Total construction period	y	2.5
Tax rate	%	15.0
CPI	%	3.0
Discount rate / cost of capital	%	5.0
Energy price		
Electricity price (sell)	EUR/kWh	0.100
Gas price	EUR/kWh	0.027
Heat price	EUR/kWh	0.032
Operaitional costs		
Cost of land (rent)	**EUR/y**	**41,800**
Required land for geothermal	ha	7.2
Required land for PV	m^2/MW	27,500
Cost of land (rent)	EUR/ha/y	2000
Electricity costs	**EUR/y**	**-**
Electricity consumption (production and injection)	kWh/y	5,600,000
Electricity consumption (DH pumps)	kWh/y	360,000
Maintenance cost	**EUR/y**	**169,700**
Maintenance cost for subsurface (1,5% of investment)	EUR/y	88,500
Maintenance cost for surface (1% of investment)	EUR/y	21,200
Maintenance cost for PV	EUR/kW/y	12.0
Maintenance cost for PV	EUR/y	60,000
Property tax	**%**	**0.4**
SG&A (% of turnover)	**%**	**0.5**
Insurance	**%**	**0.75**
Other operation costs (% of total operational costs)	**%**	**1**
Labor cost	**EUR/y**	**200,000**
Headcount	person	8
Headcount cost	EUR/person/year	25,000

Table 8.5: GeoT-PV system economical model input data

Year	Discounted CF	Nominal CF	Investment, Replacement& Residual Value	Revenue			Income / bank loan	Bank loan payment		Depreciation	O&M costs							Tax	Nominal Costs	Discounted Costst
				Total	Heat Sales	Electricity Sales		Payment of bank loan	Interest rate		*Labor cost*	*Land costs*	*Electricity costs*	*Maintenance*	*Proprety tax*	*Other costs (SG&A, insurance and ect.)*	TOTAL incl. add costs			
0	(3,506,013)	(3,506,013)	(4,674,684)				1,168,671												(4,674,684)	(4,674,684)
1	357,515	375,391	(4,674,684)	613,880		613,880	4,674,684			(311,646)	*(51,500)*	*(30,138)*	*0*	*(34,958)*	*(17,452)*	*(90,942)*	*(227,240)*	(11,249)	(4,913,173)	(4,679,212)
2	101,223	111,598	(2,337,342)	1,148,419	674,197	474,222	2,337,342	(247,405)	(409,035)	(467,468)	*(106,090)*	*(44,346)*	*0*	*(90,017)*	*(43,630)*	*(92,531)*	(380,381)	0	(3,374,163)	(3,060,465)
3	126,536	146,481		1,388,846	1,388,846			(259,776)	(396,665)	(779,114)	*(218,545)*	*(45,676)*	*0*	*(185,436)*	*(40,514)*	*(89,952)*	(585,924)	0	(1,242,364)	(1,073,201)
4	149,392	181,587		1,430,511	1,430,511			(272,765)	(383,676)	(779,114)	*(225,102)*	*(47,046)*	*0*	*(190,999)*	*(37,397)*	*(86,074)*	(592,484)	0	(1,248,924)	(1,027,493)
5	170,691	217,850		1,473,426	1,473,426			(286,403)	(370,038)	(779,114)	*(231,855)*	*(48,458)*	*0*	*(196,729)*	*(34,281)*	*(81,882)*	(599,136)	0	(1,255,576)	(983,777)
6	190,518	255,312		1,517,629	1,517,629			(300,723)	(355,717)	(779,114)	*(238,810)*	*(49,911)*	*0*	*(202,631)*	*(31,165)*	*(77,361)*	(605,877)	0	(1,262,317)	(941,960)
7	(9,561)	(13,453)	(307,468)	1,563,158	1,563,158			(315,759)	(340,681)	(779,114)	*(245,975)*	*(51,409)*	*0*	*(208,710)*	*(28,048)*	*(72,495)*	(612,703)	0	(1,576,611)	(1,120,468)
8	226,066	334,002		1,610,053	1,610,053			(331,547)	(324,893)	(779,114)	*(253,354)*	*(52,951)*	*0*	*(214,971)*	*(24,932)*	*(67,268)*	(619,610)	0	(1,276,050)	(863,681)
9	241,934	375,319		1,658,354	1,658,354			(348,124)	(308,316)	(779,114)	*(260,955)*	*(54,540)*	*0*	*(221,420)*	*(21,815)*	*(61,662)*	(626,595)	0	(1,283,035)	(827,056)
10	256,215	417,348		1,708,105	1,708,105			(365,531)	(290,910)	(779,114)	*(268,783)*	*(56,176)*	*0*	*(228,063)*	*(18,699)*	*(55,658)*	(633,653)	(664)	(1,290,757)	(792,413)
11	264,337	452,106		1,759,348	1,759,348			(383,807)	(272,633)	(779,114)	*(276,847)*	*(57,861)*	*0*	*(234,904)*	*(15,582)*	*(49,240)*	(640,778)	(10,023)	(1,307,242)	(764,317)
12	(561,887)	(1,009,069)	(1,497,049)	1,812,128	1,812,128			(402,997)	(253,443)	(779,114)	*(285,152)*	*(59,597)*	*0*	*(241,952)*	*(12,466)*	*(42,386)*	(647,967)	(19,741)	(2,821,197)	(1,570,948)
13	278,423	525,007		1,866,492	1,866,492			(423,147)	(233,293)	(779,114)	*(293,707)*	*(61,385)*	*0*	*(249,210)*	*(9,349)*	*(35,076)*	(655,214)	(29,831)	(1,341,485)	(711,418)
14	284,467	563,225		1,922,487	1,922,487			(444,305)	(212,136)	(779,114)	*(302,518)*	*(63,226)*	*0*	*(256,686)*	*(6,233)*	*(27,290)*	(662,513)	(40,309)	(1,359,262)	(686,520)
15	289,896	602,674		1,980,162	1,980,162			(466,520)	(189,920)	(779,114)	*(311,593)*	*(65,123)*	*0*	*(264,387)*	*(3,116)*	*(19,005)*	(669,857)	(51,191)	(1,377,488)	(662,595)
16	294,746	643,394		2,039,567	2,039,567			(489,846)	(166,594)	(779,114)	*(320,941)*	*(67,077)*	*0*	*(272,319)*		*(10,198)*	(677,240)	(62,493)	(1,396,173)	(639,603)
17	62,993	144,380	(413,212)	2,100,754	2,100,754			(514,338)	(142,102)		*(330,570)*	*(69,089)*	*0*	*(280,488)*		*(10,504)*	(697,557)	(189,164)	(1,956,373)	(853,559)
18	244,956	589,516		2,163,776	2,163,776			(540,055)	(116,385)		*(340,487)*	*(71,162)*	*0*	*(288,903)*		*(10,819)*	(718,484)	(199,336)	(1,574,260)	(654,138)
19	246,273	622,321		2,228,689	2,228,689			(567,058)	(89,382)		*(350,701)*	*(73,297)*	*0*	*(297,570)*		*(11,143)*	(740,038)	(209,890)	(1,606,369)	(635,695)
20	247,250	656,028		2,295,550	2,295,550			(595,411)	(61,030)		*(361,222)*	*(75,495)*	*0*	*(306,497)*		*(11,478)*	(762,239)	(220,842)	(1,639,522)	(617,919)
21	247,428	689,326		2,013,760	1,182,208	831,552		(625,181)	(31,259)		*(186,029)*	*(77,760)*	*0*	*(157,846)*		*(10,069)*	(436,022)	(231,972)	(1,324,434)	(475,395)

NPV, EUR	*203,398*	*NPV of Costs, EUR*	*(28,316,518)*
PI	*1.02*	*Annuity of Costs, EUR*	*(2,272,191)*
IRR	*5.5%*	*LRGC (incl. Cost Escal.), EUR/MWh*	*(56.8)*
Annuity, EUR	*16,321*		

Table 8.6: GeoT-PV system economical model.

The GeoT-PV scenario has positive NPV 203,398 euro and profitability Index PI = 1.02. (table 9.6). Starting from year the 1st project will be having positive annual nominal cash flow except years 7 and 12 than repair works have to be executed and required investment are planned. Planned break even time is foreseen after 15 years, as we can see in the figure 8.6.

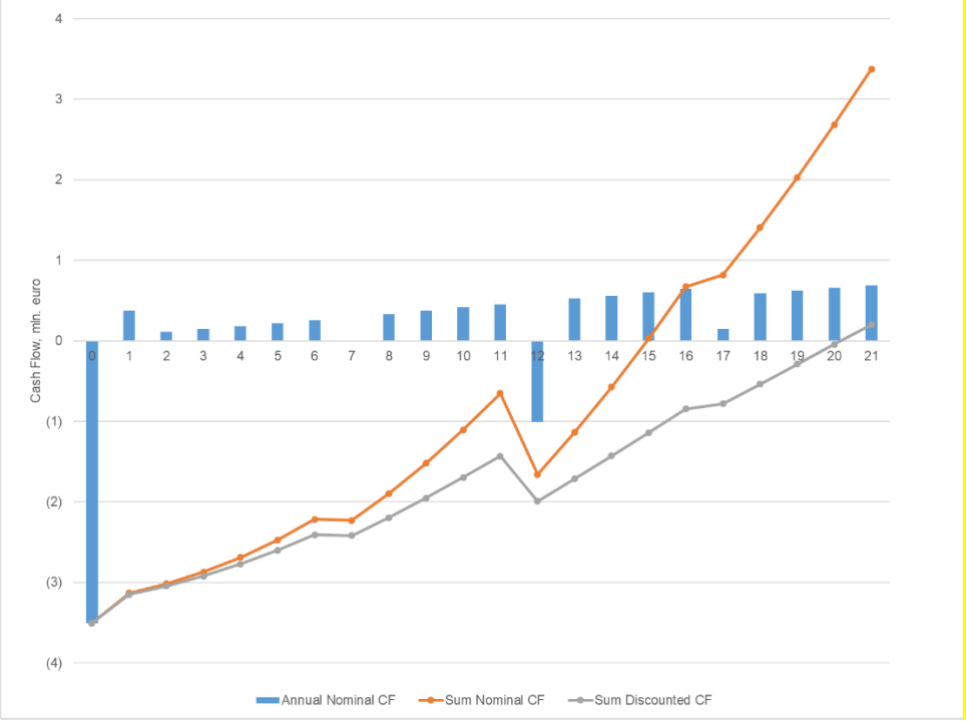

Figure 8.7: Nominal and discounted CF. GeoT-PV system.

Sensitivity analyses is presented in the figure 8.7. As NPV is close to zero any changes will have a critical impact on the project. However, gas price drop is not expected, but it growth will support project. At the same time, we should work on investment costs optimization that makes project more sustainable.

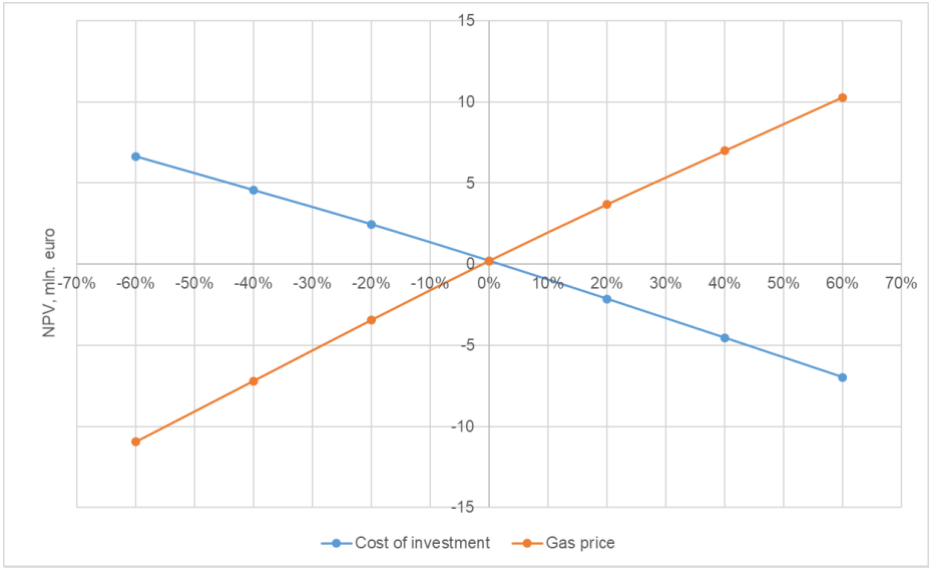

Figure 8.8: Sensitivity analysis for NPV. GeoT-PV system.

9. CONCLUSION

The goal of this Mater Thesis was research of potential use-case of geothermal direct heat usage in city of Subotica. Overall study of this topic including systematic analyses of exist technologies and expiries in geothermal worldwide, in Europe and Serbia, geothermal potential in Pannonian basin with a focus on the area near the city of Subotica, design of geothermal heat plant and finance analyses was done.

Based on DHS of Subotica analyses geothermal heat plant installed capacity $10MW_{th}$, 4000 hours of full load hours and temperature mode 85/55°C was chosen. It is important to mention that during the coldest days in the last 5 years, January 6th-12th of 2017, when the outside temperature dropped below minus 20 Celsius degrees the temperature mode was 95/65°C. The annually average supply temperature in DH is around 60^0C than return temperature is around 40^0C. Therefore, it looks reasonable to study a possible use case with a lower temperature mode that consequence lower depth and investment costs for drilling.

Also, a distribution of produced heat is an open issue. The total heat needs of the city of Subotica is appraised as 250-300 GWh_{th} per heating season. Only 27% of households are connected to DHS, that owned by “Suboticka Toplana” and more than 70% use natural gas and other sources for heating. In addition, according with “General plan of Subotica-Palic area development until 2030”, building more than 250,000 square meters of new apartments are projected that will require roughly 25 MWth of installed heat power. Nevertheless, heat demand forecasts based on urban planning should be interpreted prudently.

Therefore, two optioned were announced in the research. The first is the connection to exist DH and the second is heat supply in districts, which are not connected to DH. Particularly decentralized gas heating and geothermal local district heating may become serious competitors. A critical factor for the competitiveness of DH will be the pricing for natural gas.

Brief analyses of current and projected conditions of heat market showed that potentially exist room for 10MWth geothermal heat plant, which can help to cover growing heat demand and support a transition to “green” heating.

According with geological assessment of the city of Subotica area, the 1500 m depth layers were defined as priority for a future DH geothermal system. The temperature of geothermal water on this depth is ~1150C that is corresponds to DH temperature regime requirements. However, Paleozoic formations presented on this depth are challenging for development. It has a wide range of basic reservoir characteristics , which are crucial for geothermal system design, and complex for studing by conventional methods and predicting . The key uncertainties relate to the permeability of the reservoir and thickness of aquifers.

Having wide range of permeability and thickness of aquifers in a different wells in Paleozoic formation, probabilistic approach, including alternative numerical simulation models (most likely, pessimistic and optimistic) creation, was chosen for further calculations as common tool for such cases.

Different technological scenarios were modeled with a goal to achieve required fluid flow and geothermal energy production. Besides conventional vertical drilling, two technologies were applied in addition - horizontal drilling and hydraulic fracturing. These technologies are widely used to stimulate production from low-permeability and tiny layer reservoir in oil&gas industry. As a result, 10 MW thermal power doublet geothermal system with two horizontal wells (one production and one injection) and

two plate exchangers, 5 MW_{th} each, was chosen. This scenario has probability not less than P50 ("most likely").

Economical evaluation of this scenario showed that due to high investment costs related to subsurface part and high electricity price geothermal heat production is positive only in a case of CO_2 trading. It has positive NPV 2,996,717 euro and Profitability Index PI = 1.35

Sensitivity analyses showed that project is stable and even investment increase by 40% will not make NPV negative. Gas price has crucial impact on the project, but it not expected its drop. Gas price decrease by 20% makes project inexpedient. As, electricity consumption is significant its price also crustily influence on the project stability. Electricity price growth more than 29% makes NPV negative.

CO2 trading is not a regular business in Serbia and as Serbia is not a member of EU there is no sustainable mechanisms and legal base to manage this. On the other hand, significant amount of electricity, almost 6 GWh annually, is required to operate geothermal heat plant. We should take into account, that around than 70% of electricity generation in Serbia comes from coal burning power plants. Only consumption of “green” electricity will make this project renewable. This dilemma may be a theme for another research.

Aiming to build sustainable business-case with a low carbon footprint additional scenario was set up - PV power plant and geothermal heat plant together, as one energy asset. From the geographical point of view, Serbia looks attractive for PV power and we can observe a rise of interest to PV power projects on a local market nowadays. PV plant must cover annual electricity demand of geothermal heat plant. It is obvious that outlet power curve of PV plant and demand curve of electric power of geothermal plant will not concur. It is assumed that it will be agreed with electrical grid provider that annual electric power balance will be “zero”. The GeoT-PV scenario has positive NPV 203,398 euro and profitability Index PI = 1.02.

At the end, it is important to mention two things. Firstly, the creation of sustainable geothermal energy business case strongly required regional geological study and maybe exploration works. Base on that potential “hot-spots” could be defined which has the best potencial and geological conditionns. Secondly, it important to have a strong commitment and need of local municipality and heat consumers in a new heat energy source. These two things are key element of success business case. Moreover, geothermal energy source has features as high electricity demand, high load factor and ect. Its combination with other renewable energy sources can created additional value and should be taken into account for creation carbon-neural sustainable energy source.

In addition, as geothermal projects has significantly complex and expensive subsurface part, oil & gas companies experience must be taken into account in researched areas if it is possible. It will help to reduce risks and costs.

BIBLIOGRAPHY

1. Anderson, A. and Rezaie, B. (2019): *Geothermal technology: Trends and potential role in a sustainable future*, Applied Energy, Vol. 248/August, p. 18-34.
2. Andritsos N. / Karabelas A.J. / Koutsoukos P. G. (2014): Scale Formation in Geothermal Plants. In: *International Summer School on Direct Application of Geothermal Energy*, 179-189.
3. Aydin H. / Merey S. (2021): Changing Casing-Design of New Geothermal Wells in Western Anatolia for Adapting to the Changes in Reservoir Conditions. In: *46th Workshop on Geothermal Reservoir Engineering Stanford University, Stanford, California, February 15-17, 2021*
4. Beckers K. and Young K. (2017): Performance, Cost, and Financial Parameters of Geothermal District Heating Systems for Market Penetration Modeling under Various Scenarios. In: *42nd Workshop on Geothermal Reservoir Engineering Stanford University*, Stanford, California, February 13-15, 2017
5. DiPippo, R. (2012): *Geothermal Power Plants: Principles, Applications, Case Studies and Environmental Impact*, Butterworth-Heinemann, Oxford, United Kingdom.
6. Dövényi P. / Horváth F. (1988): A Review of Temperature, Thermal Conductivity, and Heat Flow Data for the Pannonian Basin. In: *The Pannonian Basin: A Study in Basin Evolution*, AAPG Memoir 45, eds. Royden L, Horváth F., 195-233.
7. EGEC (1999): Ferrara Declaration / Dichiarazione di Ferrara. In: *EGEC Business Seminar Ferrara,* Brussels, 1-2.1999.
8. EGEC (2020): *Geothermal market report. Key Findings*. 10th edition, Brussels.
9. Electric Power Research Institute (2015): *Budgeting for solar PC plant Operations & Maintenance: Practices and pricing.* Palo Alto California USAO, December 2015
10. Energy balance of Republic of Serbia (2022): In: *Official Gazette of RS, 4/2022,* January 14, 2022.
11. Energy manager of the City of Subotica (2021): *Energy efficiency program of the city of Subotica for the period 2022-2024,* the City of Subotica, August 2021.
12. Energy Sector Development Strategy of the Republic of Serbia for the period by 2025 with projections by 2030 (2016): Republic of Serbia, Ministry of Mining and Energy, Kosmos Ltd, Belgrade, 2016.
13. Gasketed plate heat exchangers. Instruction Manual (2023): Industrial line - M15, TL10, T15, TL15, T20, T21, TS20, T25, MX25, MA30,WideGap 100, WideGap 200. Alfa Laval. https://www.alfalaval.com/products/heat-transfer/plate-heat-exchangers/gasketed-plate-and-frame-heat-exchangers/
14. Golusin M. / Munitlak Ivanovic O. / Bagaric I. / Vranjes S. (2014): Exploitation of geothermal energy as a priority of sustainable energetic development in Serbia. In: *Renewable and Sustainable Energy Reviews 14 (2010), 868–871*

15. H.F. Mijnlieff / A.N.M. Obdam/ J.D.A.M. van Wees / M.P.D. Pluymaekers / J.G. Veldkamp (2014): TNO 2014 R11396, DoubletCalc 1.4 manual, English version for DoubletCalc 1.4.3

16. Hagen H. (2008): Geothermal well design – casing and wellhead. In: *Petroleum Engineering Summer School Hole. H M Dubrovnik, Croatia. Workshop #26 June 9 – 13, 08 June 2008*

17. Horváth F. / Musitz B. / Balázs A. / Végh A. / Uhrin A. / Nádor A. / Koroknai B. / Pap N. / Tóth T. / Wórum G. (2015): Evolution of the Pannonian basin and its geothermal resources. In*: Geothermics, 53, 328-352*.

18. IEA (2021): The cost of capital in clean energy transitions. https://www.iea.org/articles/the-cost-of-capital-in-clean-energy-transitions - December 17 2021.

19. IRENA (2020): *Geothermal Development in Eastern Africa*, International Renewable Energy Agency, Abu Dhabi.

20. IRENA (2021): *Renewable Power Generation Costs in 2020*, International Renewable Energy Agency, Abu Dhabi.

21. IRENA and IGA (2023): *Global geothermal market and technology assessment*. International Renewable Energy Agency, Abu Dhabi; International Geothermal Association, The Hague.

22. IRENA, IEA and REN21 (2020): *Renewable energy policies in a time of transition. Heating and cooling.* IRENA, OECD/IEA and REN21.

23. IUPCS (2018): *General plan of Subotica-Palic area development until 2030.* Institute of urban planning of the city of Subotica (IUPCS), Republic of Serbia, Autonomous Province of Vojvodina, City of Subotica.

24. Jóhannesson, T. and Chatenay, C. (2014): Industrial applications of geothermal resources. In: *Short Course VI on Utilization of Low- and Medium-Enthalpy Geothermal Resources and Financial Aspects of Utilization*, organized by UNU-GTP and LaGeo, in Santa Tecla, El Salvador, March 23-29, 2014.

25. Jorge A. Acuna / Mauro A. Parini / Noel A. Urmeneta (2002): Using a large reservoir model in the probabilistic assessment of field management strategies. In: *Twenty-Seventh Workshop on Geothermal Reservoir Engineering Stanford University, Stanford, California, January 28-30, 2002*

26. Keating T.J./ Walker A./ Ardani K. (2015): *SAPC Best Practices in PV Operations and Maintenance. Version 1.0, March 2015.Period of Performance January 1, 2014 - December 31, 2015.* National Renewable Energy Laboratory, NREL/SR-6A20-63235.

27. KWF (2016): *Serbia: Rehabilitation of District Heating System (Phase I-IV) – update & outlook*. June 1st 2016, Vienna.

28. Lenkey L. / Dövényi P. / Horváth F. / Cloetingh S. (2002): Geothermics of the Pannonian basin and its bearing on the neotectonics. In: *EGU Stephan Mueller Special Publication Series*, 3, 29–40

29. Local sustainable development strategy of the city of Subotica 2013-2022 (2012): The city of Subotica. http://www.subotica.rs/documents/slor/slor_sr.pdf

30. Lund J.W. / Lienau P.J. (2009): *Geothermal district heating. In: International Geothermal days. Slovakia 2009. Conference & summer school.*

31. Mattson D. and Ghanashyam Neupane G. (2017): LCOH Estimated from Existing Geothermal District Heating Systems in the U.S. In: *Geothermal Resources Council Annual Meeting*, October 2017

32. Meissner R. / Stegena L. (1988): Lithosphere and Evolution of the Pannonian Basin. In: *The Pannonian Basin: A Study in Basin Evolution*, AAPG Memoir 45, eds. Royden L, Horváth F., 147-152.

33. Mijnlieff H.(2020): Introduction to the geothermal play and reservoir geology of the Netherlands. In: *Netherlands Journal of Geosciences, Volume 99.*

34. Milivojevic M. / Martinovic M. (2005): Geothermal Energy Possibilities, Exploration and Future Prospects in Serbia. In: *Proceedings World Geothermal Congress 2005,* Antalya, Turkey, 24-29 April 2005

35. Moumin A.O. (2013): Geothermal well design. In: *Geothermal training program reports 2013, Orkustofnun, Grensasvegur 9, Number 28, IS-108 Reykjavik, Iceland.*

36. Moumin A.O. (2015): Geothermal Well Design for the Future 4 Wells in the Lava Lake Area in Caldera Fiale in Djibouti. In: *World Geothermal Congress 2015, Melbourne, Australia, 19-25 April 2015*

37. National bank of Serbia (2023): *Inflation report.* Maj 2023., Belgrade

38. National Renewable Energy Action Plan (NREAP) Implementation Report for 2020 (2022): Republic of Serbia, Ministry of Mining and Energy, Belgrade, 2022.

39. National Renewable Energy Action Plan of the Republic of Serbia (NREAP) (2013): Republic of Serbia, Ministry Energy, Development and Environmental Protection, Belgrade, 2013.

40. Rman N. / Bălan L. / Bobovečki I. / Gál N. / Jolović B. / Lapanje A. / Marković T. / Milenić D. / Skopljak F. / Rotár-Szalkai A. / Samardžić N. / Szőcs T. / Solaja D. / Toholj N. / Vijdea A. / Vranješ A. (2019): Geothermal sources and utilization practice in six countries along the southern part of the Pannonian basin. In: *Environmental Earth Sciences*, 79, 12pp.

41. Rman N. / Kun E. / Samardžić N. / Sram D. / Atanackov J. / Markič M. / Lapanje A. / Rajver D. / Selmeczi I.S. / Maros G. / Marković T. / Budai T. / Babinszki E. (2021): A Joint Report on Geomanifestations in the Pannonian basin. In: *Deliverable 4.2 of the GeoConnect3D Horizon 2020 Project*, 105pp.

42. Patsa E. / Sadiq J. Zarrouk S.J. / Van Zyl D. (2015): The Lindal Diagram for Mining Engineering. In: *GRC Transactions, Vol. 39, 2015, 151-156.*

43. Sanner B. / Antics M. / Baresi M. / Javier F. Urchueguía / Dumas P. (2022): Summary of EGC 2022 Country Update Reports on Geothermal Energy in Europe. *In: European Geothermal Congress 2022,* Berlin, Germany, 17-21 October 2022.

44. Stipić Z. / Vidović S. / Spasojević M. (2012): The potential of renewable energy sources in the Republic of Serbia with a detailed description of the exploitation of geothermal sources in the autonomous province of Vojvodina. https://geothermalcommunities.geonardo.com/assets/elearning/1.40.CLANAK%20KOMPLET.pdf

45. Tchobanoglous G. / Burton F. / Stensel H.D. (2003): *Wastewater Engineering: Treatment and Reuse*, 4th ed, McGraw Hill, New York.

46. The theory behind heat transfer. Plate heat exchangers (2004): Alfa Laval. https://www.alfalaval.com/globalassets/documents/microsites/heating-and-cooling-hub/alfa_laval_heating_and_cooling_hub_the_theory_behind_heat_transfer.pdf

47. U.S. Department of Energy (2015): *GeoVision. Harnessing the Heat Beneath Our Feet.* https://www.energy.gov/eere/geothermal/articles/geovision-executive-summary

48. U.S. Department of Energy (2016): Geothermal Energy – Direct-Use. https://www.wbdg.org/resources/geothermal-energy-direct-use - November 12, 2016.

49. Uihlein A. (2018): *JRC Geothermal Power Plant Dataset*. Documentation, EUR 29446 EN, Publications Office of the European Union, Luxembourg.

50. Waples D.W. / Pacheco J. / Vera A. (2004): A method for correcting log-derived temperatures in deep wells, calibrated in the Gulf of Mexico. In: *Petroleum Geoscience*, 10, 239-245.

51. Waples D.W. / Ramly M. (2001): A statistical method for correcting log-derived temperatures. In: *Petroleum Geoscience,* 7, 231-240.

52. Zalevskii N. (2022): *Comparison of different technologies for transport energy for the region of Serbia*. Unpublished homework 2, TU Wien, Vienna

LIST OF ABBREVIATIONS

AGS - advanced geothermal system
BHT - bottom hole temperature
CPI - consumer price index
DH- district heating
DHS - district heating systems
EGS - enhanced geothermal system
EPS - Elektroprivreda Srbije
ESP - electrical submersible pump
EU – European Union
GDP - gross domestic product
GFEC - gross final energy consumption
GHP – geothermal heating pumps
HD – hydrodynamic
LMTD - logarifmic mean temperature difference
LSI - Langelier Saturation Index
NIS – Naftna Industrija Srbije
NPV - Net Present Value
NREAP - National Renewable Energy Action Plan
OI3-M1- Oligocene-Miocene
ORC – organic Ranikne cycle
P - Paleocene
PI - Pliocene
PI - Profitability Index
Pn – Pannonian
Pt - Pont
PV – photovoltaic
Pz - Paleozoic
Q - Quaternary
RES - renewable energy sources
RI - Ryznar Stability Index
Sm - Sarmatian
TDS - total dissolved solids
TEC - total energy consumption
UTES - underground thermal energy storage
WAAC - weighted average cost of capital
WHP- wellhead pressure

LIST OF FIGURES

LIST OF TABLES

LIST OF APPENDIXES

APPENDIXES